Aus dem Max von Pettenkofer-Institut für Hygiene und Medizinische Mikrobiologie der Ludwig-Maximilians-Universität München

A genome-wide analysis of protein-protein interactions in Kaposi's sarcoma-associated herpesvirus (KSHV)

Dissertation
zum Erwerb des Doktorgrades der Medizin
an der Medizinischen Fakultät der
Ludwig-Maximilians-Universität zu München

vorgelegt von

Christine Zeretzke

aus Münster

2006

Mit Genehmigung der Medizinischen Fakultät
der Universität München

Berichterstatter: Priv. Doz. Dr. Dr. J. Haas

Mitberichterstatter: Prof. Dr. M. Volkenandt
                         Prof. Dr. H.-G. Klobeck
                         Prof. Dr. Th. Kirchner

Mitbetreuung durch
den promovierten Mitarbeiter:

Dekan: Prof. Dr. med. D. Reinhardt

Tag der mündlichen Prüfung: 19.10.2006

In Liebe und Dankbarkeit,
meinen Eltern gewidmet

1 ZUSAMMENFASSUNG

Das Kaposi Sarkom assozierte Herpesvirus (KSHV) oder humanes Herpesvirus 8 (HHV-8) ist das zuletzt entdeckte humane Herpesvirus. Es gilt als das infektiöse Agens des Kaposi Sarkoms (KS), des Primary Effusion Lymphoms (PEL) und der Multicentric Castleman's Disease (MCD).

Ähnlich wie andere Spezies der Familie der Herpesviren kodiert es für die vergleichsweise hohe Zahl von mindestens 89 viralen Proteinen. Die meisten von ihnen wurden bisher nicht näher funktionell charakterisiert. Um nähere Informationen über die Funktion dieser Proteine zu erhalten, wurde im Rahmen dieser Studie eine genomweite Analyse von viralen Protein-Protein-Interaktionen durchgeführt. Zu diesem Zweck wurden alle KSHV „open reading frames" kloniert und in einer Yeast two-hybrid (Y2H) Matrix Analyse auf Protein-Protein Interaktionen gescreent. In diesen Screen wurden sowohl komplette Proteine als auch Protein-Fragmente eingefügt, so dass insgesamt mehr als 12.000 virale Protein-Interaktionen getestet und letztlich 125 Protein-Interaktionen identifiziert werden konnten (71 % der bisher bekannten intraviralen Protein-Interaktionen konnten in dieser Studie ebenfalls nachgewiesen werden).

Um die Ergebnisse aus dem Y2H-Screen abzusichern und um ein Set von „high-confidence"-Interaktionen zu generieren, wurden alle positiven Y2H-Interaktionen erneut duch Co-Immunoprezipitationen (Co-IP) getestet. Auf diese Weise konnten zirka 50 % der Interaktionen bestätigt werden.

Die erweiterte bioinformatische Analyse des viralen Protein-Interaktionsnetzwerkes zeigte deutliche Unterschiede zu zellulären Netzwerken auf.

Diese Studie bietet zudem eine Vielzahl neuer biologischer Ansätze an, welche es künftig noch im Detail zu untersuchen gilt.

Weiter könnten diese Untersuchungsergebnisse zu einem vertieften Verständnis der viralen Pathogenese und möglicherweise zu neuen Ansatzpunkten für therapeutische Strategien führen.

1   SUMMARY

Kaposi's Sarcoma Associated Herpesvirus (KSHV) or Human Herpesvirus 8 (HHV-8), which represents the most recently identified human herpesvirus, is considered to be the etiological infectious agent of Kaposi's sarcoma (KS), primary effusion lymphoma (PEL) and multicentric Castleman's disease (MCD).

Similarly to other species of the herpesvirus family, it encodes a rather large number of at least 89 viral proteins, most of which are not functionally characterized. In order to get some hints to the functions of these proteins, the goal of this study was a genome-wide analysis of viral protein-protein interactions. For this purpose, all KSHV open reading frames (ORFs) were cloned and screened for protein-protein interactions in a yeast two-hybrid matrix analysis. In this screen, in which more than 12,000 viral protein interactions involving both full-length proteins and protein fragments were tested, 125 interacting protein pairs were identified (71% of the small number of intraviral protein interactions reported for KSHV were captured). To confirm the quality of the Y2H results and generate a set of high-confidence interactions, all positive Y2H interactions were retested by coimmunoprecipitation (CoIP) and approximately 50% could be confirmed. The extended bioinformatical analysis of the resulting viral protein interaction network including published sequence, functional and expression profiling data revealed marked differences to cellular networks. This study evokes a plethora of novel biological hypotheses which remain to be investigated in detail. It may also lead to an improved understanding of viral pathogenesis and eventually initiate novel therapeutic strategies.

2   INTRODUCTION

2.1   Herpesviridae

Herpesviruses are widely spread throughout vertebrates. Presently, more than 100 different herpesvirus species have been classified, including eight species isolated from man. A herpesvirus virion encompasses a linear double-stranded DNA, which is wrapped on a fibrillar spoole, the core. The core with the associated DNA is protected by a protein shell called capsid. Together, capsid and nucleic acid form the nucleocapsid. The capsid measures about 100 to 110 nm in diameter and is composed of proteins organized in subunits known as capsomers. One capsid consists of 162 capsomers (150 hexameric and 12 pentameric). They form the icosaedric structure of the viral capsid. The nucleocapsid is enclosed by the tegument, a globular material that is frequently asymmetrically distributed and may be variable in amount. The tegument consists of different proteins with varying function. Tegument and capsid are encased by the envelope, a lipoprotein bilayer that may contain material from the membrane of a host cell as well as that of viral origin. The virus obtains the lipid molecules from the cell membrane during the viral budding process.
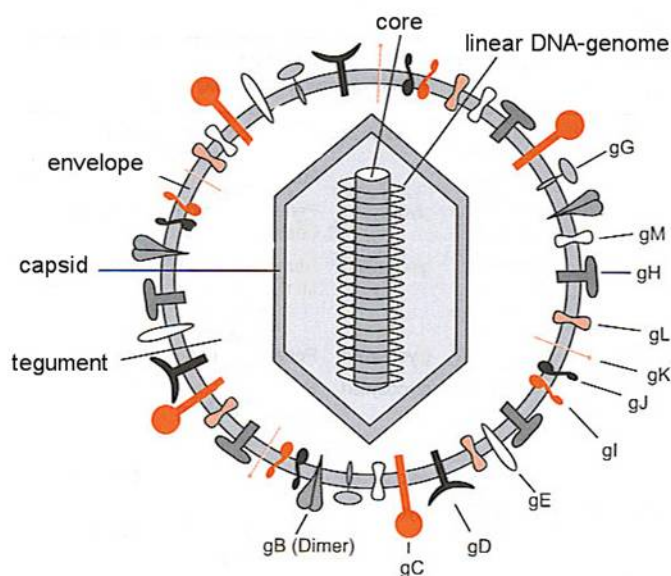
Figure 1:   **The herpesvirus particle**

The virus replaces the proteins in the cell membrane with its own proteins, creating a hybrid structure of cell-derived lipids and virus-derived glycopproteins (spikes) (Figure 1). The size of herpesvirus genomes ranges from 125 000 bp (VZV) to 230 000 bp (CMV) (Chee et al., 1990; Rawlinson et al., 1996), coding for 60 to >170 genes. In all types of herpesviruses, one can find unique and multiple repeat sequences (terminal and internal). Depending on the number of these, genome size of various isolates of a particular virus can vary by up to 10 kbp.

Replication of herpesviruses takes place inside the nucleus. Thus, herpesviruses can use both the host's transcription machinery and DNA repair enzymes to support a large genome with complex arrays of genes (e.g. DNA polymerase, helicase, primase). Genes of herpesviruses are not arranged in operons, and in most cases they have individual promoters. In this regard herpesvirus genes are similar to their eukaryotic hosts, but unlike eukaryotic genes, only view herpesvirus genes are spliced.

As a common feature, herpesviruses are not eliminated after acute infection, but rather persist life-long in their hosts by establishing a latent state. They can reactivate following cellular stress (immunosuppression, UV-light, hormones etc.). Latency involves stable maintenance of the viral genome in the nucleus with limited expression of a small subset of viral genes.

The herpesvirus family is divided into three subfamilies: the *Alphaherpesviridae*, *Betaherpesviridae*, and *Gammaherpesviridae*. This division is based on biological properties of the different members of the herpesvirus family and not solely on their genetic structure (Roizman and Pellet, 2001).

Important characteristics of *Alphaherpesviridae* are a variable host range, relatively short reproductive cycle, a rapid spread in culture, an efficient destruction of infected cells, and the capacity to establish latent infections primarily but not exclusively in sensory ganglia.

Betaherpesviridae are characterized by a more restricted host range, a long reproductive cycle and a slow progress of infection. Infected cells are frequently enlarged (cytomegalia). The virus can be maintained in latent form in secretory glands, lymphoreticular cells, kidneys, and other tissues.

The host range of *Gammaherpesviridae* is even more restricted. *In vitro,* all members of this family replicate in lymphoblastoid cells, and some also cause lytic infections in

some types of epitheloid and lymphoblastic cells. Viruses are specific for either T or B lymphocytes. The latent virus is frequently detected in lyphoid tissue. This subfamily contains two genera: Lymphocryptovirus (EBV) and Rhadinovirus (KSHV, HVS). (Table 1)

Table 1:   Human Herpesviruses

Subfamily	Genera	Viruses	Clinic
Alphaherpesviridae		HHV-1 (Herpes simplex virus 1)	Gingivostomatitis, Conjunctivitis, Keratitis
		HHV-2 (Herpes simplex virus 2)	Herpes genitalis, Herpes neonatorum, a.o.
		HHV-3 (Varicella-zoster virus, VZV)	Varicella, Herpes zoster
Betaherpesviridae		HHV-5 (Human Cytomegalovirus)	congenital infection, infection in immuno-suppressed individuals
		HHV-6A and B (Human B cell lymphotrophic virus)	Roseola infantum
		HHV-7	no clear evidence for a direct involvement of HHV-7 in any human disease
Gammaherpesviridae	*Lymphocryptovirus*	HHV-4 (Epstein-Barr virus, EBV)	infectious mononucleosis, Burkitt's lymphoma, nasopharyngeal carcinoma and others
	Rhadinovirus	**HHV-8 (Kaposi's sarcoma-associated herpesvirus, KSHV)**	**Kaposi's sarcoma, primary effusion lymphoma (PEL), multicentric Castleman's diseases (MCD)**

2.2 The replication cycle of herpesviridae

A herpesvirus infection starts with an interaction of viral envelope-associated glycoproteins with a cellular receptor (adsorption). This interaction results in a fusion of the envelope and cell membrane. Subsequently, the nucleocapsid is released into the cytoplasm, where it migrates to the nucleus. The core enters via a nuclear pore where the genome is circularized. Inside the nucleus transcription and replication takes place. The replicated viral DNA is transferred into capsids. Tegument and envelope are acquired as the virion buds out through the nuclear membrane or endoplasmic reticulum. Virions are transported to the cell membrane via the Golgi complex, and the host cell dies as mature virions are released (Figure 2).
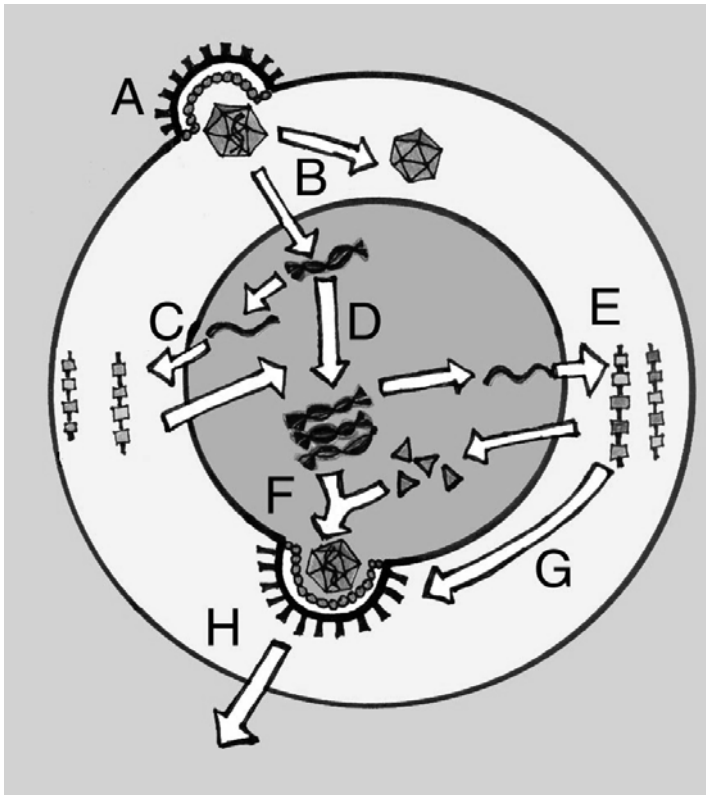
Figure 2:   The herpesvirus replication cycle
A. Viral glycoproteins allow the virus to attach to and enter the cell. The envelope and cell membrane fuse and the viral capsid is released into the cytoplasm. B. Viral DNA enters the nucleus and the capsid is discarded. C. Host enzymes catalyze the early transcription, and viral mRNA directs the production of viral enzymes. D. These enzymes facilitate the replication of viral DNA. E. Late transcription produces the mRNA encoding the production of glycoproteins and capsid elements. F. The capsid components return to the nucleus and the DNA is packaged. G. The glycoproteins fix themselves to the nuclear membrane and the DNA-filled capsid acquires this coat as it buds out of the nucleus. H. The virus is released from the cell by unknown mechanisms. (*According to C. Fowler from Ackerman et al., 1998*)

Viral genes are expressed in a specific order: immediate-early (IE) genes, which encode predominantly regulatory proteins, early genes (E), which mainly encode enzymes for replicating viral DNA, and late genes (L), which encode structural proteins (Honess et al., 1974). Viral DNA replication is the target for a number of successful anti-herpesvirus drugs (e.g. acyclovir, gancyclovir, etc).

2.3   The Kaposi's sarcoma-associated herpesvirus (KSHV)

2.3.1   The Kaposi's sarcoma (KS)

Moritz Kaposi, a Hungarian dermatologist working in Vienna, first described KS lesions in 1872. He published a report portraying the cases of five men with 'idiopathic multiple pigmented sarcoma of the skin' including a patient who had developed visceral disease in the lung and gastrointestinal tract. Two decades later, this 'pigmented sarcoma' was designated Kaposi's sarcoma (KS) at the suggestion of another prominent dermatologist, Heinrich Köbner. It is now referred to as classic KS (Antman and Chang, 2000; Russo et al., 1996)

Before the outbreak of the AIDS epidemic, Kaposi's sarcoma remained a rare curiosity to cancer researchers, predominantly found in men of Mediterranean, Eastern European or Jewish heritage. With the onset of the AIDS epidemic, the Kaposi's sarcoma became the most common malignancy seen in the setting of HIV infection (Ahmed et al., 2001).

Kaposi's sarcoma has four major clinical presentations: classical (chronic), endemic (lymphadenopathic; african), immunosuppression-associated (transplant) and epidemic (AIDS-associated KS). KSHV can be isolated from KS tissue biopsies of all four types. As mentioned, classic KS is mainly found in the lower extremities of elderly men. Most commonly, it runs a relatively benign, indolent course with slow enlargement. Up to one third of the patients with classic KS develop a second primary malignancy, mostly a non-Hodgkin's lymphoma (Reynolds et al., 1965; Safai and Good, 1980a; Safai et al., 1980b).

Lymphadenopathic KS is endemic in prepubescent African children (male/female ratio: 3:1). It occurs as localized or generalized lymphadenopathy. The disease frequently follows a fulminating course with visceral organ involvement and usually

7

minimal skin or mucous membrane involvement (Taylor, 1971; Templeton and Bhana, 1975).

One to four percent of all renal transplant patients and a number of other organ allograft recipients receiving prednisone and azathioprine develop transplantation-associated Kaposi's sarcoma. The average time to develop KS after transplantation is approximately 16 months. The extent and progression of the disease correlates with the loss of cellular immunity of the patient. After reduction or changes of immunosuppressive therapy, KS tumors may regress, suggesting a modulation by the host immune system (Penn, 1978). Transplantation-associated KS often remains localized to the skin, but visceral organ involvement is possible.

Due to the AIDS epidemic, the AIDS-associated KS is currently one of the most common cancers in sub-Saharan Africa. Worldwide, it is the fourth most common cancer caused by an infectious agent – after gastric cancer (Helicobacter pylori), cervical cancer (human papillomavirus) and liver cancer (hepatitis viruses). In contrast to classic KS, AIDS-associated KS is rather aggressive. It often involves skin and mucosal surfaces in visceral organs.

AIDS patients often develop KS as an early sign of the disease. A continuing downtrend in the incidence of KS as an AIDS-defining illness is currently observed (in 1981, 48% of all AIDS patients developed KS, compared to 12% today). This development is probably due to the introduction of highly active antiretroviral therapy (HAART), which may delay and reduce the risk of opportunistic infections (Flexner, 1998; Palella, Jr. et al., 1998; Selik et al., 1987).

The histopathology of all of its clinical subtypes of KS is similar. It is a multifocal neoplasm characterized by dark purple lesions, which contains multiple cell types with the dominant cell being the spindle cell, derived from endothelial origins (Boshoff et al., 1997). In addition, KS lesions contain numerous infiltrating inflammatory cells as well as a profusion of neovascular elements (Monini et al., 1999). Often large numbers of extravasated erythrocytes and abundant hemosiderin deposits can be detected. The lack of a histological obvious neoplastic cell suggests that the disease is not neoplastic *per se*, but rather a hyperproliferative and highly vascularised cell mass (Figure 3).

The observation that KS is present mainly in gay men infected with HIV-1, and not in individuals, who have acquired HIV-1 through a blood transfusion or intravenous drug use, lead the pathologist Yuan Chang and the epidemiologist Patrick Moore to

search for an infectious agent in KS. In co-operation with their colleagues at Columbia University (New York), in 1994 they identified sequences of a new human herpesvirus, which they called KSHV, in an AIDS-KS lesion (Chang et al., 1994; Ensoli et al., 1989).

Similar to EBV, its closest human relative, KSHV infects B lymphocytes and is associated with B-cell lymphomas. KSHV has also been isolated from primary effusion lymphoma (PEL) (Cesarman et al., 1995) and multicentric Castleman's disease (MCD) (Soulier et al., 1995; Chee et al., 1990).

Figure 3:   A Kaposi's sarcoma lesion.
KS lesions show extended areas of brown-blue-red plain maculae and patches with hyperkeratosis and skin ulceration.

2.3.2   The primary effusion lymphoma (PEL)

PEL, or BCBL (body cavity-based lymphomas), is a rare, rapidly fatal, non-Hodgkin's malignancy associated with KSHV infection. It is generally present as a pleural or pericardial effusion without a detectable mass or peripheral lymphoadenopathy. Alternatively, PEL can form a solid mass in the lymph nodes, in the lungs or in the gastrointestinal tract. PEL occurs predominantly in HIV seropositive individuals in advanced stages of immunosuppression, but it is also seen in HIV seronegative patients. Moreover, PEL cells are frequently co-infected with EBV and KSHV, although EBV negative and KSHV- positive PEL have also been described (Arvanitakis et al., 1996).

2.3.3   The multicentric Castleman's disease (MCD)

In contrast to the benign, localized hyperplasia of lymphatic tissue, first described by Castleman, KSHV-associated multicentric Castleman's disease is a highly malignant

lymphoproliferative disease (Castleman et al., 1956; Oksenhendler et al., 1996). It is associated with cytokine dysregulation. In particular IL-6 and IL-10 are elevated (Ablashi et al. 439-64) and closely associated to the KSHV viral load (Oksenhendler et al., 2000).

Half of the patients with MCD do also develop a Kaposi's sarcoma.

KSHV can be detected in most HIV seropositive cases of MCD as well as in approximately 40% of HIV seronegative MCD cases. KSHV positive MCD cases are now recognized as a distinct subset of MCD termed plasmablastic MCD, which contains large plasmablastic cells harbouring KSHV (Dupin et al., 2000). Unlike PEL cells, co-infection by EBV has not been detected in MCD plasmablasts.

2.3.4   The virus particle

The morphological structure of KSHV is typical for a member of the herpesvirus family. The virion of KSHV is approximately 120 to 150 nm in diameter. The electron-dense core is of toroidal shape with the DNA genome wound around a proteinaceous spindle (Renne et al., 1996a).

The icosahedral capsid – consisting of 162 hexagonal capsomeres – surrounds the core. It spans about 125 nm in diameter (Wu et al., 2000). The capsid is surrounded by an amorphous proteinaceous tegument and a lipid bilayer envelope containing numerous glycoproteins (e.g., gB, gD, and gH).

Capsids are composed of four structural proteins: the major capsid protein (MCP / ORF25) forming the hexameric and the pentameric capsomers. One molecule of ORF62 / TRI-1 and two molecules of ORF26 / TRI-2 compose the capsid floor. The small basic capsid protein (ORF65) is associated with the tip of pentons and hexons on the capsid surface (Nealon et al., 2001; Trus et al., 2001). With the exception of the small basic capsid protein, which lacks significant sequence homology to its structural counterparts from the other subfamilies, each of these proteins has significant amino-acid sequence homology to capsid proteins in alpha- and betaherpesviruses. Lytic replication of KSHV leads to the formation of at least three capsid species: A, B, and C. A capsids are empty, B capsids consist of a fifth structural protein, ORF17.5. C capsids contain the viral genome.

2.3.5   The KSHV genome

The KSHV genome encodes >89 open reading frames, many of which are conserved in most herpesviruses. A long unique region of 145 kb is flanked by two terminal repeats consisting of several 801 bp repeat subunits of high G-C content (85%) (Neipel et al., 1997a; Neipel et al., 1997b; Russo et al., 1996). All presently known ORFs are encoded within the long unique region (Figure 4).
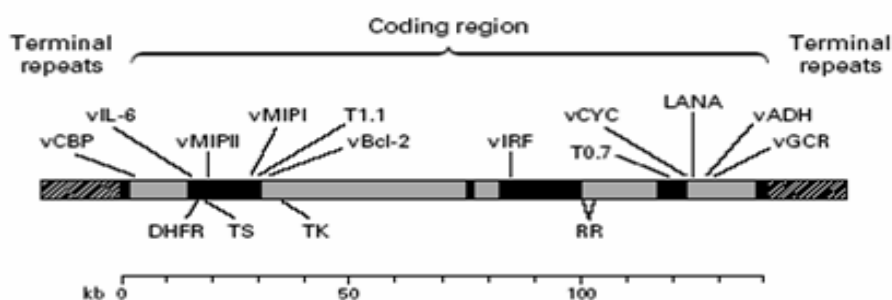
Figure 4:   The 165-kb Kaposi's sarcoma associated herpesvirus (KSHV) genome.
The entire coding region is flanked by terminal-repeat sequences (hatched boxes). The genome encodes numerous proteins that are homologous to cell-signalling and regulatory-pathway proteins found in human cells (solid boxes) and that are unique to KSHV and related rhadinoviruses. The proteins encoded include viral complement-binding protein (vCBP), viral interleukin-6 (vIL-6), viral macrophage inflammatory protein type 1 (vMIPI) and type II (vMIPII), viral Bcl-2 (vBcl-2), viral interferon regulatory factor (vIRF), viral cyclin (vCYC), latency-associated nuclear antigen (LANA), viral adhesin (vADH), G-protein-coupled receptor (vGCR), dihydrofolate reductase (DHFR), thymidylate synthase (TS), thymidine kinase (TK), and ribonucleotide reductase (RR). Stippled boxes indicate regions that are homologous to those of other herpesviruses. T1.1 and T0.7 denote nonhomologous ORFs with undetermined activities. (according to Antman and Chang, New England Journal of Medicine, April 2000)

The sequence analysis of the KSHV genome suggests that it is belonging to the genus Rhadinovirus. Members of this genus share a colinear genomic organisation with each other. The complete sequence of KSHV (GenBank accession numbers U75698 and U 93872) was provided by sequencing viral DNA of a PEL cell line and of KS biopsy specimens (Russo, 1996; Neipel, 1997). It revealed that several blocks of genes are conserved among gammaherpesviruses. These genes are predicted to encode viral replication and structural proteins. Genes that are conserved in all mammalian herpesviruses are taken together in a set of "ancient" genes (McGeoch and Davison, 1999; Simas and Efstathiou, 1998). The gene with the highest intervirus identity is the viral DNA polymerase (ORF9), others are the DNA helicase primase (ORF40, ORF41 and ORF44), the processivity factor (ORF 59), the thymidylate synthase (ORF70), and the thymidine kinase (ORF21).

Between the blocks of conserved genes, there are clusters of genes which are unique for KSHV. Among these unique KSHV genes are several homologues of cellular proteins, which seem to be involved in the control of cell proliferation.

Unique genes are designated with the prefix "K" for KSHV and are numbered sequentially K1 to K15 (Russo et al., 1996).

Although K8 and K13 were subsequently found to have homologues, and additional unique ORFs (K4.1, K4.2, K8.1, K10.1, K10.5, K10.7, K11.1 and K14.1) have since been included.

Later on, more information regarding the gene expression of KSHV became available and additional gene products were detected. Among these rather new open reading frames are K8 (a bZIP protein), K8.1 (a glycoprotein) and K10.5 + K10.7 (latent nuclear antigen-2). These genes were not identified in the first sequence analysis of the KSHV genome because they are encoded by spliced mRNAs.

Current results suggest that KSHV uses mRNA splicing more than any other herpesvirus. Up to 15 KSHV genes are regarded to be regulated by mRNA splicing. As another interesting feature many KSHV transcripts are polycistronic. One of these transcripts is ORF50 / Rta (replication and transcriptional activator) (Gradoville et al., 2000; Lukac et al., 1998; Lukac et al., 1999; Sun et al., 1999). ORF 50 is tricistronic and also encodes the downstream genes K8/K-bZIP/RAP and K8.1 (Gruffat et al., 1999; Lin et al., 1999; Lukac et al., 1998; Seaman et al., 1999; Sun et al., 1998; Sun et al., 1999; Zhu et al., 1999).

A comparison of several recently isolated complete or partial KSHV sequences suggests that K1 and K15 of KSHV, located at the very left and the very right end of the KSHV genome, exhibit greater variability than other KSHV genes studied so far (Lagunoff and Ganem, 1997; Lee et al., 1998; Neipel et al., 1997a; Nicholas et al., 1998; Russo et al., 1996). Based on the analysis of K1 and K15, five KSHV variants (groups A to E) have been identified. Whereas group B is dominant in Africa, groups D and E are confined to Pacific Island and Amerindian populations. In Europe and North America, groups A and C predominate (Schulz, 2000).
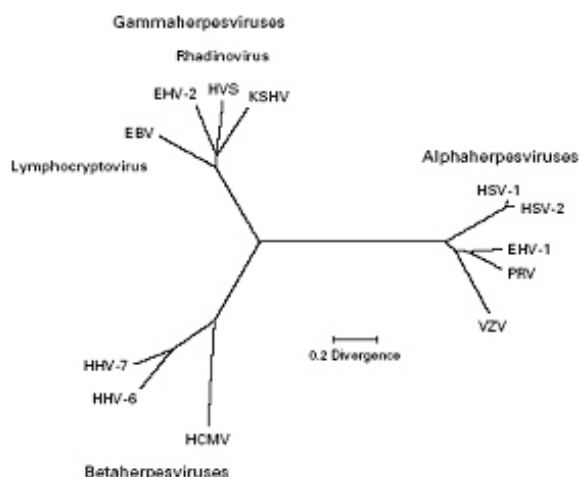
Figure 5:   **Phylogenetic tree**
The tree was constructed based on a comparison of the amino acid sequences of the major capsid protein gene. EBV denotes Epstein-Barr virus, EHV-2 equine herpesvirus type 2, HVS herpesvirus saimiri, HSV herpes simplex virus, HSV-1 herpes simplex virus type 1, HSV-2 herpes simplex virus type 2, EHV-1 equine herpesvirus type 1, PRV pseudorabies virus, VZV varicella-zoster virus, HCMV human cytomegalovirus, HHV-6 human herpesvirus 6, and HHV-7 human herpesvirus 7. (according to Moore et al., 1996)

2.3.6   The life cycle of KSHV

Analogous to other herpesviruses, KSHV can establish a latent or lytic replication. In both states a characteristical set of genes is expressed (Miller et al., 1996; Miller et al., 1997; Renne et al., 1996b; Staskus et al., 1997; Zhong et al., 1996). The classification of individual KSHV ORFs into latent and lytic allows prediction of potential roles of these genes in the pathogenesis of virus infection**.**

The PEL cell lines BCBL, BCP-1, BC-3, and KS-1 (which are free of EBV, HIV and other herpesviruses) have shown to be very beneficial for studies of KSHV. These cells are latently infected with the virus and rarely produce many virus particles. But if they are chemically induced with phorbol myristate acetate (PMA) and butyrate, the virus switches from the latent program to an ordered cascade of lytic gene expression, leading to viral replication, virion production, cell lysis, and viral release (Renne et al., 1996b; Sarid et al., 1998; Zhong et al., 1996)

KSHV, like other members of the gammaherpesvirus subfamily, latently infects B-cells and endothelial cells. Infected cells maintain the virus throughout cellular replication and can immortalize the infected cells (Ganem, 1997). During latent infection, the virus exists as a multicopy circular episomal DNA in the nucleus expressing a subset of viral genes: vIRF1 (K9), vIRF2 (K11), vIRF3 (K10.7), vIRF4

(K10), kaposin (K12), Lana1 (ORF73), FLIP (K13), v-cyc (ORF72), LAMP (K15) (Boshoff et al., 1995).

The majority or KSHV genes remain silent during latent infection. The first groups of genes expressed after the induction of lytic replication are typically regulators of gene expression including the immediate early transactivators ORF50 (Rta), K8 (Zta or K-bZIP), and ORF57 (posttranscriptional regulator of gene expression). These are followed by the expression of sets of genes, involved in replication of the viral DNA (Jenner et al., 2001). The structural genes and those involved in viral expression and maturation are expressed later, generally 24 hours after infection.

Patterns of gene expression were examined by two different kinds of genome-wide approaches. The first one compared the expression patterns of each viral ORF during normal culture of PELs (i.e. latency) to the response of each to TPA treatment and lytic viral induction (Sarid et al., 1998). Class I consisted of constitutively expressed genes, they are considered to be latent transcripts. Class II genes were defined as those that have shown some basal level of transcription that could be further induced by TPA treatment. These are mainly immediate-early, or early, viral transcripts. The third class of viral genes are only inducible by TPA. These genes typically encode late genes, which are associated with viral replication.

More recent approaches are based on DNA microarrays which permit a simultaneous comparison of the transcription kinetics of virtually all KSHV genes (Dittmer, 2003; Jenner et al., 2001; Paulose-Murphy et al., 2001).

2.4   The KSHV Y2H screen

2.4.1   From sequencing to understanding

Large-scale sequencing projects provide new insight into the function of viral proteins which have not been characterized before. The sequence alone sheds little or no light on their function. Thus the development of standardized functional assays has become necessary. Such approaches are referred to as 'functional genomics'. One approach to investigate the properties of a genome is the systematic analysis of protein-protein interactions which are essential for the structural and functional organization of the cell. The most common system used for the identification of novel interactions is the yeast two-hybrid system.

Although complications from false negative and false positive results, protein-protein interactions derived from Y2H screens contribute to the understanding of molecular processes, for at least four reasons: first, the interaction of an unknown protein, with proteins of known function can lead to a tentative assignment of a function to the unknown protein. Second, multiple interactions between a set of proteins belonging to the same functional group can hint at molecular mechanisms. Third, interactions can also occur between orthologous proteins of related organisms. Such protein pairs have been termed 'interlogs'. Fourth, starting from the interaction results, maps can be generated depicting complicated networks of proteins interacting with several other partners.

Here, we report the examination of two-hybrid interactions in all possible pairwise combinations between proteins of KSHV.

2.4.2   The yeast two-hybrid system

The basic concept of the yeast two-hybrid system is to detect the interaction between two proteins via transcriptional activation of one or several reporter genes. A classical eukaryotic transcription activator contains a domain that specifically binds to DNA sequences (the binding domain, BD) and a domain that recruits the transcription machinery (the activation domain, AD). In the two-hybrid system, these two domains are both fused to a polypeptide, X and Y, respectively. The resulting fusion proteins are directed into the yeast nucleus.

The reporter genes will only be transcribed if X and Y interact with each other (Figure 6).
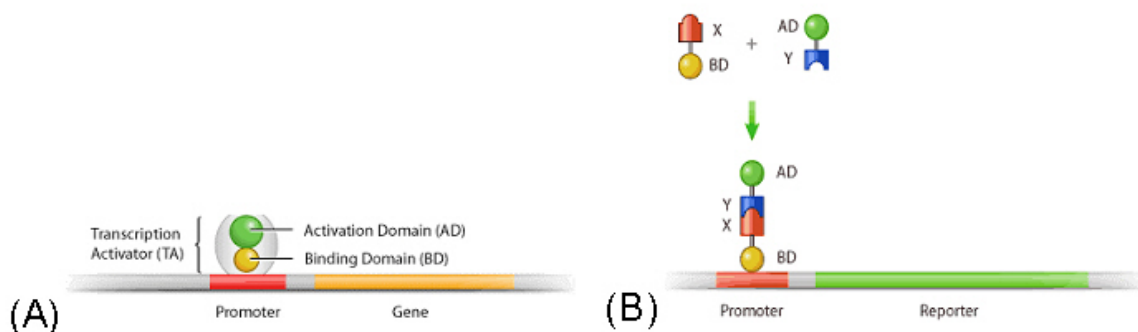
Figure 6   Transcriptional activation by the Y2H system.
(A) Normal transcription. (B) Y2H transcription (according to Jiang Long)

15

2.4.3   Libraires versus arrays

The two-hybrid system was originally intended to detect interactions between characterized proteins (Fields and Song, 1989). Quickly, it became clear that the system could be used to identify new interactions when expression libraries were screened. This has typically been done by screening a protein of interest fused to the DNA-binding domain against cells expressing a random cDNA library of potential protein partners fused to the activation domain, and applying a genetic selection for interaction. Plasmid DNA is recovered from cells expressing interacting proteins, and their identities are determined by DNA sequencing. Potential interaction partners obtained are frequently retrieved as fragments, since AD-cDNA fusion libraries are generated by reverse transcription and therefore do not exclusively contain full-length ORFs. The AD-cDNA approach possesses the advantage of partially defining the region of the AD protein required for the interaction.

An alternative two-hybrid 'matrix' approach is to test all possible pairwise protein combinations in order to identify interacting partners. A set consisting of defined ORFs is often referred to as an 'array' or, in case it deals with a whole genome, as an 'ORFeome'. These arrays are fused to BD as well as AD, BD fusions and AD fusions are transformed into yeast of opposite mating types (Mat a and Mat α, respectively). Each pairwise combination of BD and AD fusions is generated by mating and examined on the expression of reporter genes.

Arrays have the advantage that many tests can be performed under identical conditions at the same time. The results of these colonies, expressing a defined pair of proteins, can be compared directly. In addition, since arrays allow the rapid identification of positive interactions by their position, it is not necessary to sequence them as in a library screen.

We constructed a 'KSHV-ORFeome', consisting of all full length ORFs and several protein domains of KSHV. These ORFs are easily transferable to various vector types. Thus, the ORFeome is not only available to the yeast two-hybrid system, but also to studies on a variety of other topics including the expression of recombinant proteins.

2.4.4   Genome-wide yeast two-hybrid screens

Genome-wide protein-protein analyses have been performed in few organisms, including yeast (Uetz et al., 2000), *helicobacter pylori* (Rain et al., 2001), *C. elegans* (Reboul et al., 2003) and *D. melanogaster* (Giot et al., 2003).

Two papers describe large-scale approaches to detect protein-protein interactions in yeast using sets of predefined open reading frames. The ultimate aim was to test all possible combinations between annotated ORFs of *Saccharomyces cerevisiae* (i.e. 4 x 107 combinations). In one case, PCR products were cloned into BD and AD vectors, transformed into BD and AD vectors and then transformed into yeast cells of the opposite mating type (Ito et al., 2000). In the second strategy, PCR products were co-transformed with linear plasmids into yeast cells and gap repair occurred *in vivo* (Uetz et al., 2000). Ultimately, yeast cells transformed with BD fusion plasmids or AD fusion plasmids were collected, stored and assayed individually or in pools. A common intrinsic limitation of this strategy is to test only full-length proteins that were predefined.

In 2001, Rain and colleagues performed another large-scale screen on *Heliobacter pylori* (Rain et al., 2001). They assayed 261 *H. pylori* proteins against a library of genome-encoded polypeptides. Over 1200 interactions were identified, connecting 46.6% of the proteome.

An even more complex organism, which has been screened in various ways, is the nematode *Caenorhabditis elegans*. This model organism was analyzed by several groups using a combination of DNA microarray, yeast two-hybrid analysis, and RNA interference (RNAi).

The first yeast two-hybrid assays, focused on defined biological processes in *C.elegans*. Walhout and colleagues studied the vulval development in *C. elegans* by using a small array of 29 proteins (Walhout et al., 2000).

Other aspects studied in *C.elegans* by the yeast two-hybrid system were the DNA damage response (DDR) pathway (Boulton et al., 2002) and components of the 26S proteasome (Davy et al., 2001).

By now, Reboul and colleagues have generated a set of reference clones for most predicted ORFs in the *C. elegans* genome (Reboul et al., 2003). In this study, they also used Recombinatorial Cloning (GATEWAY), similar to the study presented here.

2.4.5   Yeast two-hybrid screens for viral protein interactions

Surprisingly, few viral genomes have been studied systematically for protein interactions, although their small size makes them an ideal target for such approaches. The first organism screened was the T7 bacteriophage (Bartel et al., 1996). A library of random T7 protein fragments against random libraries of T7 activation domain fusions. Among the 55 phage proteins, the authors found 25 interactions, including four that had been described previously.

Several RNA viruses express a precursor polyprotein which is fractionized into a couple of mature viral proteins either autocatalytically or by cellular proteases. The translation of the precursor polyprotein and its cleavage is obligatory for correct folding and processing of the mature proteins. Individually expressed mature proteins may not be processed correctly (Flajolet et al., 2000). Thus, it is no surprise that testing such mature proteins for pairwise interactions has not been very successfully. Neither in *hepatitis C virus* (HCV), nor in *wheat streak mosaic virus* (WSMV) interactions between mature proteins have been detected by two-hybrid assays (Choi et al., 2000a; Flajolet et al., 2000). In contrast, testing of random fragments resulted in the detection of a number of interactions. Apart from incorrect processing, an alternative explanation for this phenomenon might be that only certain protein fragments can efficiently act in conjunction with a fused activation or binding domain. Therefore the interaction can only be detected if these fragments are used. In WSMV, which belongs to the filamentous potyvirus (+) strand RNA virus family, the polyprotein precursor is cleved into nine mature proteins. When Choi and colleagues tested the mature proteins by two-hybrid assays, they could not observe any heterologous interactions, but when random fragments were used, multiple interactions were detected: the proteins P1, HC-Pro, P3 and CI interacted with each other in all possible combinations. Interactions involving the P3 protein could only be detected in *in vitro* assays, but not in yeast.

According observations have been made in HCV, a flavivirus (+) strand RNA virus: by testing full-length proteins in a two-hybrid assay no interactions could be detected (Flajolet et al., 2000). In contrast, by screening of random fragments five interactions were observed, such as the known interaction between the capsid homodimer and the protease dimer and between the nonstructural proteins NS3 and NS4a, as well as multiple novel interactions such as between NS2 and NS4a.

However, expression and processing of polyproteins is not necessary for all interactions to be detected among processed RNA virus proteins. In both *pea seed-borne mosaic virus* (PsbMV) and *potato virus A*, which belong to the potyvirus (+) strand RNA virus family similar to WSMV (Guo et al., 2001), as well as in a subset of poliovirus proteins (Cuconati et al., 1998), interactions have been detected among cloned mature proteins.

Recently, Fields and colleagues reported a protein-protein interaction screen of a member of the poxvirus family, which constitute the other known family of large DNA viruses. It is thus far the largest virus screen performed in a systematic way for protein interactions. This array screen was performed with 266 genes from vaccinia virus, The screen of about 70 000 protein pairs revealed only 37 protein-protein interactions of which 13 (35%) were self interactions (i.e. homodimers or homomultimers). Of the 24 remaining interactions, five (i.e., 13.5%) were detected in both orientations, i.e., with the two proteins as both bait and prey construct (McCraith et al., 2000). Thus two-hybrid screens should always include all possible combinations with every protein as bait and prey construct (for N proteins this requires N^2 combinations and not just $N^2/2$). Double-checking each pair not only confirms each combination but also avoids false negative interactions if one of the two partners is a transcriptional activator and therefore cannot be used as a bait. One of the reasons for the small number of interactions detected in vaccinia virus may be caused by the fact that vaccinia virus replication and transcription take place in the cytoplasm. This means, that viral splicing signals have not been eliminated in the course of evolution. If these sequences are expressed in the nucleus of eukaryotic cells from transfected plasmids, a considerable number of transcripts may be artificially spliced and the proteins encoded either disrupted or structurally altered. In fact, 282 putative introns were found in the Vaccinia genome. That is more than one putative intron per ORF (Uetz et al., 2004). Another disadvantage of the Vaccinia screen might be that transmembrane proteins were only expressed as full-length proteins. The two-hybrid system bases on an interaction of bait and prey fusion proteins in the nucleus, thus membrane-anchored may have contributed to the large number of interactions not detected in this study.

However, protein-protein interaction maps have not been reported for any member of the herpesvirus family yet. Large DNA viruses contain approximately one order of magnitude fewer genes than eubacteria and are thus particularly well suited for

genome-wide analyses. Herpesviral replication, transcription, and capsid assembly occur in the nucleus, and herpesviral transcripts can be spliced similarly to host mRNAs.

The limited number of genes makes it possible to combine the results of several genome-wide functional screens focusing on different aspects.

Several protein interactions have been shown before for KSHV, for example the interaction between the two capsid proteins ORF25 and ORF65, as well as the protein interaction between the immediate early transcriptional activator ORF57 (RTA) and ORF50. In addition, a reasonable number of protein interactions have been predicted, for example the interaction between different DNA packaging and tegument proteins.

2.5 Topology of protein interaction networks

2.5.1 Scale-free networks

Complex networks are rarely connected randomly. Most complex networks fall under the category scale-free network. Scale-free networks are characterized by an uneven distribution of connectedness. Some nodes are "highly connected hubs", but most nodes only have one or few interaction partners (Figure 7).

(a) Random network (b) Scale-free network
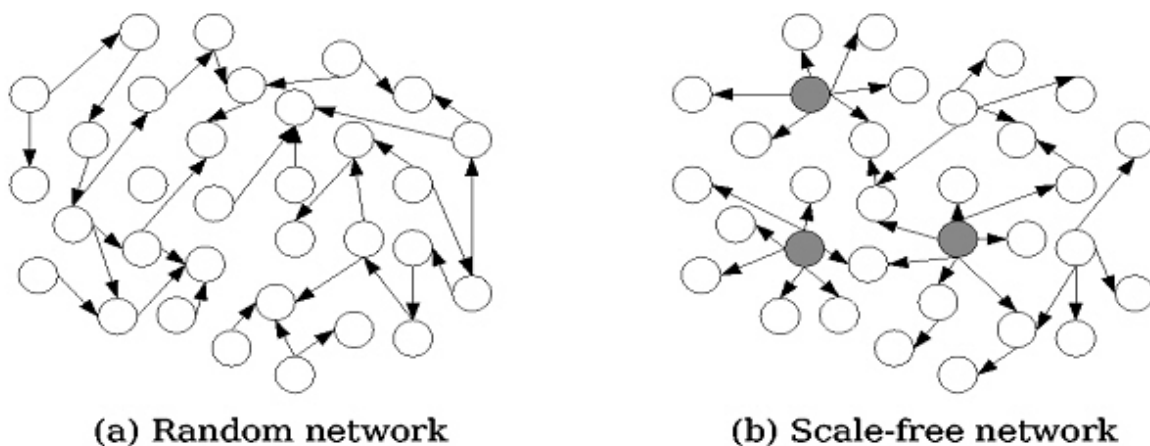
Figure 7: Scale-free and random networks:
Most complex networks, such as airline traffic routes, weblog links and terrorist networks are scale-free networks, since few hubs are far more connected than other nodes.

The term "scale-free" was established by Albert-Laszlo Barabasi and his colleagues (Barabasi and Albert, 1999). In 1999, they mapped the connectedness of the World

Wide Web and found that the the structure of the Web did not conform to the model of random connectivity, but that few nodes were far more connected than others. They found that scale-free networks follow a so-called power law distribution, what means that the probability P(k) that a node connects with k other nodes is proportional to k^{-y}, what means that there is no specific number of links per node, but that there are many nodes with few links and some nodes with many interaction partners. Such highly connected nodes are called hubs. Scale-free networks have been used to explain networks as diverse as those of social networks, cancerous cells, the dispersal of sexually transmitted disease and protein interaction networks.

A strength of scale-free networks is that a random node failure has very little effect on its connectivity or effectiveness, while in random networks a small number of random failures can collapse the network.

The weakness of scale-free networks is that they fail, when they stand under intentional attack on their hubs. If a certain number of the hubs are eliminated simultaneously, the network will collapse. Simultaneity of the attacks is important, because scale-free networks are able to heal themselves rapidly if only an insufficient number of hubs are removed.

Cellular protein interaction networks exist for several model organisms. It has been found that their degree distribution follows a power-law decay and they exhibit thus scale-free properties. Here, we establish the first viral protein network and examine topology and behaviour in comparison to known cellular networks

2.5.2   The small world phenomenon

The expression "small world phenomenon" was originally coined by Stanley Milgram, a sociologist, who published in 1967 the hypothesis that two random US citizens were connected by an average of six acquaintances (Milgram, 1967). The concept gave rise to the famous phrase "six degrees of separation". Although there was some doubt to whether the "whole world" was a small world, it became matter of fact that there is a large number of small worlds within most complex networks.

Since then, a number of studies have dealt with the problem more analytically. Watts and Strongatz formulated the expression "small world networks" by analogy with Milgram's "small world phenomenon" (Watts and Strongatz, 1998). They provided evidence that small-world properties are arising in a multitude of physical and biological networks.

Small-world networks can be found at the boundary between regular networks, like lattices, and random networks. A small-world network can be created out of a regular network by rewiring of a few short cuts.

Small world networks are characterized by a short average path length or distance between two nodes (also named the diameter of a network). The distance between two nodes is defined as the number of edges along the shortest pathway connecting them.

Another typical property of these networks is their high clustering coefficient. High clustering implies that, if a node A is linked to node B, and B is linked to node C, there is an increased probability that A will also be linked to C. In contrast, linking with a distant node is relatively rare. We distinguish between a local and a global "clustering coefficient". The local clustering-coefficient C measures to how many links one node is connected, in comparison to the maximal number of connections. It is 1 if the node is connected to all neighbors and 0, if it is not connected.

The global clustering coefficient measures the linking of a whole network. It is 1, if each node is connected to every other node.

All known cellular protein interaction networks display small-world properties. In this work the characteristics of a viral network have been examined.

2.6   Aims of this project

Herpesviruses possess a large double-stranded DNA genome encoding approximately 80 to 160 viral proteins. The function of the majority of viral proteins is currently not or only poorly understood. In particular, very little is known about how these proteins interact and are attuned to each other. The aims of this study were (i) to generate a set of plasmids representing the KSHV ORFeome by recombinatorial cloning, (ii) to perform a yeast two-hybrid matrix screen (iii) iv) to verify positive Y2H interactions by co-immunoprecipitation and (iv) to perform a bioinformatical analysis of the results received.

.

3 MATERIAL AND METHODS

3.1 Materials

3.1.1 Equipment

Bacterial Shaker	Kühner, Bürsfelden, Switzerland
Balances	Sartorius, Göttingen, Germany
Centrifuge GP	Beckman, Palo Alto, USA
Centrifuge J2-21	Beckman, Palo Alto, USA
Centrifuge Varifuge 3.0R	Heraeus, Hanau, Germany
Centrifuge Minifuge RF	Heraeus, Hanau, Germany
Centrifuge Labofuge T	Heraeus, Hanau, Germany
Centrifuge, refrigerated and non-refrigerated	Heraeus, Hanau, Germany
Eagle Eye	Stratagene, Amsterdam, The Netherlands
Film Developing Machine	Optimax Typ TR MS Laborgeräte, Heidelberg, Germany
Fluorescence/light Microscope Axiovert 35	Zeiss, Oberkochen, Germany
Fluorescence/light Microscope Axiovert 200M	Zeiss, Oberkochen, Germany
Fridge (4°C)	Liebherr, Ochsenhausen, Germany
Freezer (-20°C)	Liebherr, Ochsenhausen, Germany
Freezer (-80°C)	Forma Scientific, Inc., Marietta, Ohio, USA
Cryo 1°C Freezing Container	Nalgene Nunc, Wiesbaden, Germany
Gel Dryer	Bio-Rad, Munich, Germany
GelAir Drying System	Bio-Rad, Munich, Germany
Incubators for Cell Culture (37°C)	Forma Scientific, Inc., Marietta, Ohio, USA
Inverted Microscope TMS	Nikon, Düsseldorf, Germany
Laminar Flow Hood Steril Gard II A/B3	The Baker Company, Sanford, Maine,USA
Magnetic Stirrer with heating block	Janke & Kunkel, Staufen, Germany
Microwave	AEG, Berlin, Germany

PCR Thermal Cycler GeneAmp 2400	Perkin Elmer, Weiterstadt, Germany
pH-Meter	WTW, Weilheim, Germany
Photometer Gene Quant II	Pharmacia/LKB, Freiburg, Germany
Pipettes	Gilson, Villies Le Bel, France;
	EppendORF, Hamburg, Germany
Pipetting Aid	Technomara, Zürich, Switzerland
Electrophoresis Power supply EPS200	Amersham-Pharmacia, Freiburg, Germany
Overhead Mixer	Heidolph, Schwabach, Germany
384-Pin Replicator	Nalge Nunc International
Robotic Workstation	Biomek 2000, Beckman Coulter
Sonifier 450	Branson Ultrasonics Corp., Danbury, USA
Thermomixer	Eppendorf, Hamburg, Germany
UV-Transilluminator (366 nm)	Vetter, Wiesloch, Germany
(254 nm)	Konrad Benda, Wiesloch, Germany
Vortex Mixer	IKA Works, Inc, Wirmington, USA
Water Bath	Julabo, Seelbach, Germany
	GFL, Burgwedel, Germany

3.1.2 Chemicals

Acetic Acid	Roth, Karlsruhe, Germany
Acrylamide/Bisacrylamide 37,5/1 (Rotiphorese Gel 30)	Roth, Karlsruhe, Germany
Agar for plates	Gibco BRL, Karlsruhe, Germany
Agarose Electrophoresis Grade	Invitrogen, Karlsruhe, Germany
Ammonium Persulfate (APS)	Sigma, Munich, Germany
Ampicillin	Roche Diagnostics, Mannheim, Germany
Bacto Peptone	BD Biosciences Clontech, Heidelberg, Germany
Bacto Tryptone	BD Biosciences Clontech, Heidelberg, Germany
Bacto Yeast Extract	BD Biosciences Clontech, Heidelberg,

	Germany
Bicine	Sigma, Munich, Germany
Bromophenol Blue	Serva, Heidelberg, Germany
BSA (Bovine Serum Albumin)	Sigma, Munich, Germany
Calcium Chloride	Merck, Darmstadt, Germany
Chloramphenicole	Sigma, Munich, Germany
Coomassie Brilliant Blue R-250	Bio-Rad, Munich, Germany
Dextrose	BD Biosciences Clontech, Heidelberg, Germany
Dimethylsulfoxid (DMSO)	Merck, Darmstadt, Germany
Dithiothreitol (DTT)	Roth, Karlsruhe, Germany
dNTPs	Roche Diagnostics, Mannheim, Germany
Dulbecco's modified Eagle's medium (DMEM)	Gibco BRL, Karlsruhe, Germany
Ethanol (EtOH)	Riedel-de Haën, Seelze, Germany
Ethidium Bromide	Sigma, Munich, Germany
Ethylendiamintetraacetate Disodium Salt (EDTA)	Roth, Karlsruhe, Germany
Ethylene Glycol	Sigma, Munich, Germany
Fetal Calf Serum (FCS)	Gibco BRL, Karlsruhe, Germany
Gentamycin	Serva, Heidelberg, Germany
Glucose	Merck, Darmstadt, Germany
Glutathione-Sepharose 4B	Amersham-Pharmacia, Freiburg, Germany
Glycerol	Roth, Karlsruhe, Germany
Glycine	Serva, Heidelberg, Germany
Histogel	Linaris, Wertheim-Bettingen, Germany
Hydrochloric Acid (HCl)	Merck, Darmstadt, Germany
Imidazole	Fluka, Seelze, Germany
Isopropanol	Riedel-de Haën, Seelze, Germany
Isopropylthio-b-D-galactosid (IPTG)	Roth, Karlsruhe, Germany
Kanamycin	Serva, Heidelberg, Germany
L-Glutamine	Gibco BRL, Karlsruhe, Germany

L-Glutathione (reduced)	Merck, Darmstadt, Germany
L-Glutathione (oxidized)	Fluka, Seelze, Germany
Magnesium Chloride	Merck, Darmstadt, Germany
Magnesium Sulfate	Merck, Darmstadt, Germany
2-Mercaptoethanol	Merck, Darmstadt, Germany
Methanol	Merck, Darmstadt, Germany
Nonidet P40 (NP-40)	Fluka, Seelze, Germany
Pefabloc	Roche Diagnostics, Mannheim, Germany
Polyethylene Glycol (PEG 1000)	Sigma, Munich, Germany
Penicillin-Streptomycin	Gibco BRL, Karlsruhe, Germany
Phenylmethylsulfonfluoride (PMSF)	Roche Diagnostics, Mannheim, Germany
Phosphate Buffered Saline (PBS)	Dulbecco's Gibco BRL, Karlsruhe, Germany
Ponceau S	Sigma, Munich, Germany
Potassium Acetate	Riedel-de Haën, Seelze, Germany
Potassium Chloride	Merck, Darmstadt, Germany
Potassium Phosphate Salts	Merck, Darmstadt, Germany
Protein G Sepharose Fast Flow	Amersham-Pharmacia, Freiburg, Germany
RPMI (Rosswell Park Memorial Institute)1640	Gibco BRL, Karlsruhe, Germany
SD Base Medium	BD Biosciences Clontech, Heidelberg, Germany
Skim Milk Powder	Merck, Darmstadt, Germany
Sodium Acetate	Riedel-de Haën, Seelze, Germany
Sodium Azide	Serva, Heidelberg, Germany
Sodium Borate	Merck, Darmstadt, Germany
Sodium Chloride	Riedel-de Haën, Seelze, Germany
Sodium Thiosulfate	Merck, Darmstadt, Germany
Sodium Codecylsulfat (SDS)	Merck, Darmstadt, Germany
Sodium Carbonate	Merck, Darmstadt, Germany
Sodium Hydroxid	J.T.Baker B.V., Deventer, Holland
Sodium Phospate salts	Merck, Darmstadt, Germany

Tetramethylethylendiamin (TEMED)   Amersham-Pharmacia, Freiburg, Germany

12-O-tetradecanoylphorbol-13-acetate (TPA)   Sigma, Munich, Germany

Tris(hydroxymethyl)aminomethan (Tris)   Roth, Karlsruhe, Germany

Triton X-100   Serva, Heidelberg, Germany

Trypsin   Gibco BRL, Karlsruhe, Germany

Tween 20   Merck, Darmstadt, Germany

Urea   Roth, Karlsruhe, Germany

3.1.3   Additional materials

Autoradiography Films BIOMAX-MR   Eastman-Kodak, Rochester, USA

Cell Culture Plastic Ware   Greiner, Nürtingen, Germany

                                          Nunc, Wiesbaden, Germany

                                          Falcon/Becton Dickinson, Heidelberg,
                                          Germany

Filter Paper (3 mm)   Whatman Ltd., Maidstone, England

Glass Slides for IF   Marienfeld, Bad Mergentheim,
                                          Germany

Protran Nitrocellulose Transfer Membranes   Schleicher & Schuell, Dassel,
                                          Germany

Sterile Filter Units   Millipore

Single-well Microtiter Plates   Omnitray; Nalge Nunc International

3.1.4   Cell lines

293   human embryonal kidney cell line (ATCC: CRL-1573)

HeLa   human cervix carcinoma (ATCC :CCL-2)

BCBL-1   body cavity-based lymphoma cell line, kindly provided by
                        Dr. Don Ganem, USCF, San Francisco, USA

3.1.5   Recombinant vaccinia viruses

Recombinant vaccinia virus vTF-7 expressing T7 polymerase was provided by the NIH AIDS reagent program (Fuerst et al., 1986).

3.1.6 Bacterial strains

DH5a   Invitrogen, Karlsruhe, Germany

Genotype: F⁻ φ80d*lacZ*ΔM15 *endA1 recA1 hsdR17* (r$_k$⁻ m$_k$⁺) *supE44 thi-1* λ⁻ *gyrA96 relA1* Δ(*lacIZYA-argF*)*U169*

DB3.1   Invitrogen, Karlsruhe, Germany

Genotype: F⁻ *gyr*A462 *end*A .(*s*r1-*re*cA) *mc*rB *mrr hs*dS20 (r B - m B -) *su*pE44 *ar*a14 *ga*lK2 *la*cY1 *pro*A2 *rp*sL20(Str R) *xyl*5 ë - *leu mt*l1

DH10B   Invitrogen, Karlsruhe, Germany

Genotype: F⁻ *mcr*A Δ(*mrr-hsdRMS-mcrBC*) φ80d*lacZ*ΔM15 Δ*lacX74 deoR recA1 araD139* Δ(*ara leu*)7697 *galU galK rpsL endA1 nupG*

Top10:   Invitrogen, Karlsruhe, Germany

Genotype: F⁻, *mcr*A, Δ(*mrr-hsd*RMS-*mcr*BC), φ80*lacZ*ΔM15Δ*lac*X74, *deo*R, *rec*A1, *ara*D139 D(*ara-leu*)7697, *gal*K, *rps*L(StrR), *end*A1, *nup*G .

3.1.7 Yeast strains

AH109   BD Biosciences Clontech, Heidelberg, Germany

Genotype: MAT a, trp1-901, leu2-3, 112, ura3-52, his 3-200, gal4Δ, LYS2 : : GAL1$_{UAS}$-GAL1$_{TATA}$-HIS3, GAL2$_{UAS}$-GAL2$_{TATA}$-ADE2, URA3 : : MEL1$_{UAS}$-MEL1$_{TATA}$-lacZ

Y187   BD Biosciences Clontech, Heidelberg, Germany

Genotype: MATα, ura3-52, his3-200, ade2-101, trp 1-901, leu2-3, 112, gal4Δ, met⁻, gal 80Δ, URA3 : : GAL1$_{UAS}$-GAL1$_{TATA}$-lacZ
(Harper et al., 1993)

3.1.8 Plasmids

pGADT7 (Ap^r)   BD Biosciences Clontech, Heidelberg, Germany
pGBKT7 (Km^r)   BD Biosciences Clontech, Heidelberg, Germany
pDONR207 (Gm^r)   Invitrogen, Karlsruhe, Germany

- HA epitope tag
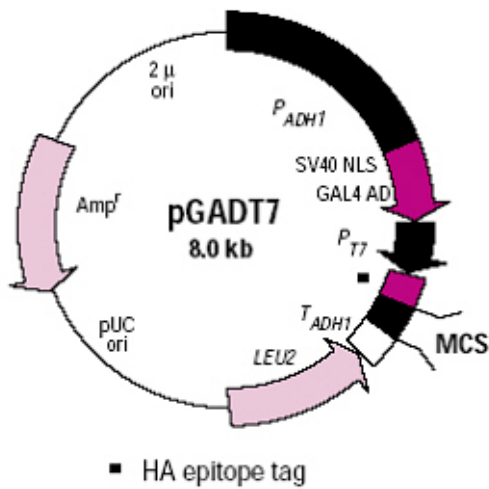
Figure 8a: Map of the pGADT7 vector.
pGADT7 consists of an ampicilin resistance gene for selection in E.coli and the LEU2 nutritional marker for selection in yeast. In yeast, pGADT7 expresses a protein of interest as a GAL4 activation domain (GAL4 AD) fusion. Transcription starts with the constitutive ADH1 promoter (P_{ADH1}) and ends with the ADH1 termination signal (T_{ADH1}). The GAL4 AD sequence includes the SV40 nuclear localization signal (SV40 NLS; 1) so that fusions translocate to the yeast nucleus. GAL4 AD fusions also contain a hemagglutinin (HA) epitope tag for identification with HA-Tag antibody.

▲ c-Myc epitope tag
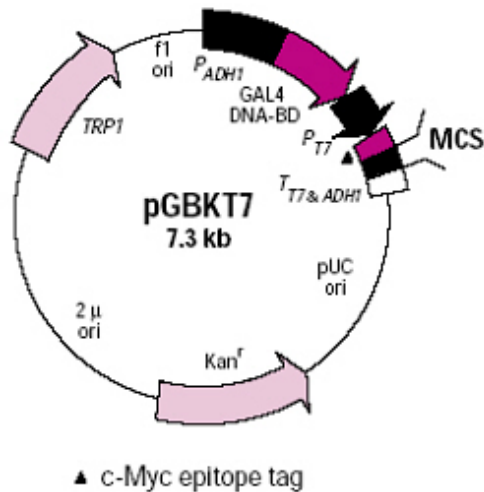
Figure 8b: Map of the pGBKT7 vector.
GBKT7 carries a kanamycin resistance for selection in E. coli and the TRP1 nutritional marker for selection in yeast. The pGBKT7 vector expresses proteins fused to the GAL4 DNA binding domain (DNA-BD). In yeast, fusion proteins are expressed from the constitutive ADH1 promoter (P_{ADH1}); transcription is terminated by the T7 and ADH1 transcription termination signals ($T_{T7\,\&\,ADH1}$). pGBKT7 also contains the T7 promoter, a c-Myc epitope tag and the SV40 nuclear localization signal (SV40 NLS)

The DNA-BD and AD fusion vectors pGBKT7 and pGADT7 express fusion proteins at high levels to make even weak and transient protein interactions detectable. pGADT7 and pGBKT7 express different bacterial selection markers to simplify their independent isolation in E.coli. Bait and prey inserts are expressed as GAL 4 fusions with c-Myc and hemagglutinin (HA) tags, respectively. The epitope tags eliminate the need to generate specific antibodies for each new protein. The T7 promoter is included to facilitate *in vitro* transcription and translation of the epitope-tagged bait and prey proteins. The T7 promotor was also used as priming site for DNA sequencing. It can also be used to express the insert in mammalian cells expressing the T7 RNA polymerase, for example by infection with recombinant vaccinia virus.

3.1.9 Oligonucleotides

Genes that encode for glycoproteins were amplified in three versions: as a full length (FL) product, as cytoplasmatic (cyt/d2) and external (ext/d1) domain. For genes that undergo splicing events, BC-1 RNA or plasmid DNA was used as template.

Table 2:   KSHV ORFs and Oligonucleotides

ORF	Size	*Template*		Primer- Sequence
K1 (FL)	860 bp	BC-1, gDNA *	for	AAAAAGCAGGCTCCGCCATGTTCCTGTATGTTGTCTGC
			rev	AGAAAGCTGGGTTCAGTACCAATCCACTGGTTGC
K1 cyt	113 bp	BC-1, gDNA	for	AAAAAGCAGGCTCCGCCCATTGTCAAAAACAACGTGAC
			rev	AGAAAGCTGGGTTCAGTACCAATCCACTGGTTGC
K1 ext	693 bp	BC-1, gDNA	for	AAAAAGCAGGCTCCGCCATGTTCCTGTATGTTGTCTGC
			rev	AGAAAGCTGGGTTATACAAGAAAATGCACTTCAAT
ORF 4	1653 bp	BCBL-1, gDNA *	for	GGGGACAAGTTTGTACAAAAAAGCAGGCTCCGCCATGGCCTTTTTAAGACAAAC
			rev	GGGGACCACTTTGTACAAGAAAGCTGGGTGCTAACGAAAGAACAGATAG
ORF 6 I	1800 bp	BC-1, gDNA	for	AAAAAGCAGGCTCCATGGCGCTAAAGGGACCAC
			rev	AGAAAGCTGGGTTAATGGACGGATTTGATGTTCTCTG
ORF 7	2088 bp	BCBL-1, gDNA	for	AAAAAGCAGGCTCCGCCATGGCAAAGGAACTGGCGGCG
			rev	AGAAAGCTGGGTCTAGACCTGGGAGTCATTGTGG
ORF 8 cyt	180 bp	BAC **	for	GGGGACAAGTTTGTACAAAAAAGCAGGCTCCGCCCGCCGCACCAATACCATAGC
			rev	GGGGACCACTTTGTACAAGAAAGCTGGGTGTCACTCCCCCGTTCCGG
ORF 9	3039 bp	BC-1, gDNA	for	AAAAAGCAGGCTCCGCCATGGATTTTTTCAATCCATTTATC
			rev	AGAAAGCTGGGTCTAGGGCGTGGGAAAAGTC
ORF 10	1257 bp	BAC	for	GGGGACAAGTTTGTACAAAAAAGCAGGCTCCGCCATGCAGACAGAGGCAACG

			rev	GGGGACCACTTTGTACAAGAAAGCTGGGTGTCACGATTGCATGGGTTC
ORF 11	1224 bp	BAC	for	GGGGACAAGTTTGTACAAAAAAGCAGGCTCCGCCATGGCGCAGGAGTCAGAG
			rev	GGGGACCACTTTGTACAAGAAAGCTGGGTGCTAACTGCGTCCGGTGGC
K 2	615 bp	BAC	for	GGGGACAAGTTTGTACAAAAAAGCAGGCTCCGCCATGTGCTGGTTCAAGTTG
			rev	GGGGACCACTTTGTACAAGAAAGCTGGGTGTTACTTATCGTGGACGTC
ORF 02	633 bp	BAC	for	GGGGACAAGTTTGTACAAAAAAGCAGGCTCCGCCATGGATCCTACACTTTAC
			rev	GGGGACCACTTTGTACAAGAAAGCTGGGTGTTACGAAGTCTCACTGAAG
K3 (FL)	1002 bp	BAC	for	GGGGACAAGTTTGTACAAAAAAGCAGGCTCCGCCATGGAAGATGAGGATGTTC
			rev	GGGGACCACTTTGTACAAGAAAGCTGGGTGTTAATGAAACATAAGGGC
K3c1	246 bp	JSC-1, gDNA *	for	GGGGACAAGTTTGTACAAAAAAGCAGGCTCCGCCATGGAAGATGAGGATGTTC
			rev	AGAAAGCTGGGTTATTCCAGACCCTCCTGGTAAG
K3c2	575 bp	BC-1, gDNA	for	AAAAAGCAGGCTCCGCCCACATGATGCGCCACGTGGGG
			rev	GGGGACCACTTTGTACAAGAAAGCTGGGTGTTAATGAAACATAAGGGC
ORF 70	1014 bp	BAC	for	AAAAAGCAGGCTATGTTTCCGTTTGTACCTTTAAG
			rev	AGAAAGCTGGGTCTATACTGCCATTTCCATAC
K 4	285 bp	BAC	for	AAAAAGCAGGCTATGGACACCAAGGGCATC
			rev	AGAAAGCTGGGTTCAGCGAGCAGTGACTGG
K 4.1	345 bp	BAC	for	AAAAAGCAGGCTATGTGGAGCATGTGCTGG
			rev	AGAAAGCTGGGTCTAGGGGCATAACCCTTTAC
K 4.2	550 bp	BAC	for	AAAAAGCAGGCTATGCAAATTAGCAAAGCC
			rev	AGAAAGCTGGGTTTATTGAAGCCCAGGCGAC
K5 (FL)	771 bp	BCBL-1, gDNA	for	AAAAAGCAGGCTATGGCGTCTAAGGACGTAG
			rev	AGAAAGCTGGGTTCAACCGTTGTTTTTTGG
K5c1	259 bp	BC-1, gDNA	for	AAAAAGCAGGCTATGGCGTCTAAGGACGTAG
			rev	AGAAAGCTGGGTTATTCAAAAATTTCTTGGCGCTCC
K5c2	344 bp	BC-1, gDNA	for	AAAAAGCAGGCTCCGCCGGCGGCATATGCCGCGTAAGTGG
			rev	AGAAAGCTGGGTTCAACCGTTGTTTTTTGG
K 6	288 bp	BAC	for	AAAAAGCAGGCTATGGCCCCCGTCCACGTTTTATG
			rev	AGAAAGCTGGGTCTAAGCTATGGCAGGCAG
K 7	381 bp	BAC	for	AAAAAGCAGGCTATGGGAACACTGGAGATAAAAG
			rev	AGAAAGCTGGGTCTACAACTGGCCTGGAGATTG
ORF 16	528 bp	BCBL-1, gDNA	for	AAAAAGCAGGCTATGGACGAGGACGTTTTG
			rev	AGAAAGCTGGGTTTATCTCCTGCTCATCGC
ORF 17	1662 bp	BCBL-1, gDNA	for	AAAAAGCAGGCTATGAGCCTCCTAAGCCCC
			rev	AGAAAGCTGGGTCTACTGCTTGTTCAGGAG
ORF 18	774 bp	BC-1, gDNA	for	AAAAAGCAGGCTATGCTCGGAAAATACGTG
			rev	AGAAAGCTGGGTTTAAACCGCGTTGTTGTTAAAC

ORF 19	1650 bp	BCBL-1, gDNA	for	AAAAAGCAGGCTCCGCCATGCTGACATCAGAAAGG
			rev	AGAAAGCTGGGTTTAAACGACCGCGAGGAC
ORF 20	963 bp	BCBL-1, gDNA	for	AAAAAGCAGGCTCCGCCATGTACGAGGTTTTTACAG
			rev	AGAAAGCTGGGTTCATGGACCTGAACAAGC
ORF 21	1743 bp	BCBL-1, gDNA	for	AAAAAGCAGGCTCCGCCATGGCAGAAGGCGGTTTTG
			rev	AGAAAGCTGGGTCTAGACCCTGCATGTCTC
ORF 22 (FL)	2193 bp	L74 ***	for	AAAAAGCAGGCTCCGCCGCTTTGTTTCTAATTCTC
			rev	AGAAAGCTGGGTCTAATAAAGGATGGAAAAC
ORF 23	1215 bp	BCBL-1, gDNA	for	AAAAAGCAGGCTCCGCCATGTTACGAGTTCCGGAC
			rev	AGAAAGCTGGGTTTAGACGGTCAATAAAGC
ORF 24	2259 bp	BCBL-1, gDNA	for	AAAAAGCAGGCTCCGCCATGGCAGCGCTCGAGGGC
			rev	AGAAAGCTGGGTTTAGACCAGCGGACGGAC
ORF 25	4131 bp	BCBL-1, gDNA	for	AAAAAGCAGGCTCCGCCATGGAGGCGACCTTGGAG
			rev	AGAAAGCTGGGTCTAATACACCACCTTGTTTC
ORF 26	918 bp	BCBL-1, gDNA	for	AAAAAGCAGGCTCCGCCATGGCACTCGACAAGAGTATAG
			rev	AGAAAGCTGGGTTTAGCGTGGGGAATACCAAC
ORF 27	873 bp	BCBL-1, gDNA	for	AAAAAGCAGGCTCCGCCATGGCGTCATCTGATATTC
			rev	AGAAAGCTGGGTTTATTTAAAATTTAGAATC
ORF 28 (FL)	309 bp	BCBL-1, gDNA	for	AAAAAGCAGGCTCCGCCATGAGCATGACTTCCCCG
			rev	AGAAAGCTGGGTCTAATCTGGCATGTATATTG
ORF 28 d2	132 bp	BCBL-1, gDNA	for	AAAAAGCAGGCTCCGCCATTCGCGTGTTCCTGGCGGC
			rev	AGAAAGCTGGGTCTAATCTGGCATGTATATTG
ORF 28 ext	218 bp	BCBL-1, gDNA	for	AAAAAGCAGGCTCCGCCATGAGCATGACTTCCCCGTCTCC
			rev	AGAAAGCTGGGTTTAGGGAGGCTTGGTGGCCATTC
ORF 29b	1056 bp	BCBL-1, gDNA	for	AAAAAGCAGGCTCCGCCATGCTTCAGAAAGACGCC
			rev	AGAAAGCTGGGTTTATTGTGGGGATATGGG
ORF 30	234 bp	BCBL-1, gDNA	for	AAAAAGCAGGCTCCGCCATGGGTGAGCCAGTGGATC
			rev	AGAAAGCTGGGTTCATTTCGCACCGGTGTC
ORF 31	675 bp	BCBL-1, gDNA	for	AAAAAGCAGGCTCCGCCATGTCACAAAACAGAAAG
			rev	AGAAAGCTGGGTCTACGTATCTTTCGTTGATAG
ORF 32	1365 bp	BCBL-1, gDNA	for	AAAAAGCAGGCTCCGCCATGGATGCGCATGCTATC
			rev	AGAAAGCTGGGTCTAGCCATAGCGGCCTCG
ORF 33	939 bp	BCBL-1, gDNA	for	AAAAAGCAGGCTCCGCCATGGCTAGCCGGAGGCGC
			rev	AGAAAGCTGGGTTCAGACATTCGTAAGAGG
ORF 29a	939 bp	BCBL-1, gDNA	for	AAAAAGCAGGCTCCGCCATGCTGCTCAGCCGTCAC
			rev	AGAAAGCTGGGTTTAAGGCCCTGGGCTTAC
ORF 34	984 bp	BCBL-1, gDNA	for	AAAAAGCAGGCTCCGCCATGTTTGCTTTGAGCTCG

			rev	AGAAAGCTGGGTTTAGAGTTGGTTGAGTCC
ORF 35	453 bp	BCBL-1, gDNA	for	AAAAAGCAGGCTCCGCCATGGACTCAACCAACTCTAAAAG
			rev	AGAAAGCTGGGTTTAGGGAGTTTCAGGGCAC
ORF 36	1335 bp	BCBL-1, gDNA	for	AAAAAGCAGGCTCCGCCATGCGCTGGAAGAGAATG
			rev	AGAAAGCTGGGTTCAGAAAACAAGTCCGCG
ORF 37	1461 bp	BCBL-1, gDNA	for	AAAAAGCAGGCTCCGCCATGGAGGCCACCCCCACAC
			rev	AGAAAGCTGGGTCTACGGGCTGTGAGGGAC
ORF 38	186 bp	BCBL-1, gDNA	for	AAAAAGCAGGCTCCGCCATGGGATTTCTCCTATCTATC
			rev	AGAAAGCTGGGTTTAATAAATTGCTTCTTTATTTTTTTTC
ORF 39 (FL)	1203 bp	BC-1, gDNA	for	AAAAAGCAGGCTCCGCCCGCGTTATAAGGAGCGACTG
			rev	AGAAAGCTGGGTTCTAAATGAATATCATTTG
ORF 39d2	240 bp	BCBL-1, gDNA	for	AAAAAGCAGGCTCCGCCCGCGTTATAAGGAGCGACTG
			rev	AGAAAGCTGGGTTCTAAATGAATATCATTTGCGTTTC
ORF 40	1374 bp	BCBL-1, gDNA	for	AAAAAGCAGGCTCCGCCATGGCAACGAGCGAAGAAAC
			rev	AGAAAGCTGGGTCAAGCAGGGACAGTAGG
ORF 41	618 bp	BCBL-1, gDNA	for	AAAAAGCAGGCTCCGCCATGGCCGGGTTTACTCTG
			rev	AGAAAGCTGGGTTCAAAATAAAGATAAAAG
ORF 42	837 bp	BCBL-1, gDNA	for	AAAAAGCAGGCTCCGCCATGTCCCTGGAAAGGGCC
			rev	AGAAAGCTGGGTTTATTTTGAAAAAAGGGAAAC
ORF 43	1818 bp	BCBL-1, gDNA	for	AAAAAGCAGGCTCCGCCATGTTGAGGATGAACCCG
			rev	AGAAAGCTGGGTCTATGCACTTCCAGGACAAG
ORF 44	2367 bp	BCBL-1, gDNA	for	AAAAAGCAGGCTCCGCCATGGACAGCTCGGAAGGG
			rev	AGAAAGCTGGGTTCAGTAGATCAGAGTAGTC
ORF 45	1224 bp	BCBL-1, gDNA	for	AAAAAGCAGGCTCCGCCATGGCGATGTTTGTGAGG
			rev	AGAAAGCTGGGTTCAGTCCAGCCACGGCCAG
ORF 46	767 bp	BCBL-1, gDNA	for	AAAAAGCAGGCTCCGCCATGGACGCATGGTTGCAAC
			rev	AGAAAGCTGGGTTTACTGCTCCAACAGGCC
ORF 47(FL)	504 bp	BC-1, gDNA	for	AAAAAGCAGGCTCCGCCCAGGCATCGGCAGCCTCTAC
			rev	AGAAAGCTGGGTTTATTTTCCCTTTTGACC
ORF 47(CyD)		BC-1, gDNA	for	AAAAAGCAGGCTCCGCCCACTCTATCCACTTCGCC
			rev	AGAAAGCTGGGTTTATTTTCCCTTTTGACC
ORF48 (FL)	1209 bp	BC-1, gDNA	for	AAAAAGCAGGCTCCGCCATGGAGGTGTGTATCCCA
			rev	AGAAAGCTGGGTTCAATCATACTCATCGTC
ORF 48 cyt	586 bp	BCBL-1, gDNA	for	AAAAAGCAGGCTCCGCCATGGAGGTGTGTATCCCAATTC
			rev	AGAAAGCTGGGTCCGCCGGAACTCCACATC
ORF 48 ext	552 bp	BCBL-1, gDNA	for	AAAAAGCAGGCTCCGCCATTACCTCGGACGTGAGAC
			rev	AGAAAGCTGGGTTCAATCATACTCATCGTCGG

ORF 49	909 bp	BCBL-1, gDNA	for	AAAAAGCAGGCTCCGCCATGACATCGAGAAGGCCC
			rev	AGAAAGCTGGGTTTATTGTATACTGAACAATG
ORF 50	1896 bp	BCBL-1, gDNA	for	AAAAAGCAGGCTCCGCCATGAAAGAATGTTCCAAG
			rev	AGAAAGCTGGGTTCAGTCTCGGAAGTAATTAC
K 8	720 bp	BCBL-1, gDNA	for	AAAAAGCAGGCTCCGCCATGCCCAGAATGAAGGAC
			rev	AGAAAGCTGGGTCTATACCTGCTGCAGCTG
K8(spliced)	330 bp	BC-1-RNA *	for	AAAAAGCAGGCTCCGCCATGCCCAGAATGAAGGAC
			rev	AGAAAGCTGGGTCTATACCTGCTGCAGCTG
K 8.1	594 bp	BCBL-1, gDNA	for	AAAAAGCAGGCTCCGCCCAGGACCACGCGAATTCG
			rev	AGAAAGCTGGGTCTATTTCTGCCGTTTTCTG
K8.1(B) (spliced)	722bp	BC-1-RNA	for	AAAAAGCAGGCTCCGCCCAGGACCACGCGAATTCG
			rev	AGAAAGCTGGGTCTATTTCTGCCGTTTTCTG
K8.1 (CyD)	98 bp	BC-1, gDNA	for	AAAAAGCAGGCTCCGCCCAGGACCACGCGAATTCG
			rev	AGAAAGCTGGGTCTATTTCTGCCGTTTTCTGC
ORF 52	396 bp	BCBL-1, gDNA	for	AAAAAGCAGGCTCCGCCATGGCCGCGCCCAGGGGC
			rev	AGAAAGCTGGGTTCAGTCATCAACCCCCGC
ORF 53	333 bp	BCBL-1, gDNA	for	AAAAAGCAGGCTCCGCCATGACAGCGTCCACGGTG
			rev	AGAAAGCTGGGTCTATGCATGGACCACCTC
ORF 54	957 bp	BCBL-1, gDNA	for	AAAAAGCAGGCTCCGCCATGAACAACCGCCGAGGC
			rev	AGAAAGCTGGGTCTAAAACCCAGACGACCC
ORF 55	684 bp	BCBL-1, gDNA	for	AAAAAGCAGGCTCCGCGTCTCCATGGTACCATGTC
			rev	AGAAAGCTGGGTCTATGTCGAACCTATCGC
ORF 56	2532 bp	BCBL-1, gDNA	for	AAAAAGCAGGCTCCGCCATGGAGACGACATACCGC
			rev	AGAAAGCTGGGTTTAACTGGCCAGTCCCAC
ORF 57 (FL)	828 bp	Z8 ***	for	AAAAAGCAGGCTCCGCCATGATAATTGACGGTGAG
			rev	AGAAAGCTGGGTTTAAGAAAGTGGATAAAAG
ORF 57 (spliced)	1368 bp	BC-1-RNA	for	AAAAAGCAGGCTCCGCCATGGTACAAGCAATGATAG
			rev	AGAAAGCTGGGTTTAAGAAAGTGGATAAAAG
K 9	1350 bp	BCBL-1, gDNA	for	AAAAAGCAGGCTCCGCCATGGACCCAGGCCAAAGAC
			rev	AGAAAGCTGGGTTTATTGCATGGCATCCCATAAC
K 10	2091 bp	BCBL-1, gDNA	for	AAAAAGCAGGCTCCGCCATGGGGTCCTCTGGGACG
			rev	AGAAAGCTGGGTTCAATGTAGACTATCCCAAATG
K 10.5	942 bp	BCBL-1, gDNA	for	AAAAAGCAGGCTCCGCCATGTACCACGTGGGACAG
			rev	AAAAAGCAGGCTTTAGTCATCACATGTAAC
VIRF3	1607 bp	Plasmid-DNA ****	for	AAAAAGCAGGCTCCGCCATGGCGGGACGCAGGCTTACC

			rev	AAAAAGCAGGCTTTAGTCATCACATGTAAC
K 11	1404 bp	BCBL-1, gDNA	for	AAAAAGCAGGCTCCGCCATGCACAGTTTGTTTTTTG
			rev	AGAAAGCTGGGTTTAGTCTCTGTGGTAAAATG
ORF 58	1074 bp	BCBL-1, gDNA	for	AAAAAGCAGGCTCCGCCATGTGCCGCCTGGACAGTG
			rev	AGAAAGCTGGGTTTAGCCAACAACTTTATTTATTAC
ORF 59	1191 bp	Z8	for	AAAAAGCAGGCTCCGCCATGCCTGTGGATTTTCAC
			rev	AGAAAGCTGGGTTCAAATCAGGGGGTTAAATG
ORF 60	918 bp	Z8	for	AAAAAGCAGGCTCCGCCATGGATTCAGTTGATCGA
			rev	AGAAAGCTGGGTTCACAAATCGTCAGTCAC
ORF 61	2279 bp	Z8	for	AAAAAGCAGGCTCCGCCATGTCTGTCCGGACATTTTG
			rev	AGAAAGCTGGGTCTACTGACAGACCAGGCAC
ORF 62	996 bp	BCBL-1, gDNA	for	AAAAAGCAGGCTCCGCCATGAAGGTGCAGGCTGAAAATG
			rev	AGAAAGCTGGGTTTACAGAAACACAGTCCAG
ORF 63 l	1642 bp	BC-1, gDNA	for	AAAAAGCAGGCTCCGCCATGGACGGCACAGACGCTC
			rev	AGAAAGCTGGGTTACAAGTGACTCTTGGTAAACGC
ORF 65	513 bp	BCBL-1, gDNA	for	AAAAAGCAGGCTCCGCCATGTCCAACTTTAAGGTG
			rev	AGAAAGCTGGGTCTATTTCTTTTTGCCAGAG
ORF 66	1290 bp	BCBL-1, gDNA	for	AAAAAGCAGGCTCCGCCATGGCCCTGGATCAGCGC
			rev	AGAAAGCTGGGTTCAGGAGGAACACTTCCC
ORF 67	816 bp	BCBL-1, gDNA	for	AAAAAGCAGGCTCCGCCATGAGTGTCGTTGGTAAG
			rev	AGAAAGCTGGGTTCAGCTGGGCCTCATCCAAAC
ORF 67.5	243 bp	BCBL-1, gDNA	for	AAAAAGCAGGCTCCGCCATGGAGTACGCGTCTGACCAG
			rev	AGAAAGCTGGGTTCAGGGCCGTGCCCGCGC
ORF 68 (FL)	1638 bp	BC-1, gDNA	for	AAAAAGCAGGCTCCGCCATGTCACGAGGCAGAAGC
			rev	AGAAAGCTGGGTTCAAGCGTACAAGTGTGACGTC
ORF 68 d2	1120 bp	BC-1, gDNA	for	AAAAAGCAGGCTCCGCCGCAGACCTGTGCGAGATC
			rev	AGAAAGCTGGGTTCAAGCGTACAAGTGTGACGTC
ORF 68 d1	463 bp	BC-1, gDNA	for	AAAAAGCAGGCTCCGCCATGTCACGAGGCAGAAGC
			rev	AGAAAGCTGGGTTTAGGCATAGTCCTCGAAGAAAC
ORF 69	678 bp	BCBL-1, gDNA	for	AAAAAGCAGGCTCCGCCATGGAGACCCCGATATGC
			rev	AGAAAGCTGGGTTTATAGGGCGTTGACAAG
K 12cyt	107 bp	BC-1, gDNA	for	AAAAAGCAGGCTCCGCCAGTGGCCAGCGTGGCCCC
			rev	AGAAAGCTGGGTTCAGTGCGCGCCGTTGC
K 13/ORF 71	567 bp	BC-1, gDNA	for	AAAAAGCAGGCTCCGCCATGGCCACTTACGAGGTTC
			rev	AGAAAGCTGGGTCTATGGTGTATGGCGATAG
ORF 72	774 bp	BCBL-1, gDNA	for	AAAAAGCAGGCTCCGCCATGGCAACTGCCAATAAC
			rev	AGAAAGCTGGGTTTAATAGCTGTCCAGAATG

K 14	1047 bp	BCBL-1, gDNA	for	AAAAAGCAGGCTCCGCCATGATACACACATTTTTTG
			rev	AGAAAGCTGGGTTCACTGGGTGGATAGGGG
K 14.1	231 bp	BCBL-1, gDNA	for	AAAAAGCAGGCTCCGCCATGCCTAGAGGGCGCACC
			rev	AGAAAGCTGGGTCTAGGACCACAGCATTTTTC
ORF 74 (FL)	1029 bp	BC-1, gDNA	for	AAAAAGCAGGCTCCGCCATGGCGGCCGAGGATTTCC
			rev	AGAAAGCTGGGTCTACGTGGTGGCGCCGGAC
ORF 74 (CyD)	125 bp	BC-1, gDNA	for	AAAAAGCAGGCTCCGCCTCCCTCTTTAGGCAGAGG
			rev	AGAAAGCTGGGTCTACGTGGTGGCGCCGGAC
ORF 75 (I)	2034 bp	BCBL-1, gDNA	for	AAAAAGCAGGCTCCGCCATGGCCTACGACGTCACTG
			rev	AGAAAGCTGGGTTAGTAGGCCTGCTCCCCCATGGCC
K 15	303 bp	BCBL-1, gDNA	for	AAAAAGCAGGCTCCGCCAAGGAAAAAAAAGTGGTGGC
			rev	AGAAAGCTGGGTCTAGTTCCTGGGAAATAAAACC
K15 (spliced)	1470 bp P-Allel	Plasmid-DNA *****	for	AAAAAGCAGGCTCCGCCATGAAGACACTCATATTC
			rev	AGAAAGCTGGGTCTAGTTCCTGGGAAATAAAACC

* kindly provided by Gergana Iotzova, Genzentrum, München, Germany

** kindly provided by Maria Roupelieva, Genzentrum, München, Germany

*** lambda (L) and cosmid clones (Z), Russo et al, PNAS 1996, 93:14862-7

**** kindly provided by Prof. Dr. Paula M. Pitha-Rowe, Oncology Center, The Johns Hopkins University School of Medicine, Baltimore, Maryland 21231, USA.

***** kindly provided by Prof. Dr. Thomas F. Schulz, Institut fur Virologie, Medizinische Hochschule Hannover, D-30625 Hannover, Germany.

The oligonucleotides were obtained from Invitrogen (Karlsruhe, Germany) and thermo hybaid (Ulm, Germany).

3.1.10 Molecular weight markers

Gene Ruler 100 bp DNA ladder   MBI Fermentas, St. Leon-Rot, Germany

Gene Ruler DNA 1 kb ladder   MBI Fermentas, St. Leon-Rot, Germany

See Blue Plus 2 Prestained Protein Standard Invitrogen, Karlsruhe, Germany
low range

3.1.11 Kits

Pharmacia GFX PCR DNA Gel Purification	Amersham-Pharmacia, Freiburg, Germany
Qiafilter Plasmid Maxi Kit	Qiagen, Hilden, Germany
Qiagen Plasmid Mini Kit	Qiagen, Hilden, Germany

3.1.12 Antibodies

3.1.12.1 Primary antibodies

3F10	Rat Mab against HA tag, Roche Diagnostics, Mannheim, Germany
9E10	Mouse Mab against Myc tag, Santa Cruz Biotechnology, Heidelberg, Germany

3.1.12.2 Secondary antibodies
peroxidase-conjugated:

Goat Anti-Rat	Dianova, Hamburg, Germany
Goat Anti-Mouse	Dianova, Hamburg, Germany

3.1.13 Enzymes

T4 DNA Polymerase	New England Biolabs, Beverly, USA
Calf Intestinal Alkaline	New England Biolabs, Beverly, USA
Phosphatase (CIP)	New England Biolabs, Beverly, USA
BP Clonase	Invitrogen, Karlsruhe, Germany
LR Clonase	Invitrogen, Karlsruhe, Germany
Topoisomerase I	MBI Fermentas, St. Leon-Rot, Germany
T4 DNA Ligase	MBI Fermentas, St. Leon-Rot, Germany
Vent DNA Polymeras	New England Biolabs, Beverly, USA
Polynukleotid Kinase	New England Biolabs, Beverly, USA
Proteinase K	Invitrogen, Karlsruhe, Germany
Restriction Endonuclease	MBI Fermentas, St. Leon-Rot, Germany
	Roche Diagnostics, Mannheim, Germany
	New England Biolabs, Beverly, USA

3.2 Methods

3.2.1 Bacterial cell culture

3.2.1.1 Cultivation of bacteria

E. coli bacteria were grown in LB medium or on LB agar plates. Incubation was performed at 37°C with constant shaking.

LB Medium (1 l):	10 g Bacto Tryptone
	5 g Bacto Yeast Extract
	5 g NaCl

LB Agar:	LB Medium with 1.5 % Agar
Selection Medium:	LB Medium with 100 µg/ml Ampicillin and/or 50 µg/ml Kanamycin

3.2.1.2 Preparation of competent bacteria

For preparation of competent bacteria a single clone of DH5α was picked and grown in 20 ml TYM medium at 37°C to an OD_{600nm} of 0.8. The bacterial culture was diluted with 100 ml TYM and incubated at 37°C until an OD_{600nm} between 0.5-0.9 was reached. Subsequently, the culture was again diluted by adding 500 ml of TYM and incubated at 37°C. At an OD_{600nm} of 0.6 the culture was rapidly chilled down on ice water. The following incubations were performed at 4°C or on ice. The bacteria were distributed to two 50 ml tubes and centrifuged 5 min at 3500 rpm (Heraeus Varifuge 3.0R). The supernatants were discarded and the pellets were resuspended in 100 ml ice-cold TfB I. After 40-50 min incubation on ice, the bacteria were centrifuged 10 min at 2500 rpm (Heraeus Varifuge 3.0R). The supernatants were discarded and the pellets were resuspended in 25 ml ice-cold TfB II. Aliquots of 0.4 ml were added to prechilled 0.5 ml reaction tubes and stored at -80°C.

TYM:	10 mM $MgSO_4$
	100 mM NaCl
	20 g/l Bacto Tryptone
	5 g/l Bacto Yeast Extract

TfB I: 30 mM KAc

                          50 mM MnCl$_2$

                          100 mM KCl

                          10 mM CaCl$_2$

                          15 % (v/v) Glycerol

TfB II: 10 mM MOPS pH 7.0

                          75 mM CaCl$_2$

                          10 mM CaCl$_2$

                          15 % (v/v) Glycerol

both buffers sterilized by filtration (Ø0.2 µm) and stored at 4°C.

3.2.1.3   Transformation

Different volumes of the ligation reaction mixture (5, 10, 20 µl) were added to 100 µl competent bacteria, mixed with 80 µl of 50 mM CaCl$_2$ and incubated 30 min on ice. After the heat shock, 1 min 42°C, 800 µl LB medium were added and bacteria were cultivated for 1 h at 37°C. Then 100 µl were taken and plated on LB agar plates with antibiotic(s). The residual bacteria were centrifuged (4000 g, 5 min), resuspended and plated the same way. The plates were incubated o/n at 37°C.

3.2.2   DNA techniques

3.2.2.1   Purification of plasmid DNA

Plasmid DNA was purified with the Pharmacia GFX Micro Plasmid Kit in small scale and the Qiafilter Plasmid Maxi Kit in large scale according to the manufacturer's instructions.

3.2.2.2   Determination of DNA concentration

The concentration and purity of the purified DNA was determined by measuring the UV absorbance at 260 and 280 nm. The DNA concentration was calculated with the OD_{260nm} (1 OD_{260nm} = 50 µg/ml dsDNA or 33 µg/ml ssDNA). The purity was estimated with the OD_{260nm}/OD_{280nm} ratio, with a ratio of ca. 1.8 indicating a low degree of protein contamination.

3.2.2.3   Restriction endonuclease digestion

Restriction endonuclease reactions were performed according to the manufacturer's recommendations. In general, 1.5 µg DNA was digested for 2 h at the appropriate

temperature with 10-20 U enzyme. Efficacy of the cleavage reaction was controlled by agarose gel electrophoresis.

3.2.2.4 5'-Dephosphorylation reaction

5'-dephosphorylation reactions of plasmid vector DNA after restriction endonuclease cleavage were performed with the calf intestinal alkaline phosphatase (CIP). 50 U CIP were added to about 1.5 µg restriction enzyme digested plasmid DNA. After 30 min incubation at 37 °C was stopped and the DNA was isolated by agarose gel electrophoresis.

3.2.2.5 Nested polymerase chain reaction (PCR) for recombinatorial cloning

Polymerase chain reactions (PCR) were performed with Vent DNA polymerase which consists of an integral 3'-5' proofreading exonuclease activity. Vent is produced as a recombinant protein in E.coli. The Vent DNA polymerase gene was isolated from the archae Thermococcus litoralis. As PCR templates we used either genomic DNA isolated from BCBL-1 cells, KSHV phage or cosmid clones from BC-1 cells (Cesarman et al., 1995), KSHV BAC DNA generated from virus of BCP-3 cells, or cDNA prepared from BC-1 cells for the amplification of spliced genes.

Table 3:   Primer construction for nested polymerase chain reaction (PCR)

1. attB1 internal	for	AAAAAGCAGGCT**CCGCC**ATGXXXXXXXXXXXXXXX
2. attB1 internal	rev	AGAAAGCTGGGTCTAXXXXXXXXXXXXXXXXXXXX
3. attB2 external	for	GGGGACAAGTTTGTACAAAAAAGCAGGCT
4. attB2 external	rev	GGGGACCACTTTGTACAAGAAAGCTGGGT

yellow box: attB1/attB2 sequence	red letters: Kozak sequence
bold letters: ATG (for) and stop (rev) codon	XXXXX: homologous for and rev sequence (18 – 22 nucleotides, 3' end G or C, app. 60°C annealing temperature)

1st PCR:

Components:

10 x Thermo Pol Buffer		5 µl
Internal Forward Prime	10 pmol/µl	1µl
Internal Reversed Primer	10 pmol/µl	1 µl

Template (genomic DNA)		1 µg
respectively, 200 ng Plasmid DNA		
dNTP Mix	10mM	0,7 µl
Vent Polymerase	2 u/ml	0,7 µl
H₂O		**add 50 µl**

The PCR reactions were performed as hot start reactions, i.e. first the PCR-device was started and after heating 0,7 µl of Vent Polymerase was added.

1ˢᵗ step	⟶	2ⁿᵈ step	⟶	3ʳᵈ step
		(hot start: add Vent polymerase)		

Heating 94°C, 2,5 min	**Annealing** 55°C, 30 sec **Synthesis** 68°C, 30 – 180 sec **Denaturation** 94°C, 15 sec	**Synthesis** 68°C, 7min

(ca. 10-15 cycles)
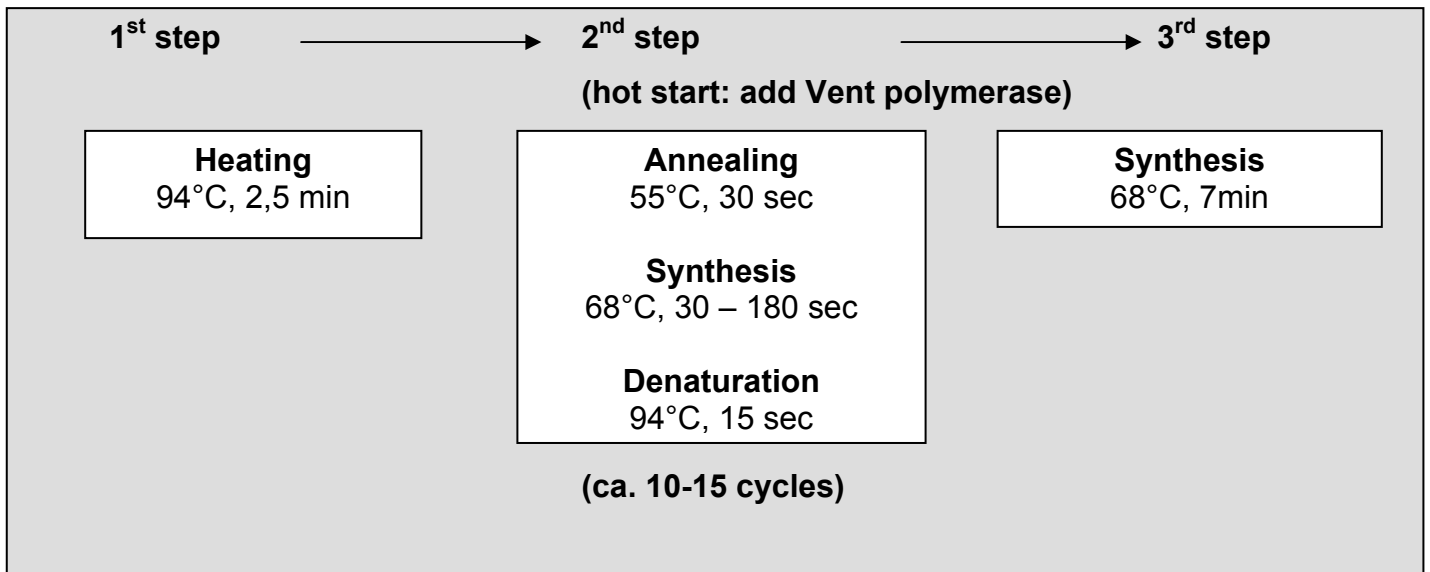
Figure 9a: Diagram of the 1ˢᵗ PCR procedure

2ⁿᵈ PCR:

Components:

10 x Thermo Pol Buffer		5 µl
External Forward Primer	10 pmol/µl	1µl
External Reversed Primer	10 pmol/µl	1 µl
Template (1ˢᵗ PCR Reaction)		10 µl
dNTP Mix	10mM	0,7 µl
Vent Polymerase	2 u/ml	0,7 µl
H₂O		**add 50 µl**
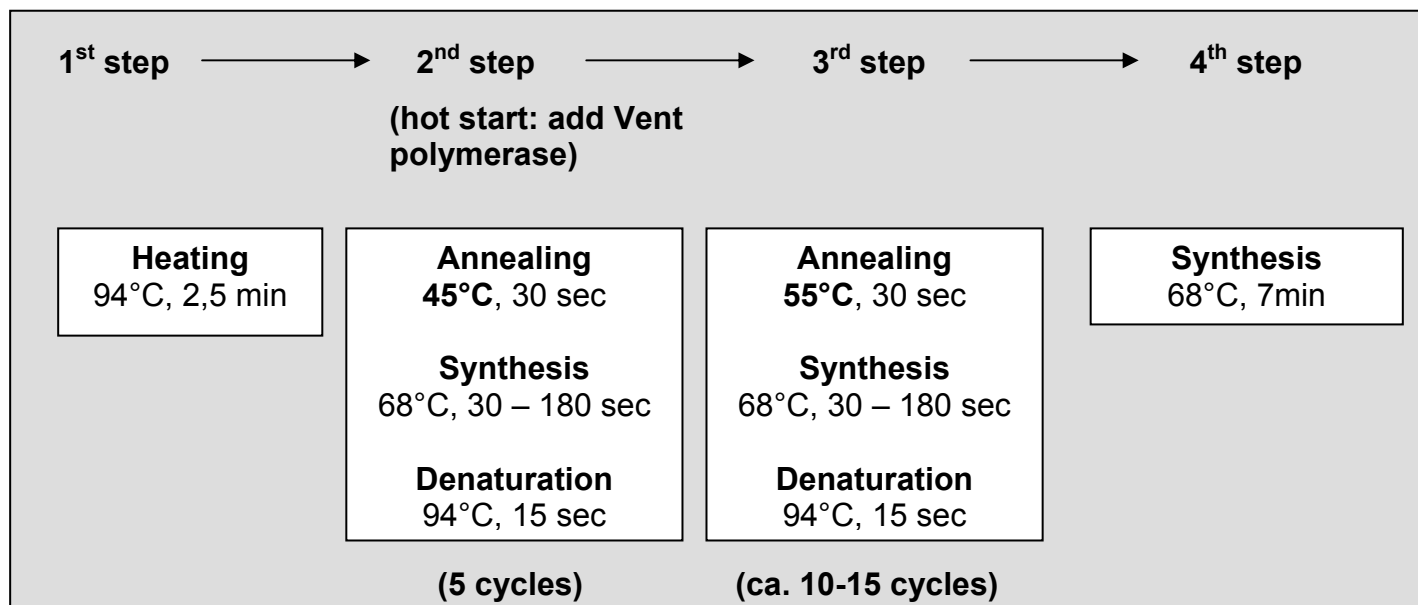
Figure 9b: **Diagram of the 2nd PCR procedure**

The time of synthesis was varied according to the length of the expected product (60 sec per 1000 bp)

3.2.2.6 Isolation of DNA fragments

DNA fragments were separated by agarose gel electrophoresis, stained with ethidium bromide, and detected with UV light (366 nm). The gel slice containing the DNA fragments was cut out and the DNA was isolated using the Pharmacia GFX PCR DNA Gel Purification Kit according to the manufacturer's instructions.

3.2.2.7 Phenol/chloroform extraction and ethanol precipitation

Proteins were removed from DNA preparations by extracting twice with 1x volume phenol/chloroform and once with 1x volume chloroform. After vigorous vortexing for 10 s, the solution was centrifuged at 14000 rpm (microcentrifuge) for 1 min and the upper DNA containing phase was recovered. Then 0.1x volume 3 M NaAc pH 5.2 and 2.5x volume 100% EtOH (cold) were added, and incubation at -80°C was performed for 20 min. The precipitated DNA was centrifuged down at 14000 rpm for 30 min (4°C). Then the pellet was washed once with 70% EtOH (cold). After another centrifugation step (14000 rpm, 15 min, 4°C, microcentrifuge) the EtOH was carefully removed, the pellet was air-dried at RT and finally resuspended in H_2O.

3.2.2.8   Ligation

For ligation, approximately 50 ng of vector DNA was used at a molar vector/insert ratio of about 1:3. The reaction was performed in a total volume of 20 µl 1x reaction buffer (MBI Fermentas) with 5 U T4 DNA Ligase (MBI Fermentas). First, vector and insert were mixed in reaction buffer, then the ligase was added. After incubation o/n in a waterbath at 16°C, the ligation was either directly transformed into competent bacteria or stored at -20°C until further usage.

3.2.2.9   Recombinatorial cloning (RC)

3.2.2.9.1   The BP reaction

Components:

PCR- product	2-7 µl
pDONR 207	1 µl
BP Reaction buffer (5x)	1.5 µl
BP Clonase	1 µl

The reaction was incubated at 25° C for at least 60 min. After incubation, 2 µl of proteinase K were added and incubated for 10 min at 37°C.

1 µl of the reaction was transformed into 50 µl DH5α, DH10B or Top10 competent cells by electroporation. 500 µl S.O.C. medium was added and incubated at 37°C for 1h. The transformation reaction was spread on LB plates containing 1,5 µg/ml gentamycin. The plates were incubated for 16 hours.

From single colonies miniprep DNA was isolated. Minipreparations were treated with RNAse, precipitated with ethanol and stored in TE. The preparations were digested with the restriction endonucleases Pst I and Apa I to determine the correct size of the inserted fragment.

3.2.2.9.2   The LR reaction

Components:

Purified Entry Clone (150ng/µl)	2 µl
pGBKT7	1 µl
pGADT7	1 µl
LR Reaction Buffer (5x)	1.5 µl
Topoisomerase	1µl

LR Clonase   1 μl

Further steps were performed as described under 'The BP reaction'. The transformation reaction was divided in two parts. One was spread on LB plates containing 50 μg/ml kanamycin for pGBKT7 (bait vector), the other on ampicillin plates (100μg/ml) for pGADT7 (prey vector).

3.2.2.10   Agarose gel electrophoresis

Analysis of DNA fragments and plasmids was performed by agarose gel electrophoresis in 1x TAE. In general agarose concentration was between 1 and 3 % in 1x TAE. The agarose was solubilised by heating in a microwave oven. Ethidium bromide was added to a final concentration of 0.25 µg/ml (2,5 µl stock to 100 ml) just before pouring the gel. Probes were mixed with 0.17x volume loading buffer. Gels (6.5 x 9.5 cm) were run horizontally at 80-120 V. DNA was detected with UV light, λ=254 nm or λ=366 nm to cut out specific fragments.

Loading Buffer (6x in water)   MBI Fermentas, St. Leon-Rot, Germany
20x TAE: 800 mM Tris
                                   400 mM NaAc
                                   40 mM EDTA
                                   adjusted to pH 7.8 with acetic acid
Ethidium Bromide (stock):   10 mg/ml

3.2.2.11   Plasmid construction

3.2.2.11.1   Inserting the recombination cassette into bait and prey vectors

A conversion cassette (Gateway) containing a chloramphenicol resistance (Cm^r) and a lethal gene (ccdB) flanked by the λ att sites was inserted blunt end into the Sma I restriction site of the Y2H bait vector pGBKT7 (Km^r) and the Sma I of the prey vector pGADT7 (Ap^r) (Clontech) resulting in pDEST-GADT7 and pDEST-GBKT7 (pGADT7 and pGBKT7 containing the attR-cassette are also referred to as destination vectors). Destination vectors must be constructed and propagated in DB3.1 cells, a gyrA462 strain of *E. coli* because the ccdB gene is lethal to other strains.

The reading frame cassettes are blunt-ended, i.e., they are inserted in both orientations and have to be tested for the proper orientation.

The destination vectors were used to make fusion proteins of a KSHV protein and the Gal4-activation domain (prey constructs), respectively KSHV protein and DNA-

binding domain. Thus, it is essential to establish the correct reading frame, starting with the Sma I restriction side, where the cassette has been inserted, over the attR1 site, the KSHV- gene, the attR2 side and activation or binding domain. In our case, we had to use reading frame cassette B.

3.2.2.11.2 Cloning the PCR products into the donor vector

114 PCR products with 25-bp terminal attB sites (+ 4Gs) were converted to entry clones by performing BP reactions, in which the PCR products containing attB sites recombine with a donor vector containing attP sites. The resulting entry clones are flanked by attL sites. As a donor vector we chose pDONR207 carrying a gentamycin resistance gene (Gm^r).

3.2.2.11.3 Subcloning of the array into bait and prey vector

The LR reaction is used to create expression clones. The recombination proteins cut to the left and right of the gene within the attL sites in the entry clone and ligate it to the corresponding attR site in the destination vector, creating an expression clone. The resultant 25-bp attB sites (attB1 on the N-terminus and attB2 on the C-terminus) created by the LR reaction are derived from the attL sites (adjacent to the gene), whereas the distal sequences are derived from the attR sites.

The KSHV array consisting of the 114 different entry clones was transferred by LR reaction into the Y2H plasmids pGADT7 (ampicillin resistance) and pGBKT7 (kanamycin resistance). Due to the three different resistances involved it was possible to perform the subcloning from the donor vector into bait and prey vector in a one-tube-reaction: The LR reactions were transformed into the competent E. coli and the bacteria were plated on kanamycin and ampicillin plates to obtain both bait and prey plasmids.

3.2.3 Tissue culture

3.2.3.1 Cultivation and cryoconservation

The KSHV-infected PEL cell line BCBL-1 was cultured in RPMI 1640 supplemented with 20% fetal calf serum, 100 IU/ml penicillin, 100 µg/ml streptomycin and 2 mM L-glutamine. Cells were induced for 48 h with 3 mM n-butyrate. 293 and Hela cells were cultured in DMEM/10% FCS plus supplements at 37°C and 5% CO2. For cryoconservation cells were detached with trypsin and centrifuged at 300 g for 5 min at 4°C. Then the cells were resuspended in 1 ml FCS/10% DMSO (4°C) with a final

concentration of 0.5-1x10^7 cells/ml and transferred to cryovials which were cooled to -80°C in a "Cryo 1°C Freezing Container" (Nalgene). Subsequently, the vials were transferred to liquid nitrogen for long term storage. Frozen aliquots were quickly thawed at 37°C in a waterbath, 10ml DMEM was added and after centrifugation at 300 g for 5 min, the supernatant was removed. Subsequently, cells were resuspended in complete medium and transferred to cell culture dishes.

3.2.3.2   Calcium phosphate transfection

For transient transfection, cells were grown on 10 cm Ø dishes to 60-70% confluency. 500 µl of 2x HBS pH 7.05 was added to a 15 ml Falcon tube. In another tube, 20 µg DNA was combined with 500 µl 250 mM CaCl$_2$. The tube with the 2x HBS was vortexed while the DNA/CaCl$_2$ solution was added dropwise. The solution was incubated at RT for 15-20 min to allow the formation of the Calcium-DNA to precipitate. Subsequently, the suspension was mixed with 6 ml fresh medium and was added to the cells after removal of the old medium. The next day, protein expression was assessed by immunofluorescence.

2x HBS pH 7.05:	50 mM HEPES
	1.5 mM Na2HPO4x 2 H2O
	280 mM NaCl
	12 mM glucose

3.2.4   Protein techniques

3.2.4.1   Co-immunoprecipitation

Co-immunoprecipitation was performed using the plasmids pGBKT7 and pGADT7 with T7 promoter and recombinant vaccinia virus vT7 expressing the T7 RNA polymerase (NIH AIDS repository). 293 cells were cultured on 10 cm dishes and infected with vTF-7 at a MOI of 10 in serum-free medium. One hour after infection, cells were transfected with 10 µg of each of the two expression plasmids by calcium phosphate transfection. Expression was controlled using a GFP plasmid under the control of a T7 promoter. After 24 h, cells were lysed by incubation in 1 ml of NP-40 lysis-buffer (1% NP-40, 140 mM NaCl, 5 mM MgCl$_2$, 20 mM Tris pH 7,6, 1 mM PMSF) for 30 min on ice. Lysates were centrifuged for 10 min at 20,500 g and 4°C to remove unsolubilized material and precleared with 50 µl of preequilibrated protein G-Sepharose.

Supernatant was divided into two parts. Subsequently, proteins were precipitated from the supernatant by adding 1 μg of the anti-HA (Roche) antibodies or the anti-myc (Santa Cruz) antibodies, respectively and 50 μl of protein G-sepharose beads, each overnight at 4°C. Beads were washed three times with ice-cold NP-40 buffer and were resuspended in 2xSDS protein sample buffer. Cellular subfractions and total cell lysates were additionally sonified for 30 s. Samples were boiled for 10 min and directly analyzed by SDS-PAGE or stored at -20°C.

Equilibration of protein G-Sepharose: 1.5 g protein G-Sepharose was washed 3x and resuspended with NP-40 lysis-buffer to obtain a 50% slurry.

3.2.4.2   SDS-PAGE

Gel electrophoresis was performed with minigels using the Protean II system (Bio-Rad) with 12 to 20% gels (80 x 50 x 1 mm). The solution for generating the separation gel was mixed and, after pouring, the gel was overlaid with isopropanol. After polymerization, the isopropanol was sucked of the gel. The stacking gel solution was poured on top of the separation gel and a comb was fixed. After polymerization, the glass plates containing the gel were assembled in the gel electrophoresis apparatus. Samples or pellets from immunoprecipitation were resuspended in the appropriate amount of 2xSDS protein sample buffer and heated for 5 min to 95°C. After cooling to RT, the samples were centrifuged for 2 min at 14000 rpm (microcentrifuge) and loaded on the gel together with a protein standard. Separation was performed at 150 V constant current for 1-2 h.

Separation Gel :	**12%**	**15%**	**20%**
Acrylamide / Bisacrylamide (37.5:1)	2 ml	2.5 ml	3.33 ml
1.5 M Tris pH 8.8	1.25 ml	1.25 ml	1.25 ml
10 % SDS	50 μl	50 μl	50 μl
H_2O	1.675 ml	1.175 ml	0.343 ml
10 % APS	20 μl	25 μl	25 μl
TEMED	2.5 μl	2.5 μl	2.5 μl

Stacking gel:	5%
Acrylamide/ Bisacrylamide (37.5:1)	1.35 ml
0.5 M Tris pH 6.8	0.625 ml
10 % SDS	25 µl
H_2O	1.53 ml
10 % APS	12.5 µl
TEMED	2.5 µl
Electrophoresis buffer (10 x):	50 mM Tris
	384 mM glycine
	0.1% SDS

3.2.4.3   Western blot

Proteins were blotted to nitrocellulose membranes (Schleicher & Schuell) using the Trans-Blot SD Semidry Transfer Cell (Bio-Rad). A piece of nitrocellulose membrane and two pieces of filter paper and two sponges of the same size as the gel were soaked with transfer buffer. A sponge, a piece of filter paper, the nitrocellulose membrane, the gel, another piece of filter paper and again a sponge were packed. Then, air bubbles were removed by rolling a test tube over the sponge, and subsequently the package was clamped into the transfer tank with the nitrocellulose facing the anode. Blotting was performed with 100 V for 1 h. Proteins were detected after 2 min incubation in Ponceau staining solution.

The membranes were labeled with a pen and washed several times with H_2O to remove the Ponceau staining solution. Unspecific binding sites were blocked by incubation in TBST (TBS, 0.05% Tween 20), 5% skim milk powder, 0.02% NaN3 either 1 h at RT or o/n at 4°C. Then incubation with the first antibody was performed in 5-10 ml TBST (used also in the following washing and incubation steps) at 4°C o/n. After five washing steps of 15 min with ca. 200 ml buffer each, incubation with the secondary antibody, coupled to peroxidase, was performed in 15 ml buffer at RT for 1 h followed by washing 5x 10 min in 200 ml buffer. The blotted proteins were detected using the ECL Western blotting detection system (Amersham-Pharmacia) according to the manufacturer's instructions. The membrane was exposed to BIOMAX-MR autoradiography films (Eastman-Kodak) for different time periods and films were developed using an automatic film developing machine.

Transfer buffer (1 l):   **Ponceau solution (100 ml):**

Tris base   5.8 g   Ponceau S   0.5 g

Glycine   2.9 g   Glacial acetic acid   1 ml

SDS   0.37 g H_2O 98.5 ml

Methanol   200 ml

H_2O to 1l

Antibody dilution

rat anti-HA tag   1 : 1000
Roche Diagnostics, Mannheim, Germany

mouse anti-myc tag   1 : 1000
Santa Cruz Biotechnology, Heidelberg, Germany

goat anti-mouse peroxidase coupled   1 : 5000
Jackson, Hamburg, Germany

goat anti-rat peroxidase coupled   1 : 5000
Jackson, Hamburg, Germany

3.2.5   Yeast cell culture

3.2.5.1   Competent yeast cells

To produce competent yeast cells, first a preculture had to be prepared: 10 ml YEPD-medium was inoculated by a colony of the yeast strain Y 187, respectively AH109. The preculture was shaken overnight at 30°C.

The next day, the preculture was added to 250 ml of fresh YEPD-medium and let grow at 30°C until it reached a density of 0,6 at OD_{600}. The cells were harvested in ten 50 ml Falcon tubes at 2000 Upm (930 x g, 5 min, 4°C). The supernatant was removed and the cells were resuspended in 12,5 ml SBEG-solution (each) and subsequently pelleted another time. The resulting cell pellet was resuspended in 500 µl SBEG-solution. The 500 µl cellsuspension was splitted into 100 µl aliquots, filled into microlitertubes and put into liquid nitrogen. The aliquots were stored at - 80°C.

YEPD medium: to 800 ml H_2O add:

for liquid medium: 10 g yeast extract
                                                   20 g peptone
                                                   20 g dextrose
                                                   add H_2O to 1 liter, autoclave

for solid medium: add 14 g agar before
                                                   autoclaving

SBEG solution: 91,1 g Sorbitol
                                                            5 ml Bicine 1M pH 8,35
                                                            15 ml Ethylenglycol (3%)
                                                            add 500 ml H2O

3.2.5.2   Transformation into yeast

For a transformation, a microlitertube with 100 μl competent yeast cells (Y187 or AH109) was thawed quickly in a waterbath at 37°C. Subsequently, 1 μg of the plasmid pGBKT7, respectively pGADT7, was pipetted into the thawed yeast cells of the appropriate yeast strain and mixed carefully by the pipet. Afterwards, 750 μl PEG/Bicine-solution was added and again mixed by the pipet. First of all, this reaction was incubated at 30°C for 1 h, then at 45°C for 5 min. The next step was to pellet the cells for 2 min at 3500 Upm (ca. 2700 x g, table centrifuge). The supernatant was removed by a pasteurpipet and the pellet was resuspended in 1ml NB-buffer by a pipet. Again, cells were pelleted, as described above, but only 800 μl of the supernatant was removed. The pellet was resuspended in the remaining 200 μl supernatant and plated on an appropriate yeast plate.

Bicine: stock solution pH 8,35, sterile

PEG/Bicine solution: PEG 1000 (40%)
                                                            Bicine, pH 8,35, sterile

NB buffer: 3 ml NaCl 5M
(0,15M NaCl/10mM Bicine)   1 ml Bicine 1M pH 8,35, sterile

Transformed yeast cells were grown to an OD_{600} of 0,6 in YEPD medium. Yeast cells were stored in 15% glycerol at -80 °C.

3.2.5.3   Mating and selection by a robot device

The steps involving a robotic workstation (Biomek 2000; Beckman Coulter) were performed in the lab of Peter Uetz in the 'Institut für Toxikologie und Genetik' in Karlsruhe.

The prey array, consisting of 111 haploid yeast transformants, was divided onto two plates, lacking leucine (the transformed yeast vector pGADT7 provides a leucine auxotrophy). By applying 5μl of appropriate yeast glycerol stock, 96 colonies were placed on the first plate and 15 on the second one (single-well microtiter plates). For reasons of transportabability the yeast-transformed bait array was treated the same

way, apart from being placed on plates lacking tryptophan. The second prey plate was splitted into triplets of 3 x 32 individual colonies. The 17 'free places' per third were filled up with preys from the first plate. This procedure was done by hand in our lab.

By robot device, each element on the prey plate was quadruplicated, thus we obtained 384 elements per plate. The quadruplication assures reproducibility of screening results.

Bait colonies from -Trp plates were picked and grown overnight in 20 ml YEPD at 30°C. The bait-medium was transferred into empty microtiter plates. The pins of the 384-pin replicator were dipped into the BD fusion-expressing culture and placed directly onto a fresh single-well microtiter plate containing solid YEPD medium. This procedure was repeated for each of the 112 baits.

Between transfer steps, the tool must be sterilized by sequential immersion into a 20% bleach solution (20sec), sterile water (1 sec), 95% ethanol (20 sec), and sterile water (1 sec). The level of these liquids should be 2 to 4 mm from the base of the pin and care must be taken that the ethanol does not evaporate.

In the next step, the prey array, transformed into haploid Mat a yeast strain, was picked up with sterilized pins and transferred directly onto the Mat α colonies expressing a single protein as a BD fusion, so that each of the 384 BD yeast spots per plate received different AD yeast cells. The plates were incubated for 1 or 2 days at 30°C to allow mating.

For selection the colonies were transferred to single-well microtiter plates containing solid -Leu -Tryp dropout medium using the sterilized pinning tool. The colonies were grown for 2 days at 30°C until they were 1mm in diameter. This was an essential control step because only diploid cells that contain Leu and Trp markers on pGADT7 and pGBKT7, respectively, will grow on this medium. This step also helps recovery of the colonies and increases the efficiency of the next selection step.

For the next step the colonies were transferred to a single-well microtiter plate containing solid -His -Leu -Trp (+ 3AT) dropout medium using the sterilized pinning tool and grow at 30°C for up to 10 days (or longer if there is little or no background growth) to select two-hybrid positive diploids.

The stringency of the screen can be varied by adding different amounts of 3AT, an inhibitor of the His3 gene product. In many cases (10% to 20%), the haploid strain expressing the BD fusion has transcriptional self-activation properties. These haploid

strains can be titrated on plates lacking histidine and containing increasing amounts of 3AT (3mM, 10mM, 20mM,

50mM). The highest level of 3AT tolerated should be added to the -His -Leu -Trp plates for selection of two-hybrid positive diploids. In many cases, the transcriptional activity is very strong ($>$200 mM 3AT), so that not all self-activators can be eliminated.

The interactions were scored by looking for growing colonies that were significantly above the background (by size) and that were present in at least 3 out of the 4 colonies. In rare cases 2 out of 4 growing colonies were scored positive, when these 2 colonies were extraordinary large.

Dropout medium:	to 800 ml H_2O add:
For liquid medium:	1,7 g yeast nitrogen base without amino acids 5 g ammonium sulfate 20 g dextrose 1,4 g dropout powder add H_2O to 1 liter, autoclave
For +3AT dropout medium:	add 3 mM 3-aminotriazole
For solid medium:	add 16 g agar before autoclaving cool to 45°C and pour into appropriate plates.

4 RESULTS

4.1. Generation of KSHV arrays in Y2H bait and prey vectors

4.1.1 Amplification of KSHV genes

To identify previously unknown viral protein-protein interactions in the human γ herpesvirus KSHV by performing a Y2H matrix screen, we amplified each viral ORF by PCR (Figure 10, Figure 11). For transmembrane proteins, extra- and intracellular domains were cloned separately. In total, we cloned 93 full-length proteins and 20 protein domains. Five genes for which splicing events are known were additionally generated from cDNA of KSHV positive cell lines or cDNA clones provided by other scientists (see Table 2), in order to amplify the spliced version. These five viral genes are: (i) one of the three alternatively spliced transcripts encoded by the K8 locus of KSHV (Gruffat et al., 1999; Lin et al., 1999; Seaman et al., 1999; Sun et al., 1998; Zhu et al., 1999), (ii) K8.1B (one of two alternatively spliced proteins identified by Chandran et al.(Chandran et al., 1998) in the genomic K8.1 region), (iii) the spliced gene product of ORF57 (Bello et al., 1999; Kirshner et al. 2000; Lukac et al., 1998; Lukac et al., 1999), (iv) the spliced K10.5/10.6 transcript encoding vIRF-3 (also termed LANA-2) (Rivas et al., 2001; Lubyova and Pitha, 2000) and (v) one of the eight exons of the K 15 gene (Choi et al., 2000b; Glenn et al., 1999; Poole et al., 1999). K 15 exists in two variants, M and P. It is thought that the P variant (for 'prototype') represents the original KSHV sequence and that the M variant (for 'minor') is the result of a recombination event with a currently unknown related rhadinovirus (Choi et al., 2000b; Glenn et al., 1999; Poole et al., 1999). The P variant was used as a template for the K15 (spliced) PCR product.
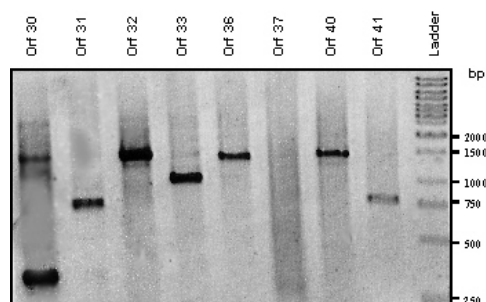
Figure 10: PCR products.
7 out of 113 PCR products. The generation of ORF 37 failed here, yet succeeded later on.
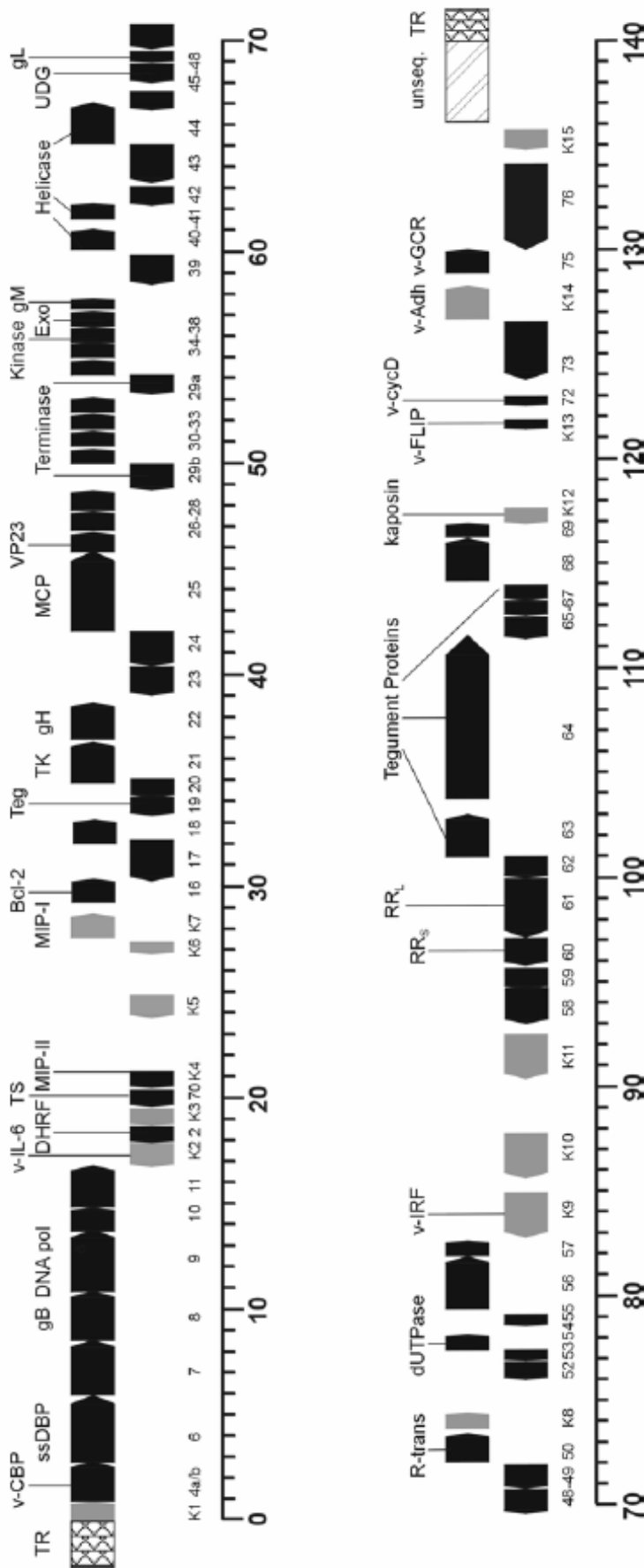
Figure 11: The KSHV-genome:
The KSHV genome consists of approximatly 100 genes, among them numerous glycoproteins, three versions of which were generated: a full length PCR-product, a cytoplasmatic and an external domain.

4.1.2   Adding attB sites to both ends of the PCR-product

First, each gene was individually amplified by PCR using forward and reverse primers with a similar annealing temperature of approximately 60°C. The internal forward primer contained a 12 nucleotide partial attB1 site, a translational initiation consensus sequence (KOZAK), the initiation codon ATG, and 15 to 22 homologous nucleotides. The internal reverse primer contained a 12 nucleotide partial attB2 site, a stop codon and 15 to 22 homologous nucleotides. By reamplification with common 29 nucleotide forward and reverse primers the complete attB1 and attB2 sites were added to both ends (Figure 12).
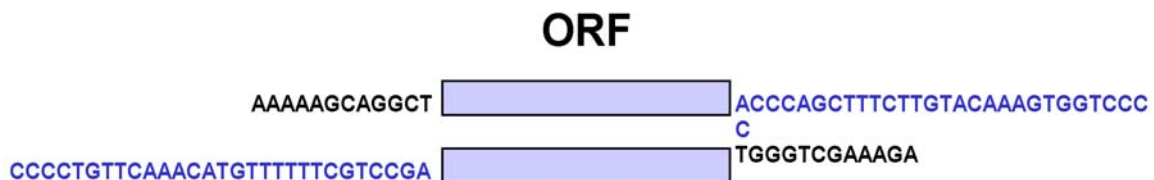
Figure 12:   PCR-product with attB1 and attB2 sites.
Indicated in black are the partial attB-sides of the internal individual primer. Indicated in blue are the external primers, which complete the attB-sites in the second PCR round.

4.1.3   Cloning the PCR-products into the entry vector

Each PCR-product was cloned into the entry vector pDONR207 by recombinatorial cloning (RC). The collection of KSHV-genes in this vector represents the KSHV ORFeome.

Starting with these vectors, the whole array or single genes can easily be subcloned into different destination vectors. Thus, an entire genome or subset of genes of interest can be examined in various ways in a short amount of time.

4.1.4   Subcloning into the bait and prey vector

Subsequently, the array was subcloned into the Y2H bait and prey vectors pGBKT7 and pGADT7, which contain kanamycin and ampicillin resistance genes. As all three vectors contain different resistance genes, the subcloning could be performed in a one-step reaction (Figure 13). The two arrays thus consist of each viral ORF fused to either the DNA binding or activation domain.
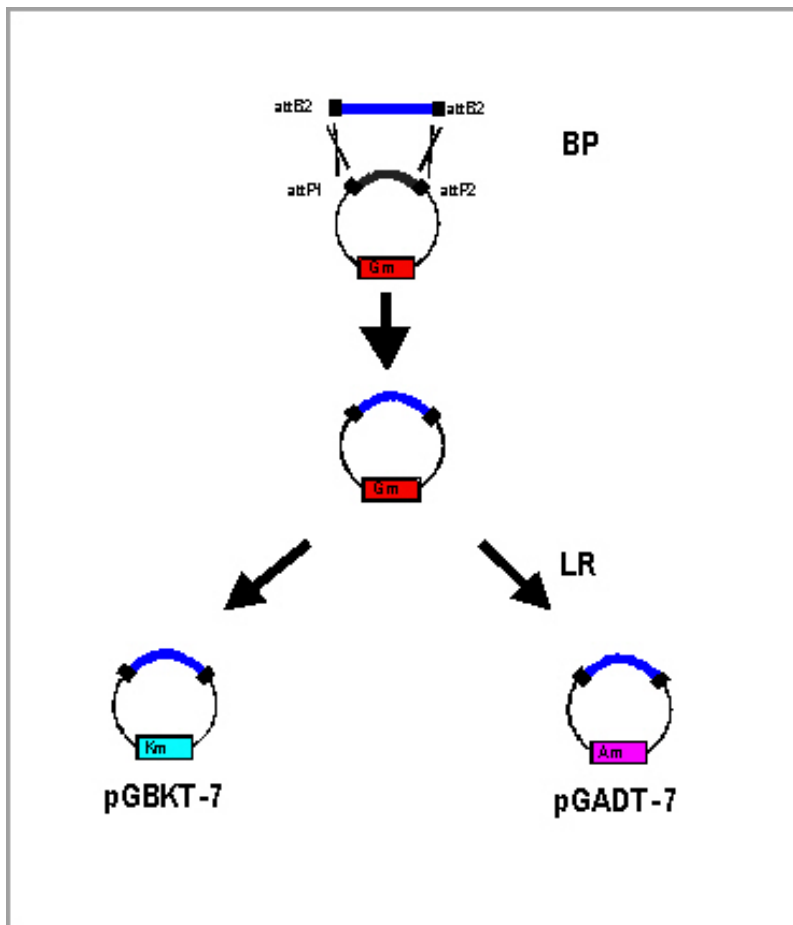
Figure 13: **Recombinatorial cloning.**
113 PCR-products were cloned into the donor vector by BP reaction. Subsequently, these sequences were subcloned in one step into two different vectors. The transformed E.colis were spread on kanamycin and ampicillin plates.

4.1.5 Transformation into yeast and arrangement of the plates

The bait array in vector pGBKT7 was transformed into the haploid Y187 yeast strain of the Mat a mating type, the prey array in the vector pGADT7 into the AH 109 yeast strain of the Mat α mating type. Transformed yeast cells were grown to an OD_{600} of 0,6 in YEPD medium and stored in 15% glycerol at -80 °C.

The 111 haploid prey transformants were distributed onto two plates, lacking leucine (the transformed yeast vector pGADT7 provides a leucine auxotrophy). 96 colonies were placed on the first plate and 15 colonies on the second one (single-well microtiter plates) by applying 5µl out of the yeast glycerol stock. The yeast-transformed bait array was placed on plates lacking tryptophan.

The second prey plate was divided into triplets of 3 x 32 individual colonies. The 17 'free places' per triplet were filled with preys from the first plate.

	1	2	3	4	5	6	7	8	9	10	11	12
A	pGADT7 empty	DR1	DR2	DR2/1	ORF73 c-term	vIRF3	ORF74 cyt/d2	ORF72	K13= ORF71	ORF68 ext/d1	ORF57 FL	ORF50
B	K1 FL	K1 cyt/d2	ORF4	ORF7	ORF8 cyt/d2	ORF9	ORF10	ORF11	K2	ORF02	K3 cyt1/d1	K3 cyt2/d2
C	ORF70	K4	K4.1	K4.2	K5 cyt1/d1	K5 cyt2/d2	K6	K7	ORF16	ORF17	ORF18	ORF19
D	ORF20	ORF21	ORF23	ORF24	ORF25	ORF26	ORF27	ORF28 cyt/d2	ORF28 ext/d1	ORF29 b	ORF30	ORF31
E	ORF32	ORF33	ORF29 a	ORF34	ORF35	ORF36	ORF37	ORF38	ORF39	ORF40	ORF41	ORF42
F	ORF43	ORF44	ORF45	ORF46	ORF47 cyt/d2	ORF48 cyt/d2	ORF48 ext/d1	ORF49	K8 spliced	ORF52	ORF53	ORF54
G	ORF55	K9	K10	K10.5	K11	ORF58	ORF60	ORF61	ORF62	ORF65	ORF66	ORF67
H	ORF67.5	ORF68 cyt/d2	ORF69	K12 cyt/d2	K14	K14.1	ORF75 II	K15	K8.1	K8.1 spliced	K8.1 cyt/d2	K15 spliced

Plate I: 96 haploid prey transformants on a single-well microtiter plate

	1	2	3	4	5	6	7	8	9	10	11	12
A	K1 ext/d1	ORF68 FL	ORF74 FL	K3 FL	K1 ext/d1	ORF68 FL	ORF74 FL	K3 FL	K1 ext/d1	ORF68 FL	ORF74 FL	K3 FL
B	K5 FL	ORF22 FL	ORF28 FL	ORF39 FL	K5 FL	ORF22 FL	ORF28 FL	ORF39 FL	K5 FL	ORF22 FL	ORF28 FL	ORF39 FL
C	ORF47 FL	ORF48 FL	K8	ORF59	ORF47 FL	ORF48 FL	K8	ORF59	ORF47 FL	ORF48 FL	K8	ORF59
D	ORF53	ORF6 I	ORF63 I	ORF56	ORF53	ORF6 I	ORF63 I	ORF56	ORF53	ORF6 I	ORF63 I	ORF56
E	ORF57 spl	ORF63 II	DR1	DR2	ORF57 spl	ORF63 II	DR1	DR2	ORF57 spl	ORF63 II	DR1	DR2
F	DR 2/1	K10	vIRF3	ORF74 cyt/d2	DR 2/1	K10	vIRF3	ORF74 cyt/d2	DR 2/1	K10	vIRF3	ORF74 cyt/d2
G	ORF72	K13	ORF68 ext/d1	ORF57 FL	ORF72	K13	ORF68 ext/d1	ORF57 FL	ORF72	K13	ORF68 ext/d1	ORF57 FL
H	ORF50	ORF61	ORF58	pGADT7 empty	ORF50	ORF61	ORF58	pGADT7 empty	ORF50	ORF61	ORF58	pGADT7 empty

Plate II: 3x32 prey transformants, 17 transformants of first plate reoccur on the second one

57

4.1.6 The robot-assisted steps
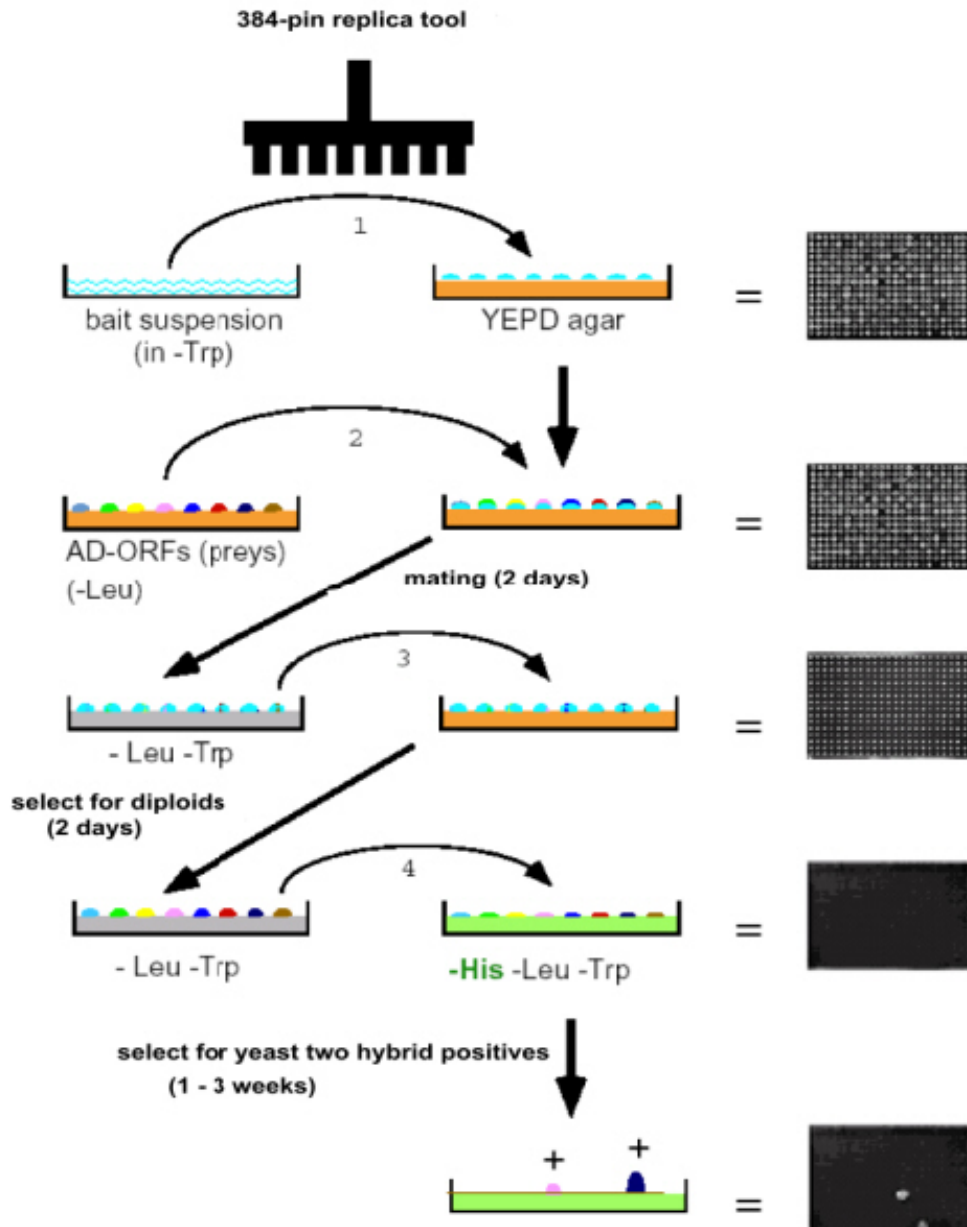
Figure 14: **Mating and selection of diploids and two-hybrid positives, using an automated pinning device**
Step 1: Haploid yeast cells expressing the binding domain-ORF fusion protein (bait) were transferred from a liquid culture to solid medium. Step 2: Haploid cells from the activation domain array (prey-array) were transferred with the same tool onto the BD-ORF fusion-expressing cells for mating. Step 3: After 2 days of growth, the colonies were transferred to -Leu-Trp medium to allow growth of diploids. Step 4: After another 2 days of growth, the diploid cells were transferred to two-hybrid selective plates (-Trp-Leu-His), on which visible colonies started to grow after a few days. (Weak two-hybrid positives may, however, take up to 3 weeks or more to form colonies.) (according to Cagney et al., 2000)

The next steps were robot-assisted: Individual yeast transformants of both arrays were mated with each transformant of the opposite mating type. Diploid yeast transformants were transfered onto plates selecting for the presense of both bait and prey vectors, and subsequently onto plates selecting for activation of the Gal4-controlled HIS auxotrophy (Figure 14).

4.2   Identification of KSHV protein-protein interactions

4.2.1   Analysis of Y2H data

The Y2H matrix screen of 113 viral KSHV genes and more than 12,000 viral protein interactions resulted in the identification of 125 interacting protein pairs, corresponding to approximately 1% of the total number of pairs. Y2H screens generate significant numbers of false positive interactions which are not reproducible. This occurrence of histidine auxotroph colonies can result from mutations of the host strain. In order to enable rapid detection of reproducible two-hybrid interactions, we tested every pairwise combination in quadruplicates. Interactions in the Y2H screen were scored positive if three or four out of four matings were positive (Figures 15a-c) or if two out of four were positive and the colonies were large compared to average colonies (Figure 15d).
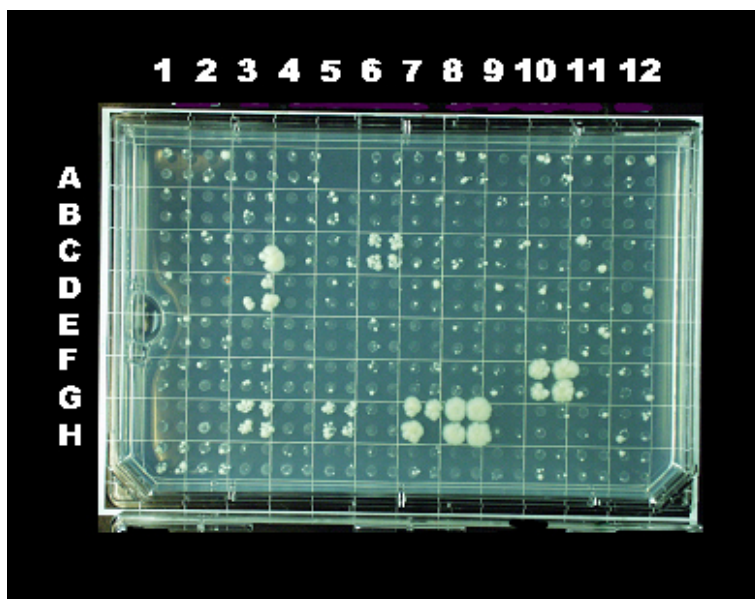
Figure 15a: Protein-protein interactions of bait ORF 60
Four out of four colonies:
6 C: K5d2
10F: ORF 52

3 G: K10
5 G: K11
8 G: ORF 61
1 H: ORF 67.5 (weak)
2 H: ORF 68d2 (weak)
Three out of four:
3 D: ORF 23
7 G: ORF 60
ORF 60 serves as an example for a highly connected viral protein. The interactions visible here are not the only ones ORF 60 is involved in, as ORF 60 also shows interactions as bait with the prey plate II and as prey protein with other baits.
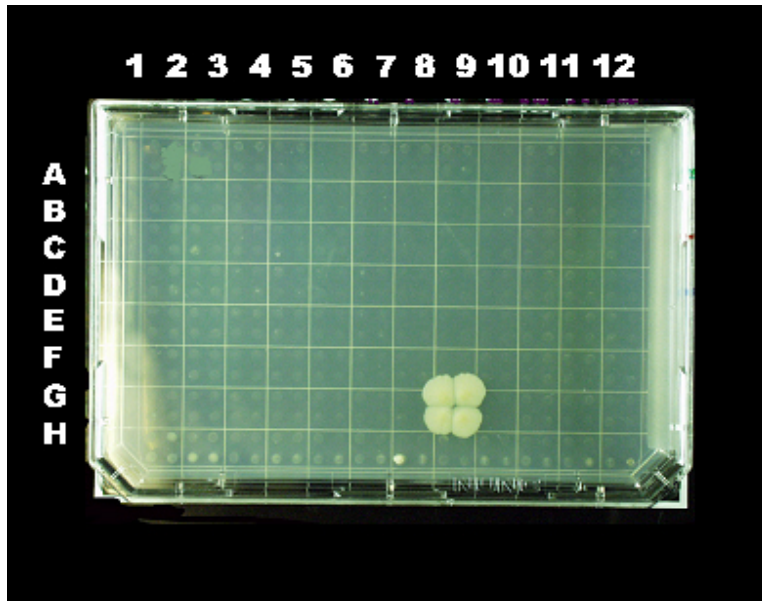
Figure 15b: Protein-protein interactions of bait ORF 61
8 G: ORF 61
Single strong interaction (four out of four). In contrast to bait ORF 60 hardly any background is visible.
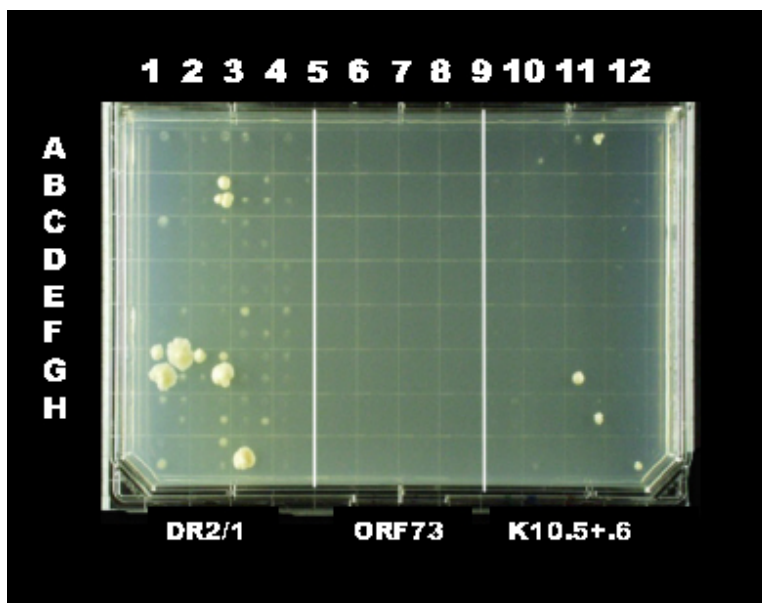
Figure 15c: Protein-protein interactions of baits DR2/1; ORF73 (c-terminal); vIRF3
Interacting preys DR2/1:
three out of four:
1 F: DR2/1

2 F: K 10
false positive:
2 B: two out of four
3 H: one out of four
ORF 73 (c-terminal): no colonies growing
K10.5+K10.6:
false positive:
11A: one out of four
11F: one out of four
11G: one out of four
12H: one out of four

One of the disadvantages limiting the number of detectable interactions is the high percentage of selfactivating baits (Figure 15e). These sequences encode polypeptides that, when fused to a binding domain, can activate transcription on their own. 15 proteins were found to be strong activators when fused to the Gal4 DNA-binding domain, and thus could only be analyzed under more stringent conditions in the bait vector, using the competitive inhibitor 3AT. But even under more stringent conditions, nine baits remained self-activating. However, self-activating ORFs in the bait vector can still be tested unidirectionally in the prey vector as fusions with the Gal4 activation domain and are thus not completely lost for the screen.
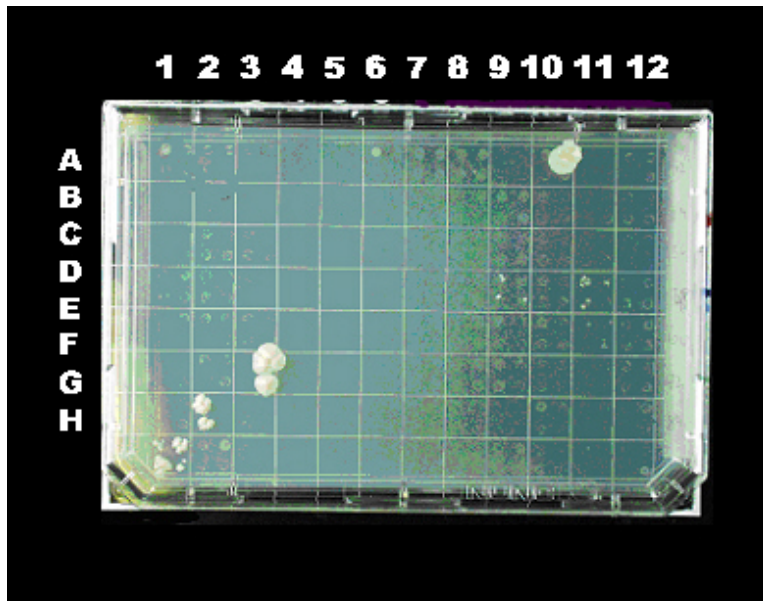
Figure 15d: Protein-protein interactions of bait ORF 23
Two out of four growing colonies were counted as positive interaction if they grew large and against faint background.
Interacting preys:
four out of four:
1 H: ORF 67.5
three out of four:
9 D: ORF 28/d1
11D: ORF 30
both better visible after a longer time of incubation.
two out of four:
3 F: ORF 45

2 G: K 9
false positive:
10A: one out of four
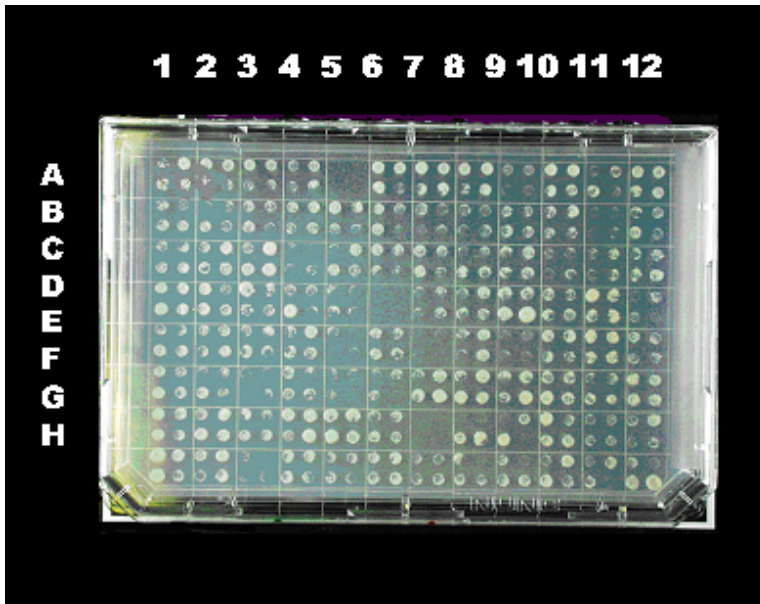
Figure 15e: Protein –protein interactions of ORF 30:
Selfactivating bait:
An inherent problem of Y2H screens is the high number of selfactivating baits (10-20%). This number can be reduced by increasing the stringency of the screen adding higher amounts of 3AT. In our case, the transcriptional activity of nine baits (from initially 15 selfactivating baits) was so strong that they could not be eliminated. Among the self-activating baits was ORF 30.

4.2.2   Protein-protein interactions identified by Y2H matrix screen

In total, 12.432 protein-protein interactions between different KSHV ORFs were tested and 125 were found to be positive. Three genes were introduced into the screen in only one of the two Y2H vectors:

        1) ORF28 d2 and ORF63 II could only be cloned into the prey vector (pGADT7).

        2) ORF73, which contains numerous internal repeats, could not be amplified by PCR, neither by using genomic-DNA, nor a cDNA clone. Instead, the C-terminal part of ORF73 was used as a bait. Unfortunately, it turned out to be self-activating.

Almost all interactions could only be observed in one direction, i.e. the interaction could only be detected if one interaction partner was fused to the activation domain and the other to the binding domain, but not vice versa.

In figure 16 the baits are indicated on the vertical axis and the preys on the horizontal axis. The mirror axis is indicated by red boxes, selfactivating baits by yellow boxes. The 125 positive protein interactions are indicated by black boxes.

The histogram on top of the table indicates the number of interaction partners of each viral ORF. Along the viral genome, proteins with many interaction partners cluster in two regions: between ORF23 and ORF31 and between ORF52 and ORF67.5.
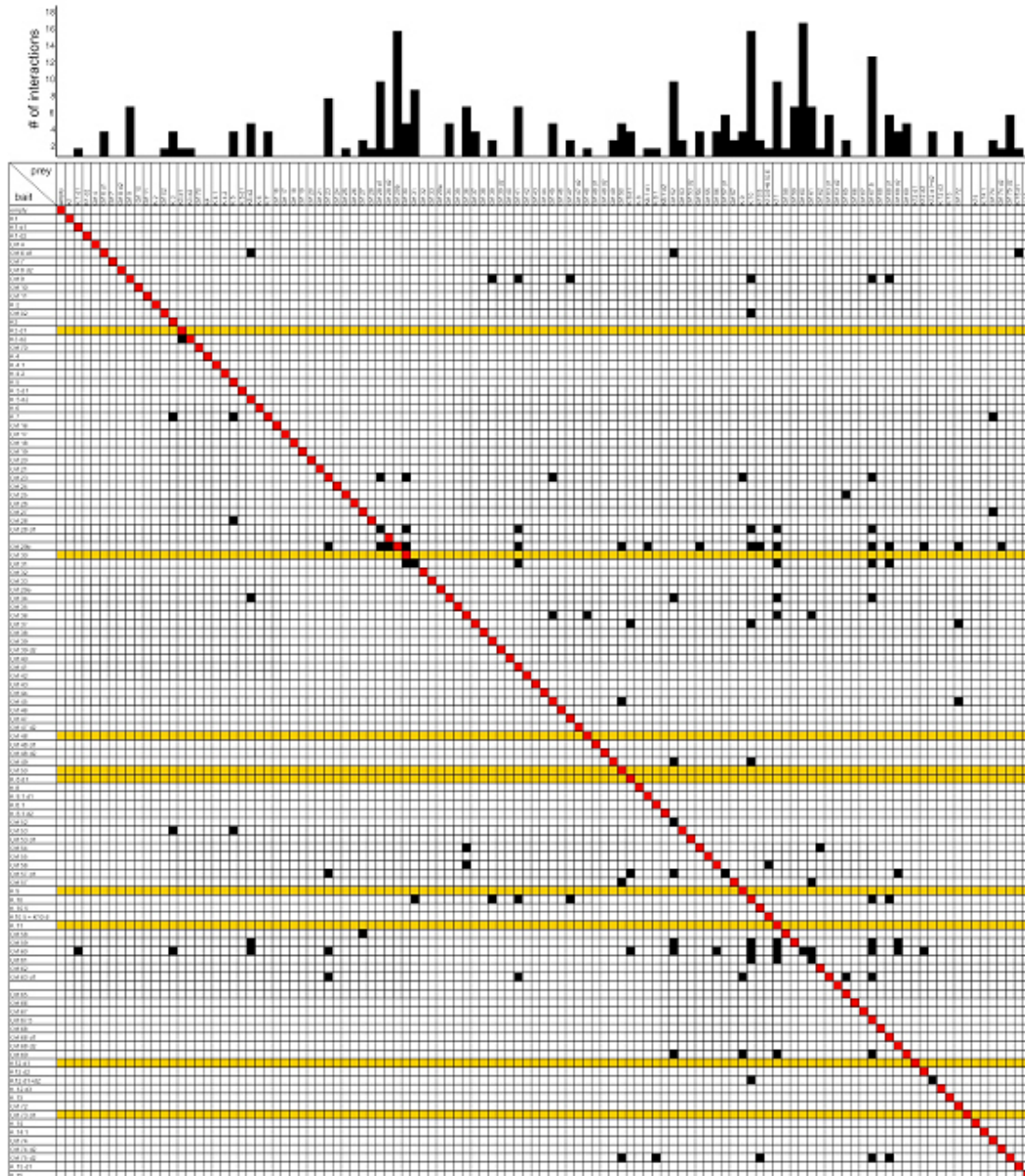
Figure 16:   Protein-protein interactions in KSHV identified by yeast two-hybrid matrix screen
Each of the individual bait clones was tested against each of the individual prey clones. Bait clones are scheduled on the vertical axis, prey clones on the horizontal axis. Self-activating baits are indicated in yellow. 125 positive protein interactions are indicated by black boxes, the mirror axis by red boxes.
Distribution of protein interactors along the KSHV genome: There are two clusters of viral hubs between ORF23 and ORF31 and between ORF52 and ORF67.5 within the KSHV genome.

4.3 Characterization of interactions

4.3.1 Classification of protein interactions in KSHV

Based on the known or suggested function of the participating proteins the interactions were divided into five functional cat

egories: DNA-replication, gene regulation, virion structure / morphogenesis, virus-host interactions and unknown function. Viral proteins were divided into 4 classes depending on wether they are specific for KSHV or possess orthologs in HSV- 1 (α), CMV (β) or EBV (λ).

To reduce the number of false positive interactions, we scrutinized all 125 interactions detected by co-immunoprecipitation.

4.3.2 Co-immunoprecipitation of Y2H positive interactions

The Y2H bait and prey vectors used in this study express the insert either as c-Myc- or HA-tagged protein under the control of a T7 promotor. This feature allowed to test each protein- protein interaction by co-immunoprecipitation (CoIP) without the need of subcloning the viral genes into new vectors. Bait and prey vectors of interacting partners were transfected into 293 cells. Simultaneously, cells were infected with recombinant vacciniavirus expressing T7 polymerase. Cell lysates were split into two parts and precipitated with either anti-c-Myc or anti-HA antibodies. Each precipitate was separated on two polyacrylamide gels. On the left side of each gel precipitating and on the right side co-precipitating proteins are indicated. The precipitations were performed to control for expression levels and correct size. Out of the 125 viral protein-protein interactions found with the Y2H-system, 62 could were also detected by co-immunoprecipitation (approximately 50 percent) (Figure 17). This number of false positive interactions was also reported in the literature (Mrowka et al., 2001).
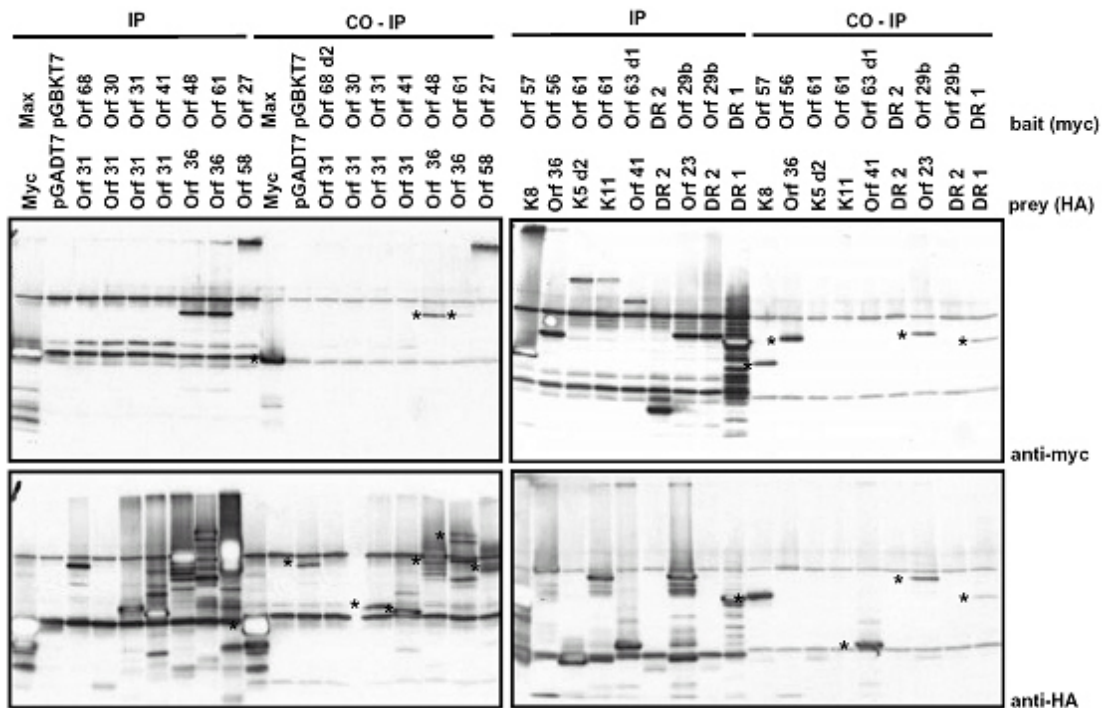
Figure 17:   Co-immunoprecipitations
Protein interactions were verified by CoIP. Cloned KSHV ORFs were expressed from pDEST-GBKT7 and pDEST-GADT7 bait and prey vectors as myc- or HA-tagged proteins by transfection into 293 cells and simultaneous infection with recombinant vaccinia virus vTF-7 expressing T7 RNA polymerase. Cell lysates were split and precipitated with either anti-myc or anti-HA antibodies. Each precipitate was separated on two polyacrylamide gels. On the left side of each gel precipitating and on the right side co-precipitating proteins are indicated. Coprecipitating proteins are indicated by asterisks (*).

4.3.3.   Expression, function and homologues genes of interacting KSHV proteins

For each interacting KSHV protein, the function or certain characteristics as portrayed in the literature and homologous genes in other herpesviruses were listed in the Figure below (Figure 18). By adding these informations, the plausibility of protein interactions can be assessed comparing functional information of interacting partners (as far as a function it is known). Listing homologous genes in other herpesvirus genera may hint at conserved protein interactions. It may thus provide the opportunity to predict interactions in other herpesvirus genomes.

The proteins were divided into five functional groups (red: *DNA replication* and nucleotide metabolism, yellow: *gene regulation* and signalling, green: virion *structure* and morphogenesis, blue: proteins involved in virus-*host interaction*, grey: *unknown* function). More than 70 % of all protein interactions occurred between viral proteins belonging to different functional classes. In general, interacting proteins are not more

likely to belong to the same functional class than random pairs of proteins (only 1.1-fold enrichment over random pairs of proteins, p=0.334), suggesting that the majority of viral proteins either have multiple, previously unknown functions, or are assigned incorrectly. Significantly increased numbers of intra-class interactions were only identified between proteins belonging to the *gene regulation* and *unknown* functional classes. Whereas interactions between proteins involved in *host interaction* were most highly suppressed (as expected, interactions between proteins involved in both *host interaction* and *replication* were significantly increased. Interactions between proteins with *unknown* function are significantly overrepresented, implying that they are within the same functional group (other than host interaction) and part of identical complexes or processes. Subsequently, we partitioned viral ORFs into 8 phylogenetic classes based on wether they are conserved across HSV-1 (α), CMV (β), and EBV (γ). The KSHV-specific phylogenetic class is dominated by proteins involved in *host interaction*, and the $\alpha\beta\gamma$ phylogenetic class (containing proteins present in all three subfamilies) by structural proteins and those involved in replication.

DNA replication, nucleotide metabolism (DN)

#	bait		exp*	α	β	γ	prey		exp*	α	β	γ	COIP
1	K 10	vIRF-4	lat/lyt	-	-	-	Orf 41	helicase/primase subunit	lytic 3	-	-	BBLF-3	1
2	Orf 2	DHRF	lytic 2	-	-	-	K 10	vIRF-4	lat/lyt	-	-	-	1
3	Orf 6	ssDNA binding protein	lytic 1	UL 29	UL 57	BALF-2	K 5	ubiquitin ligase	lytic 1	-	-	-	1
4	Orf 6	ssDNA binding protein	lytic 1	UL 29	UL 57	BALF-2	K 15	LAMP	latent	-	-	-	0
5	Orf 6	ssDNA binding protein	lytic 1	UL 29	UL 57	BALF-2	Orf 52	unknown	lytic 2	-	-	BLRF-2	0
6	Orf 9	DNA polymerase	lytic 1	UL 30	UL 54	BALF-5	K 10	vIRF-4	latent	-	-	-	0
7	Orf 9	DNA polymerase	lytic 1	UL 30	UL 54	BALF-5	Orf 39	gM glycoprotein	lytic 2	UL 10	UL 100	BBRF-3	0
8	Orf 9	DNA polymerase	lytic 1	UL 30	UL 54	BALF-5	Orf 41	helicase/primase subunit	lytic 3	-	-	BBLF-3	0
9	Orf 9	DNA polymerase	lytic 1	UL 30	UL 54	BALF-5	Orf 47	gL glycoprotein	lytic 2	UL 1	UL 115	BKRF-2	0
10	Orf 9	DNA polymerase	lytic 1	UL 30	UL 54	BALF-5	Orf 67.5	packaging protein/terminase	lytic	UL 33	UL 51	BFRF-4	1
11	Orf 9	DNA polymerase	lytic 1	UL 30	UL 54	BALF-5	Orf 68	packaging protein	lytic	UL 32	UL 52	BFLF-1	0
12	Orf 28 d1	unknown	lytic 3	-	-	BDLF-3	Orf 41	helicase/primase subunit	lytic 3	-	-	BBLF-3	1
13	Orf 29b	packaging protein/terminase	lytic 3	UL 15	UL 89	BDRF-1	Orf 41	helicase/primase subunit	lytic 3	-	-	BBLF-3	1
14	Orf 29b	packaging protein/terminase	lytic 3	UL 15	UL 89	BDRF-1	Orf 54	dUTPase	lytic 3	UL 50	UL72	BLLF-3	0
15	Orf 31	unknown	lytic 3	-	UL 92	BDLF-4	Orf 41	helicase/primase subunit	lytic 3	-	-	BBLF-3	1
16	Orf 36	kinase	lytic 3	UL 13	UL 97	BGLF-4	Orf 54	dUTPase	lytic 3	UL 50	UL72	BLLF-3	0
17	Orf 36	kinase	lytic 3	UL 13	UL 97	BGLF-4	Orf 61	ribonucleotide reductase	lytic	UL 39	UL 45	BORF-2	1
18	Orf 37	alkaline exonuclease	lytic 3	UL 12	UL 98	BGLF-5	K 8	k-bZIP, RAP	lytic 1	UL 9	UL 84	BZLF-1	1
19	Orf 37	alkaline exonuclease	lytic 3	UL 12	UL 98	BGLF-5	K 10	vIRF-4	lat/lyt	-	-	-	0
20	Orf 37	alkaline exonuclease	lytic 3	UL 12	UL 98	BGLF-5	Orf 72	vCyc	latent	-	-	-	1
21	Orf 54	dUTPase	lytic 3	UL 50	UL72	BLLF-3	Orf 36	kinase	lytic 3	UL 13	UL 97	BGLF-4	1
22	Orf 54	dUTPase	lytic 3	UL 50	UL72	BLLF-3	Orf 62	assembly, DNA maturating protein	lytic 3	-	-	BORF-1	1
23	Orf 56	helicase/primase	lytic 2	UL 52	UL 70	BSLF-1	K 10.5	vIRF-3	latent	-	-	-	1
24	Orf 56	helicase/primase	lytic 2	UL 52	UL 70	BSLF-1	Orf 36	kinase	lytic 3	UL 13	UL 97	BGLF-4	1
25	Orf 57	immediate early	lytic 1	-	-	BMLF-1	Orf 61	ribonucleotide reductase	lytic	UL 39	UL 45	BORF-2	1
26	Orf 59	polymerase processivity factor	lytic 2	-	-	BMRF-1	K 5	ubiquitin ligase	lytic 1	-	-	-	0
27	Orf 59	polymerase processivity factor	lytic 2	-	-	BMRF-1	K 10	vIRF-4	lat/lyt	-	-	-	0
28	Orf 59	polymerase processivity factor	lytic 2	-	-	BMRF-1	K 11	vIRF-2	lytic 2	-	-	-	1
29	Orf 59	polymerase processivity factor	lytic 2	-	-	BMRF-1	Orf 52	unknown	lytic 2	-	-	BLRF-2	0
30	Orf 59	polymerase processivity factor	lytic 2	-	-	BMRF-1	Orf 67.5	packaging protein/terminase	lytic	UL 33	UL 51	BFRF-4	0
31	Orf 59	polymerase processivity factor	lytic 2	-	-	BMRF-1	Orf 68	packaging protein	lytic	UL 32	UL 52	BFLF-1	0
32	Orf 60	ribonucleotide reductase	lytic	UL 40	-	BaRF-1	K 1	transforming	lytic 3	-	-	-	0
33	Orf 60	ribonucleotide reductase	lytic	UL 40	-	BaRF-1	K 3	ubiquitin ligase	lytic 2	-	-	-	1
34	Orf 60	ribonucleotide reductase	lytic	UL 40	-	BaRF-1	K 5	ubiquitin ligase	lytic 1	-	-	-	0
35	Orf 60	ribonucleotide reductase	lytic	UL 40	-	BaRF-1	K 8	k-bZIP, RAP	lytic 1	UL 9	UL 84	BZLF-1	0
36	Orf 60	ribonucleotide reductase	lytic	UL 40	-	BaRF-1	K 10	vIRF-4	lat/lyt	-	-	-	0
37	Orf 60	ribonucleotide reductase	lytic	UL 40	-	BaRF-1	K 11	vIRF-2	lytic 2	-	-	-	0
38	Orf 60	ribonucleotide reductase	lytic	UL 40	-	BaRF-1	K 12	kaposin	lytic	-	-	-	0
39	Orf 60	ribonucleotide reductase	lytic	UL 40	-	BaRF-1	Orf 23	unknown	lytic 3	-	UL 117	BTRF-1	0
40	Orf 60	ribonucleotide reductase	lytic	UL 40	-	BaRF-1	Orf 52	unknown	lytic 2	-	-	BLRF-2	0
41	Orf 60	ribonucleotide reductase	lytic	UL 40	-	BaRF-1	Orf 56	helicase/primase	lytic 2	UL 52	UL 70	BSLF-1	1
42	Orf 60	ribonucleotide reductase	lytic	UL 40	-	BaRF-1	Orf 60	ribonucleotide reductase	lytic	UL 40	-	BaRF-1	1
43	Orf 60	ribonucleotide reductase	lytic	UL 40	-	BaRF-1	Orf 61	ribonucleotide reductase	lytic	UL 39	UL 45	BORF-2	1
44	Orf 60	ribonucleotide reductase	lytic	UL 40	-	BaRF-1	Orf 67.5	packaging protein/terminase	lytic	UL 33	UL 51	BFRF-4	1
45	Orf 60	ribonucleotide reductase	lytic	UL 40	-	BaRF-1	Orf 68	packaging protein	lytic	UL 32	UL 52	BFLF-1	1
46	Orf 61	ribonucleotide reductase	lytic	UL 39	UL 45	BORF-2	K 10	vIRF-4	lat/lyt	-	-	-	1
47	Orf 61	ribonucleotide reductase	lytic	UL 39	UL 45	BORF-2	K 11	vIRF-2	lytic 2	-	-	-	1
48	Orf 61	ribonucleotide reductase	lytic	UL 39	UL 45	BORF-2	Orf 61	ribonucleotide reductase	lytic	UL 39	UL 45	BORF-2	0
49	Orf 63	tegument	lytic 3	-	-	BOLF-1	Orf 41	helicase/primase subunit	lytic 3	-	-	BBLF-3	1

gene regulation, signalling (GR)

#	bait		exp*	α	β	γ	prey		exp*	α	β	γ	COIP
1	Orf 23	unknown	lytic 3	-	UL 117	BTRF-1	Orf 45	immediate early , tegument	lytic 1	-	-	BKRF-4	0
2	Orf 29b	packaging protein/terminase	lytic 3	UL 15	UL 89	BDRF-1	Orf 50	immediate early, RTA	lytic	-	-	BRLF-1	0
3	Orf 37	alkaline exonuclease	lytic 3	UL 12	UL 98	BGLF-5	K 8	k-bZIP, RAP	lytic 1	UL 9	UL 84	BZLF-1	1
4	Orf 45	immediate early, tegument	lytic 1	-	-	BKRF-4	Orf 50	immediate early, RTA	lytic	-	-	BRLF-1	0
5	Orf 45	immediate early, tegument	lytic 1	-	-	BKRF-4	Orf 72	vCyc	latent	-	-	-	0
6	Orf 36	kinase	lytic 3	UL 13	UL 97	BGLF-4	Orf 45	immediate early, tegument	lytic 1	-	-	BKRF-4	0
7	Orf 57	immediate early	lytic 1	-	-	BMLF-1	K 8	k-bZIP, RAP	lytic 1	UL 9	UL 84	BZLF-1	1
8	Orf 57	immediate early	lytic 1	-	-	BMLF-1	Orf 23	unknown	lytic 3	-	-	BTRF-1	1
9	Orf 57	immediate early	lytic 1	-	-	BMLF-1	Orf 50	immediate early, RTA	lytic	-	-	BRLF-1	0
10	Orf 57	immediate early	lytic 1	-	-	BMLF-1	Orf 52	unknown	lytic 2	-	-	BLRF-2	1
11	Orf 57	immediate early	lytic 1	-	-	BMLF-1	Orf 57	immediate early	lytic 1	-	-	BMLF-1	1
12	Orf 57	immediate early	lytic 1	-	-	BMLF-1	Orf 61	ribonucleotide reductase	lytic	UL 39	UL 45	BORF-2	1
13	Orf 57	immediate early	lytic 1	-	-	BMLF-1	Orf 68	packaging protein	lytic	UL 32	UL 52	BFLF-1	0
14	Orf 60	ribonucleotide reductase	lytic	UL 40	-	BaRF-1	K 8	k-bZIP, RAP	lytic 1	UL 9	UL 84	BZLF-1	0
15	Orf 75	tegument, FGARAT	lytic 3	-	-	BNRF-1	Orf 50	immediate early, RTA	lytic	-	-	BRLF-1	0

virion structure, morphogenesis (VS)

#	bait		exp*	α	β	γ	prey		exp*	α	β	γ	COIP
1	K 10	vIRF-4	lat/lyt	-	-	-	Orf 47	gL glycoprotein	lytic 2	UL 1	UL 115	BKRF-2	0
2	K 10	vIRF-4	lat/lyt	-	-	-	Orf 67.5	packaging protein/terminase	lytic	UL 33	UL 51	BFRF-4	1
3	K 10	vIRF-4	lat/lyt	-	-	-	Orf 68	packaging protein	lytic	UL 32	UL 52	BFLF-1	1
4	K 10	vIRF-4	lat/lyt	-	-	-	Orf 39	gM glycoprotein	lytic 2	UL 10	UL 100	BBRF-3	0
5	Orf 9	DNA polymerase	lytic 1	UL 30	UL 54	BALF-5	Orf 39	gM glycoprotein	lytic 2	UL 10	UL 100	BBRF-3	0
6	Orf 9	DNA polymerase	lytic 1	UL 30	UL 54	BALF-5	Orf 47	gL glycoprotein	lytic 2	UL 1	UL 115	BKRF-2	0
7	Orf 9	DNA polymerase	lytic 1	UL 30	UL 54	BALF-5	Orf 67.5	packaging protein/terminase	lytic	UL 33	UL 51	BFRF-4	1
8	Orf 9	DNA polymerase	lytic 1	UL 30	UL 54	BALF-5	Orf 68	packaging protein	lytic	UL 32	UL 52	BFLF-1	1
9	Orf 23	unknown	lytic 3	-	UL 117	BTRF-1	Orf 67.5	packaging protein/terminase	lytic	UL 33	UL 51	BFRF-4	0
10	Orf 25	major capsid antigen	lytic 3	UL 19	UL 86	BcLF-1	Orf 65	small basic capsid antigen	lytic 2	UL 35	UL 48/49	BFRF-3	0
11	Orf 28 d1	unknown	lytic 3	-	-	BDLF-3	Orf 67.5	packaging protein/terminase	lytic	UL 33	UL 51	BFRF-4	0
12	Orf 29b	packaging protein/terminase	lytic 3	UL 15	UL 89	BDRF-1	K 8.1	glycoprotein	lytic 3	-	-	-	0
13	Orf 29b	packaging protein/terminase	lytic 3	UL 15	UL 89	BDRF-1	K 10	vIRF-4	lat/lyt	-	-	-	0
14	Orf 29b	packaging protein/terminase	lytic 3	UL 15	UL 89	BDRF-1	K 10.5	vIRF-3	latent	-	-	-	0
15	Orf 29b	packaging protein/terminase	lytic 3	UL 15	UL 89	BDRF-1	K 11	vIRF-2	lytic 2	-	-	-	1
16	Orf 29b	packaging protein/terminase	lytic 3	UL 15	UL 89	BDRF-1	K 12	transforming	lytic	-	-	-	0
17	Orf 29b	packaging protein/terminase	lytic 3	UL 15	UL 89	BDRF-1	Orf 23	unknown	lytic 3	-	UL 117	BTRF-1	0
18	Orf 29b	packaging protein/terminase	lytic 3	UL 15	UL 89	BDRF-1	Orf 28 d1	unknown	lytic 3	-	-	BDLF-3	1
19	Orf 29b	packaging protein/terminase	lytic 3	UL 15	UL 89	BDRF-1	Orf 28 d2	unknown	lytic 3	-	-	BDLF-3	1
20	Orf 29b	packaging protein/terminase	lytic 3	UL 15	UL 89	BDRF-1	Orf 30	unknown	lytic 3	-	-	BDLF-3,5	1
21	Orf 29b	packaging protein/terminase	lytic 3	UL 15	UL 89	BDRF-1	Orf 41	helicase/primase subunit	lytic 3	-	-	BBLF-3	1
22	Orf 29b	packaging protein/terminase	lytic 3	UL 15	UL 89	BDRF-1	Orf 50	immediate early, RTA	lytic	-	-	BRLF-1	0
23	Orf 29b	packaging protein/terminase	lytic 3	UL 15	UL 89	BDRF-1	Orf 54	dUTPase	lytic 3	UL 50	UL72	BLLF-3	0
24	Orf 29b	packaging protein/terminase	lytic 3	UL 15	UL 89	BDRF-1	Orf 67.5	packaging protein/terminase	lytic	UL 33	UL 51	BFRF-4	1
25	Orf 29b	packaging protein/terminase	lytic 3	UL 15	UL 89	BDRF-1	Orf 68	packaging protein	lytic	UL 32	UL 52	BFLF-1	1
26	Orf 29b	packaging protein/terminase	lytic 3	UL 15	UL 89	BDRF-1	Orf 72	vCyc	latent	-	-	-	0
27	Orf 29b	packaging protein/terminase	lytic 3	UL 15	UL 89	BDRF-1	Orf 74	GPCR	lytic 1	-	-	-	0
28	Orf 31	packaging protein/terminase	lytic 3	-	UL 92	BDLF-4	Orf 67.5	packaging protein/terminase	lytic	UL 33	UL 51	BFRF-4	1
29	Orf 31	unknown	lytic 3	-	UL 92	BDLF-4	Orf 68	packaging protein	lytic	UL 32	UL 52	BFLF-1	1

No	ORF	Function	Phase				ORF	Function	Phase				Score
30	Orf 34	tegument	lytic 2	UL 14	UL 95	BDLF-4	K 5	ubiquitin ligase	lytic 1	-	-	-	0
31	Orf 34	tegument	lytic 2	UL 14	UL 95	BGLF-3	K 11	vIRF	lytic 2	-	-	-	0
32	Orf 34	tegument	lytic 2	UL 14	UL 95	BDLF-4	Orf 52	unknown	lytic 2	-	-	BLRF-2	0
33	Orf 34	tegument	lytic 2	UL 14	UL 95	BGLF-3	Orf 67.5	packaging protein	lytic	UL 33	UL 51	BFRF-4	0
34	Orf 36	kinase	lytic 3	UL 13	UL 97	BGLF-4	Orf 48	gP glycoprotein	lytic2	-	-	BKRF-2	0
35	Orf 53	gN glycoprotein	lytic 2	-	UL 73	BLRF-1	K 3	ubiquitin ligase	lytic 2	-	-	-	1
36	Orf 53	gN glycoprotein	lytic 2	-	UL 73	BLRF-1	K 5	ubiquitin ligase	lytic 1	-	-	-	1
37	Orf 57	immediate early	lytic 1	-	-	BMLF-1	Orf 68	packaging protein	lytic	UL 32	UL 52	BFLF-1	1
38	Orf 59	polymerase processivity factor	lytic 2	-	-	BMRF-1	Orf 67.5	packaging protein/terminase	lytic	UL 33	UL 51	BFRF-4	0
39	Orf 59	polymerase processivity factor	lytic 2	-	-	BMRF-1	Orf 68	packaging protein	lytic	UL 32	UL 52	BFLF-1	1
40	Orf 60	ribonucleotide reductase	lytic	UL 40	-	BaRF-1	Orf 67.5	packaging protein/terminase	lytic	UL 33	UL 51	BFRF-4	1
41	Orf 60	ribonucleotide reductase	lytic	UL 40	-	BaRF-1	Orf 68	packaging protein	lytic	UL 32	UL 52	BFLF-1	1
42	Orf 63	tegument	lytic 3	-	-	BOLF-1	K 9	vIRF	lytic 2	-	-	-	1
43	Orf 63	tegument	lytic 3	-	-	BOLF-1	Orf 23	unknown	lytic 3	-	-	BTRF-1	1
44	Orf 63	tegument	lytic 3	-	-	BOLF-1	Orf 41	helicase/primase subunit	lytic 3	-	-	BBLF-3	1
45	Orf 63	tegument	lytic 3	-	-	BOLF-1	Orf 65	small basic capsid antigen	lytic 2	UL 35	**UL 48/49**	BFRF-3	1
46	Orf 63	tegument	lytic 3	-	-	BOLF-1	Orf 67.5	packaging protein/terminase	lytic	UL 33	UL 51	BFRF-4	1
47	Orf 69	capsid egress	lytic 1	UL 31	UL 53	BFLF-2	K 9	vIRF-1	lytic 2	-	-	-	1
48	Orf 69	capsid egress	lytic 1	UL 31	UL 53	BFLF-2	K 11	vIRF-2	lytic 2	-	-	-	0
49	Orf 69	capsid egress	lytic 1	UL 31	UL 53	BFLF-2	Orf 52	unknown	lytic 2	-	-	BLRF-2	0
50	Orf 69	capsid egress	lytic 1	UL 31	UL 53	BFLF-2	Orf 67.5	packaging protein/terminase	lytic	UL 33	UL 51	BFRF-4	1
51	Orf 75	tegument, FGARAT	lytic 3	-	-	BNRF-1	K 8.1	glycoprotein	lytic 3	-	-	-	0
52	Orf 75	tegument, FGARAT	lytic 3	-	-	BNRF-1	K 10.5	vIRF-3	latent	-	-	-	0
53	Orf 75	tegument, FGARAT	lytic 3	-	-	BNRF-1	Orf 50	immediate early, RTA	lytic	-	-	BRLF-1	1
54	Orf 75	tegument, FGARAT	lytic 3	-	-	BNRF-1	Orf 67.5	packaging protein/terminase	lytic	UL 33	UL 51	BFRF-4	1
55	Orf 75	tegument, FGARAT	lytic 3	-	-	BNRF-1	Orf 68	packaging protein	lytic	UL 32	UL 52	BFLF-1	1

virus-host interaction (HI)

No	ORF	Function	Phase				ORF	Function	Phase				Score
1	K 3 d2	ubiquitin ligase	lytic 2	-	-	-	K 3 d1	ubiquitin ligase	lytic 2	-	-	-	0
2	K 7	apoptosis	lytic 1	-	-	-	K 3	ubiquitin ligase	lytic 2	-	-	-	0
3	K 7	apoptosis	lytic 1	-	-	-	K 5	ubiquitin ligase	lytic 1	-	-	-	1
4	K 7	apoptosis	lytic 1	-	-	-	Orf 74	GPCR	lytic 1	-	-	-	1
5	K 10	vIRF-4	lat/lyt	-	-	-	Orf 31	unknown	lytic 3	-	UL 92	BDLF-4	1
6	K 10	vIRF-4	lat/lyt	-	-	-	Orf 39	gM glycoprotein	lytic 2	UL 10	UL 100	BBRF-3	1
7	K 10	vIRF-4	lat/lyt	-	-	-	Orf 41	helicase/primase subunit	lytic 3	-	-	BBLF-3	1
8	K 10	vIRF-4	lat/lyt	-	-	-	Orf 47	gL glycoprotein	lytic 2	UL 1	UL 115	BKRF-2	0
9	K 10	vIRF-4	lat/lyt	-	-	-	Orf 67.5	packaging protein/terminase	lytic	UL 33	UL 51	BFRF-4	1
10	K 10	vIRF-4	lat/lyt	-	-	-	Orf 68	packaging protein	lytic	UL 32	UL 52	BFLF-1	1
11	K 12	signallin g	lytic	-	-	-	K 10	vIRF-4	lat/lyt	-	-	-	1
12	K 12	signallin g	lytic	-	-	-	K 12	signalling	lytic	-	-	-	1
13	Orf 2	DHRF	lytic 2	-	-	-	K 10	vIRF-4	lat/lyt	-	-	-	1
14	Orf 6	ssDNA binding protein	lytic 1	UL 29	UL 57	BALF-2	K 5	ubiquitin ligase	lytic 1	-	-	-	1
15	Orf 6	ssDNA binding protein	lytic 1	UL 29	UL 57	BALF-2	K 15	LAMP	latent	-	-	-	0
16	Orf 9	DNA polymerase	lytic 1	UL 30	UL 54	BALF-5	K 10	vIRF-4	latent	-	-	-	0
17	Orf 23	unknown	lytic 3	-	UL 117	BTRF-1	K 9	vIRF-1	lytic 2	-	-	-	1
18	Orf 27	unknown	lytic 2	-	-	BDLF-2	Orf 74	GPCR	lytic 1	-	-	-	1
19	Orf 28	unknown	lytic 3	-	-	BDLF-3	K 5	ubiquitin ligase	lytic 1	-	-	-	1
20	Orf 28 d1	unknown	lytic 3	-	-	BDLF-3	K 10	vIRF-4	lat/lyt	-	-	-	0
21	Orf 28 d1	unknown	lytic 3	-	-	BDLF-3	K 11	vIRF-2	lytic 2	-	-	-	0
22	Orf 29b	packaging protein/terminase	lytic 3	UL 15	UL 89	BDRF-1	K 10	vIRF-4	lat/lyt	-	-	-	0
23	Orf 29b	packaging protein/terminase	lytic 3	UL 15	UL 89	BDRF-1	K 10.5	vIRF-3	latent	-	-	-	0
24	Orf 29b	packaging protein/terminase	lytic 3	UL 15	UL 89	BDRF-1	K 11	vIRF-2	lytic 2	-	-	-	1
25	Orf 29b	packaging protein/terminase	lytic 3	UL 15	UL 89	BDRF-1	K 12	transforming	lytic	-	-	-	0
26	Orf 29b	packaging protein/terminase	lytic 3	UL 15	UL 89	BDRF-1	Orf 72	vCyc	latent	-	-	-	0
27	Orf 29b	packaging protein/terminase	lytic 3	UL 15	UL 89	BDRF-1	Orf 74	GPCR	lytic 1	-	-	-	0
28	Orf 31	unknown	lytic 3	-	UL 92	BDLF-4	K 11	vIRF-2	lytic 2	-	-	-	1
29	Orf 34	tegument	lytic 2	UL 14	UL 95	BDLF-4	K 5	ubiquitin ligase	lytic 1	-	-	-	0
30	Orf 34	tegument	lytic 2	UL 14	UL 95	BGLF-3	K 11	vIRF	lytic 2	-	-	-	0
31	Orf 36	kinase	lytic 3	UL 13	UL 97	BGLF-4	Orf 45	immediate early, tegument	lytic 1	-	-	BKRF-4	0
32	Orf 36	kinase	lytic 3	UL 13	UL 97	BGLF-4	Orf 48	gP glycoprotein	lytic2	-	-	BKRF-2	0
33	Orf 36	kinase	lytic 3	UL 13	UL 97	BGLF-4	Orf 54	dUTPase	lytic 3	UL 50	UL72	BLLF-3	0
34	Orf 36	kinase	lytic 3	UL 13	UL 97	BGLF-4	Orf 61	ribonucleotide reductase	lytic	UL 39	UL 45	BORF-2	1
35	Orf 37	alkaline exonuclease	lytic 3	UL 12	UL 98	BGLF-5	K 10	vIRF-4	lat/lyt	-	-	-	1
36	Orf 37	alkaline exonuclease	lytic 3	UL 12	UL 98	BGLF-5	Orf 72	vCyc	latent	-	-	-	1
37	Orf 45	immediate early, tegument	lytic 1	-	-	BKRF-4	Orf 72	vCyc	latent	-	-	-	0
38	Orf 49	unknown	lytic 2	-	-	BRRF-1	K 10	vIRF-4	lat/lyt	-	-	-	0
39	Orf 53	gN glycoprotein	lytic 2	-	UL 73	BLRF-1	K 3	ubiquitin ligase	lytic 2	-	-	-	1
40	Orf 53	gN glycoprotein	lytic 2	-	UL 73	BLRF-1	K 5	ubiquitin ligase	lytic 1	-	-	-	1
41	Orf 54	dUTPase	lytic 3	UL 50	UL72	BLLF-3	Orf 36	kinase	lytic 3	UL 13	UL 97	BGLF-4	0
42	Orf 56	helicase/primase	lytic 2	UL 52	UL 70	BSLF-1	K 10.5	vIRF-3	latent	-	-	-	1
43	Orf 56	helicase/primase	lytic 2	UL 52	UL 70	BSLF-1	Orf 36	kinase	lytic 3	UL 13	UL 97	BGLF-4	1
44	Orf 59	polymerase processivity factor	lytic 2	-	-	BMRF-1	K 5	ubiquitin ligase	lytic 1	-	-	-	0
45	Orf 59	polymerase processivity factor	lytic 2	-	-	BMRF-1	K 10	vIRF-4	lat/lyt	-	-	-	0
46	Orf 59	polymerase processivity factor	lytic 2	-	-	BMRF-1	K 11	vIRF-2	lytic 2	-	-	-	1
47	Orf 60	ribonucleotide reductase	lytic	UL 40	-	BaRF-1	K 1	transforming	lytic 3	-	-	-	0
48	Orf 60	ribonucleotide reductase	lytic	UL 40	-	BaRF-1	K 3	ubiquitin ligase	lytic 2	-	-	-	1
49	Orf 60	ribonucleotide reductase	lytic	UL 40	-	BaRF-1	K 5	ubiquitin ligase	lytic 1	-	-	-	0
50	Orf 60	ribonucleotide reductase	lytic	UL 40	-	BaRF-1	K 10	vIRF-4	lat/lyt	-	-	-	0
51	Orf 60	ribonucleotide reductase	lytic	UL 40	-	BaRF-1	K 11	vIRF-2	lytic 2	-	-	-	1
52	Orf 60	ribonucleotide reductase	lytic	UL 40	-	BaRF-1	K 12	kaposin	lytic	-	-	-	0
53	Orf 61	ribonucleotide reductase	lytic	UL 39	UL 45	BORF-2	K 10	vIRF-4	lat/lyt	-	-	-	1
54	Orf 61	ribonucleotide reductase	lytic	UL 39	UL 45	BORF-2	K 11	vIRF-2	lytic 2	-	-	-	0
55	Orf 63	tegument	lytic 3	-	-	BOLF-1	K 9	vIRF	lytic 2	-	-	-	1
56	Orf 69	capsid egress	lytic 1	UL 31	UL 53	BFLF-2	K 9	vIRF-1	lytic 2	-	-	-	1
57	Orf 69	capsid egress	lytic 1	UL 31	UL 53	BFLF-2	K 11	vIRF-2	lytic 2	-	-	-	0
58	Orf 75	tegument, FGARAT	lytic 3	-	-	BNRF-1	K 10.5	vIRF-3	latent	-	-	-	0

unknown function (UN)

#	ORF	function	phase	α	β	λ	ORF	function	phase	α	β	λ	co-IP
1	K 10	vIRF-4	lat/lyt	-	-	-	Orf 31	unknown	lytic 3	-	UL 92	BDLF-4	1
2	Orf 6	ssDNA binding protein	lytic 1	UL 29	UL 57	BALF-2	Orf 52	unknown	lytic 2	-	-	BLRF-2	0
3	Orf 23	unknown	lytic 3	-	UL 117	BTRF-1	K 9	vIRF-1	lytic 2	-	-	-	1
4	Orf 23	unknown	lytic 3	-	UL 117	BTRF-1	Orf 28	unknown	lytic 3	-	-	BDLF-3	0
5	Orf 23	unknown	lytic 3	-	UL 117	BTRF-1	Orf 30	unknown	lytic 3	-	-	BDLF-3,5	0
6	Orf 23	unknown	lytic 3	-	UL 117	BTRF-1	Orf 45	immediate early, tegument	lytic 1	-	-	BKRF-4	0
7	Orf 23	unknown	lytic 3	-	UL 117	BTRF-1	Orf 67.5	packaging protein/terminase	lytic	UL 33	UL 51	BFRF-4	1
8	Orf 27	unknown	lytic 2	-	-	BDLF-2	Orf 74	GPCR	lytic 1	-	-	-	1
9	Orf 28	unknown	lytic 3	-	-	BDLF-3	K 5	ubiquitin ligase	lytic 1	-	-	-	1
10	Orf 28 d1	unknown	lytic 3	-	-	BDLF-3	K 10	vIRF-4	lat/lyt	-	-	-	0
11	Orf 28 d1	unknown	lytic 3	-	-	BDLF-3	K 11	vIRF-2	lytic 2	-	-	-	0
12	Orf 28 d1	unknown	lytic 3	-	-	BDLF-3	Orf 28 d1	unknown	lytic 3	-	-	BDLF-3	0
13	Orf 28 d1	unknown	lytic 3	-	-	BDLF-3	Orf 30	unknown	lytic 3	-	-	BDLF-3,5	0
14	Orf 28 d1	unknown	lytic 3	-	-	BDLF-3	Orf 41	helicase/primase subunit	lytic 3	-	-	BBLF-3	1
15	Orf 28 d1	unknown	lytic 3	-	-	BDLF-3	Orf 67.5	packaging protein/terminase	lytic	UL 33	UL 51	BFRF-4	0
16	Orf 29b	packaging protein/terminase	lytic 3	UL 15	UL 89	BDRF-1	Orf 23	unknown	lytic 3	-	UL 117	BTRF-1	1
17	Orf 29b	packaging protein/terminase	lytic 3	UL 15	UL 89	BDRF-1	Orf 28 d1	unknown	lytic 3	-	-	BDLF-3	0
18	Orf 29b	packaging protein/terminase	lytic 3	UL 15	UL 89	BDRF-1	Orf 28 d2	unknown	lytic 3	-	-	BDLF-3	1
19	Orf 29b	packaging protein/terminase	lytic 3	UL 15	UL 89	BDRF-1	Orf 30	unknown	lytic 3	-	-	BDLF-3,5	0
20	Orf 31	unknown	lytic 3	-	UL 92	BDLF-4	K 11	vIRF-2	lytic 2	-	-	-	1
21	Orf 31	unknown	lytic 3	-	UL 92	BDLF-4	Orf 30	unknown	lytic 3	-	-	BDLF-3,5	0
22	Orf 31	unknown	lytic 3	-	UL 92	BDLF-4	Orf 31	unknown	lytic 3	-	UL 92	BDLF-4	1
23	Orf 31	unknown	lytic 3	-	UL 92	BDLF-4	Orf 41	helicase/primase subunit	lytic 3	-	-	BBLF-3	1
24	Orf 31	unknown	lytic 3	-	UL 92	BDLF-4	Orf 67.5	packaging protein/terminase	lytic	UL 33	UL 51	BFRF-4	1
25	Orf 31	unknown	lytic 3	-	UL 92	BDLF-4	Orf 68	packaging protein	lytic	UL 32	UL 52	BFLF-1	1
26	Orf 34	tegument	lytic 2	UL 14	UL 95	BDLF-4	Orf 52	unknown	lytic 2	-	-	BLRF-2	0
27	Orf 49	unknown	lytic 2	-	-	BRRF-1	K 10	vIRF-4	lat/lyt	-	-	-	0
28	Orf 49	unknown	lytic 2	-	-	BRRF-1	Orf 52	unknown	lytic 2	-	-	BLRF-2	0
29	Orf 52	unknown	lytic 2	-	-	BLRF-1	Orf 52	unknown	lytic 2	-	-	BLRF-2	1
30	Orf 57	immediate early	lytic 1	-	-	BMLF-1	Orf 23	unknown	lytic 3	-	-	BTRF-1	1
31	Orf 57	immediate early	lytic 1	-	-	BMLF-1	Orf 52	unknown	lytic 2	-	-	BLRF-2	0
32	Orf 58	unknown	lytic 1	-	-	BMRF-2	Orf 27	unknown	lytic 2	-	-	BDLF-2	0
33	Orf 59	polymerase processivity factor	lytic 2	-	-	BMRF-1	Orf 52	unknown	lytic 2	-	-	BLRF-2	0
34	Orf 60	ribonucleotide reductase	lytic	UL 40	-	BaRF-1	Orf 23	unknown	lytic 3	-	UL 117	BTRF-1	0
35	Orf 60	ribonucleotide reductase	lytic	UL 40	-	BaRF-1	Orf 52	unknown	lytic 2	-	-	BLRF-2	0
36	Orf 63	tegument	lytic 3	-	-	BOLF-1	Orf 23	unknown	lytic 3	-	-	BTRF-1	1
37	Orf 69	capsid egress	lytic 1	UL 31	UL 53	BFLF-2	Orf 52	unknown	lytic 2	-	-	BLRF-2	0

Figure 18:   Protein-protein interactions in KSHV.
Indicated for each bait and prey clone are the function or putative function of the ORF and homologous genes in HSV-1 (α), CMV (β) and EBV (λ).
Viral proteins were divided into five functional groups marked by different colours: red: DNA replication, nucleotide metabolism, yellow: gene regulation and signalling, green: virion structure, morphogenesis, blue: proteins involved in virus-host interaction, grey: unknown function.
Positive protein-protein interactions identified by Y2H matrix screen were scrutinized by co-immuno-precipitation.

4.3.4   Viral protein-protein interaction map in KSHV

The interaction map was created on the basis of the data out of the Y2H matrix screen (Figure 19). Self-interacting, viral proteins are depicted with a blue square. Different domains and full length constructs of the same protein are defined as one dot. Similar to Figure 18, proteins are divided into five functional groups which are marked by different colours. This visualizes that proteins of the same functional group tent to cluster in certain regions.

We see that some proteins are forming hubs, which means that they have many interaction partners, e.g. ORF29b and ORF67.5 (packaging proteins), ORF60 (ribonucleotide reductase), K10 and K11 (viral interferon regulatory factors).

Another feature of this interaction map is that it makes interaction partners of unknown proteins visible. Unknown proteins interacting several times with proteins belonging to one functional group might as well be a member of this group. For example: ORF53 is interacting with K5 and K3, these proteins are homologous to

each other and they are both involved in the ubiquitinylation and subsequent downregulation of MHC I (Coscoy and Ganem, 2000; Coscoy and Ganem, 2001a). Thus, specific conclusions concerning the function of ORF53 might be drawn from these interactions.
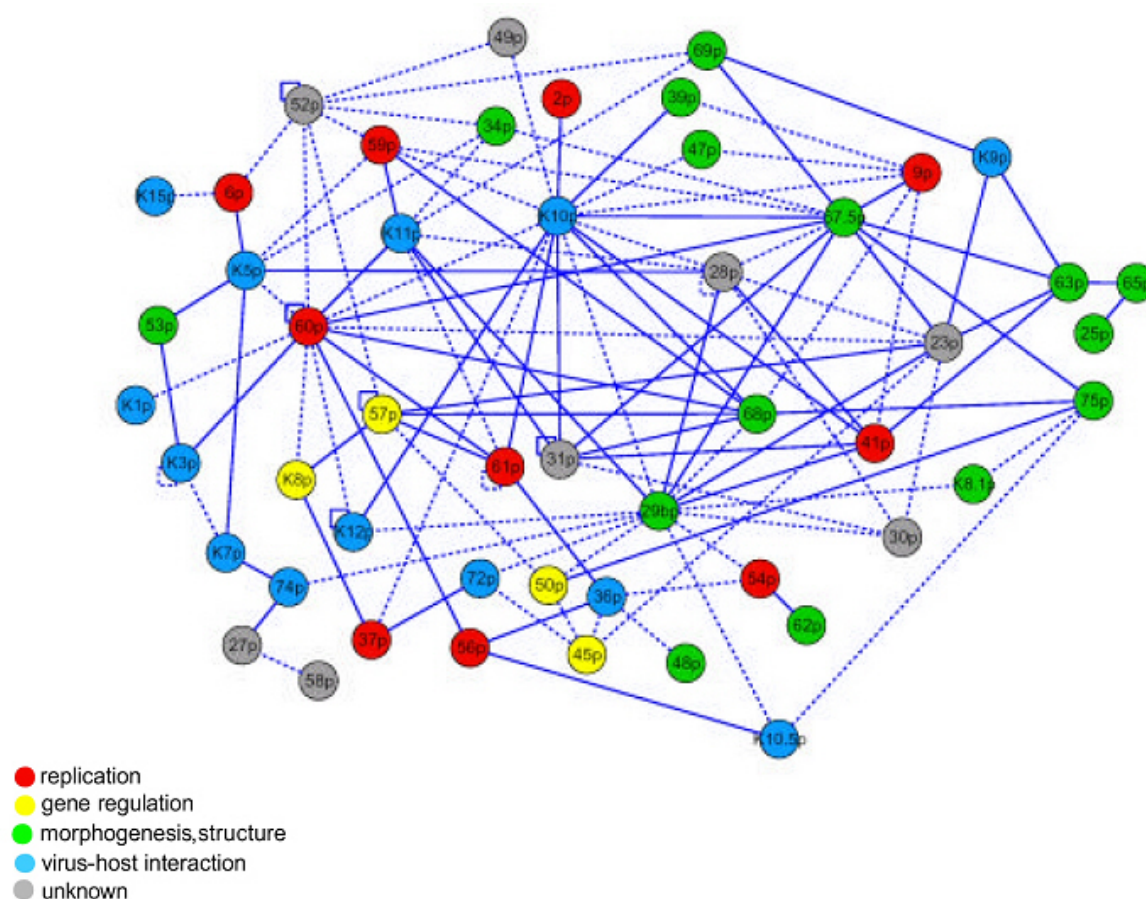
Figure 19: **KSHV protein-protein interaction map.**
Protein interaction map in KSHV evaluated by Y2H screen. KSHV proteins are indicated as nodes, protein interactions as either hatched (found only by Y2H) or solid (confirmed by CoIP) edges. The same colours as in Figure 17 were chosen to distinguish between functional groups: red: DNA replication, nucleotide metabolism, yellow: gene regulation, green: virion structure, morphogenesis, blue: proteins involved in virus-host interaction, grey: unknown function. Squares were added to self-interacting proteins.

4.4 Conserved protein interactions between herpesvirus subfamilies

KSHV encodes ORFs with 31, 38 and 54 orthologs in the main representatives of the three α, β and γ herpesvirus subfamilies, HSV-1, CMV and EBV. The 54 KSHV ORFs with orthologs in EBV possess an average sequence identity of 35.1%. Among these 54 proteins 30 are involved in viral protein interactions as shown in our data set, but

their average similarity is not increased (34.5%) when compared to the 24 non-interacting proteins (36.0%). However, hubs (proteins that interact with >5 other proteins) are more conserved, i.e. there is a positive correlation between homology and the number of interaction partners. Within the group of conserved proteins, there is a significant correlation between protein interactions and homology which is statistically significant for EBV (p=0.046). The core set of 22 KSHV ORFs that have orthologs in all three other herpesviruses have an average homology of 40.9%. Within this core set the 10 viral proteins which were found to interact have an average homology of 43.1%. This indicates that this most basic set of proteins is functionally important and thus more conserved. Since interactions between highly homologous proteins are conserved, we predict 56 interactions in EBV (Figure 20), 22 in CMV (Figure 21) and 19 in HSV-1 (Figure 22).
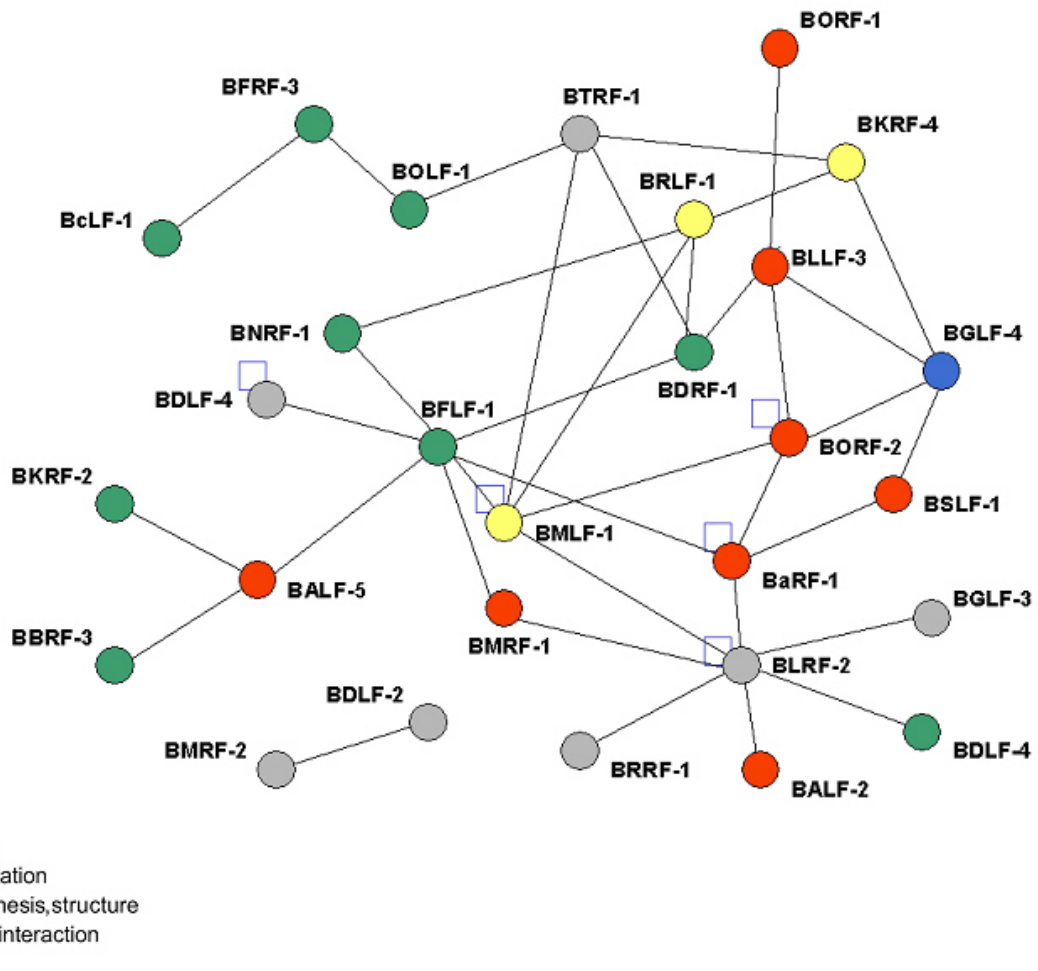
Figure 20:   Predicted protein interaction in EBV.
54 KSHV ORFs have orthologs in EBV, among which 30 have protein interactions. To self-interacting proteins a square was added. The colours of the nodes indicate the function of the KSHV orthologs.
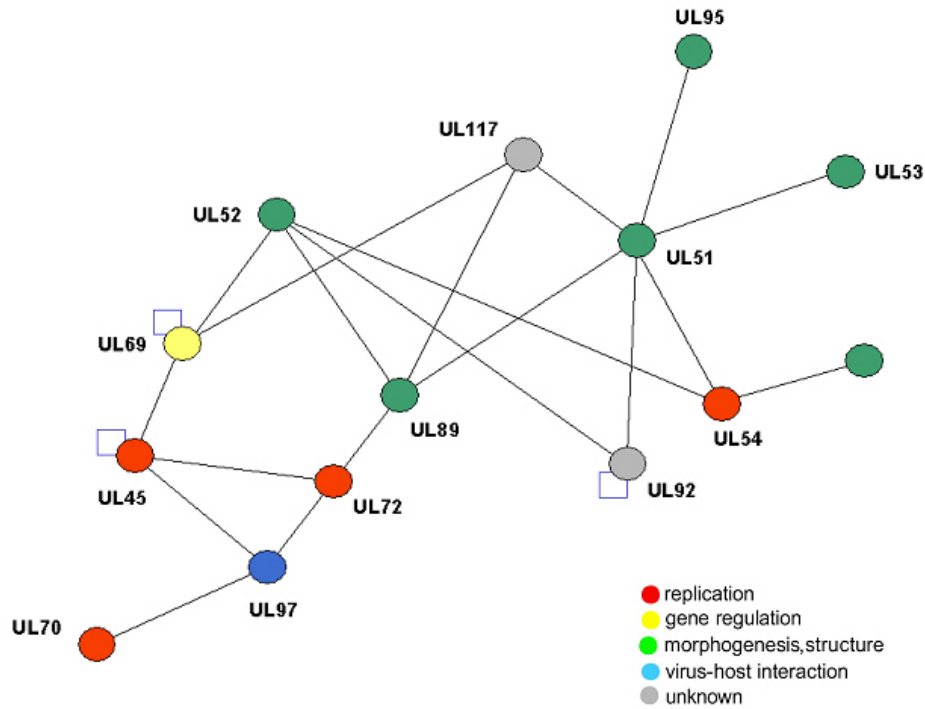
Figure 21: **Predicted protein interactions in CMV**
38 KSHV ORFs have orthologs in EBV, among which 22 have protein interactions. It is striking, that only a few interactions according virus-host-interactions and gene regulation could be predicted.
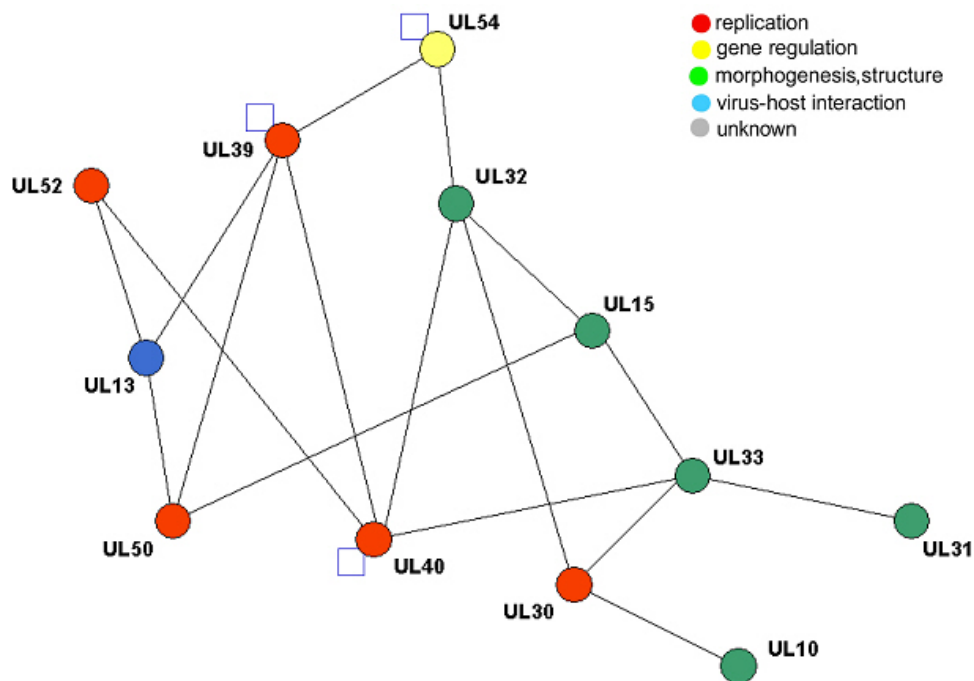
Figure 22: **Predicted protein interactions in HSV-1**
31 KSHV ORFs have orthologs in EBV, among which 19 are predicted to interact. As in EBV and CMV, most conserved interactions belong to the group of virus replication and morphogenesis/structure. From the virus-host interaction group only UL13, the ortholog of KSHV ORF36 is predicted to interact in HSV-1.

5   DISCUSSION

5.1   Analysis of protein-protein interactions

5.1.1   Herpesviruses

Surprisingly little is known about interactions between herpesviral proteins, particularly of herpesviruses which replicate poorly in cell culture including the human γ-herpesvirus KSHV. We know that more than half of the viral genes do not encode structural or replicatory proteins, but rather non-essential proteins mandatory for infection of the natural host. A considerable number of viral proteins share sequence and structural similarities with cellular proteins, however possess different functions.

5.1.2   Choice of KSHV genes, domains and templates

The first report on the KSHV sequence predicted 82 open reading frames (ORFs) (Russo et al., 1996). Several other genes including K4.1, K4.2, K8.1, K

10.5, ORF67.5, K14.1, K10.7 (vIRF3) were added in later studies (Neipel et al., 1997; Jenner et al., 2001). Although cDNAs of five spliced genes were included in this study, this is probably not the complete set of spliced KSHV genes. Since for some of the KSHV genes it is controversially discussed whether they are spliced, we only included one exon (for example: K10/K10.1 (vIRF4) and K11/K11.1 (vIRF2)). For K8 (3 exons), K15 (8 exons) and K8.1 (2 exons) only one exon was used in this study since the cDNA was not available.

Moreover, there might be more spliced genes which are currently unknown and which are therefore not introduced in the Y2H screen. Therefore, it is advisable to use cDNA as PCR template, whenever possible.

The open reading frames at the very left and the very right end of the KSHV genome, K1 and K15, are known to be highly variable (Lagunoff and Ganem, 1997; Lee et al., 1998; Neipel et al., 1997b; Nicholas et al., 1998; Russo et al., 1996). Thus, different sequences can be expected, according to the PCR template which has been used.

Proteins containing transmembrane regions will give false negative results since both bait and prey proteins have to be transported into the nucleus in order to transactivate the promotor of the selection gene in the Y2H system. To avoid this, all full-length open reading frames were screened for putative transmembrane domains

by the algorithms HMMTOP 2.0 (Tusnàdy et al., 2001) (http://www.enzim.hu/hmmtop/html/document.html) and TMpred (Hofmann and Stoffel, 1993) (http://www.ch.embnet.org/software/TMPRED_form.html). The two programs were used in parallel since both can produce false negative and false positive results, i.e. known domains are not found, and vice versa. In addition to these problems, the designated orientation of the transmembrane proteins given by these programs is not always correct.

To reduce false negative results caused by transmembrane proteins, we also cloned separate domains of proteins with known or predicted transmembrane domains. Intriguingly, several predicted external domains interacted with intracellular proteins in the Y2H screen. In some cases, these interactions could even be validated by CoIP. In these cases, the transmembrane domains might have been falsely predicted, as the algorithms used only have an accuracy of 60-80%.

Despite all efforts the array displays some blanks: ORF64, a gene of 8 kb was not included, and for ORF6 and ORF75 (3,4 and 3.9 kb, respectively) only the 5' half could be cloned into bait and prey vector. To decrease the number of PCR-induced mutations, a polymerase with a proof-reading activity (Vent polymerase) was used. However, the possibility that some constructs of the array contain mutations cannot be excluded. All ORFs with positive interactions were sequenced from both sides, and only two mutations were found (both not shifting the reading frame), indicating that the number of mutated clones is probably low.

5.1.3 ORFeome matrices versus cDNA libraires

Genome-wide analyses can be performed in several ways. In general, either cDNA libraries or ORFeome matrices containing full-length cDNAs can be used.

cDNA libraries are limited in several respects: First, they do not represent accurately the mRNA distribution of the cell, and rare mRNA's may be underrepresented or lost in the library. Second, 66.6% of the clones in cDNA libraries, which express N-terminal fusion proteins, are in the wrong reading frame.

In this study, the KSHV ORFeome was cloned by recombinatorial cloning (GATEWAY system). This cloning technology replaces restriction endonucleases and ligase by site-specific recombination and is highly efficient. The viral ORFs were amplified by PCR from initiation to termination codon using specific primers with attB1, respectively attB2 recombination sites at the 5' end. The resulting PCR

products were recombined uni-directionally into a 'donor' vector to create 'entry' clones. This reaction is reversible and ORFs in the entry vector can subsequently be transferred efficiently by recombination into any 'destination' vector of interest.

We converted the yeast vectors pGBKT7 and pGADT7 into destination vectors by cloning a conversion cassette into the multiple cloning site.

These vectors were chosen because of their numerous useful features: Both vectors contain a T7 promoter and tag sequences at the 5' end of the insert, so that protein-protein interactions can be tested by co-immunoprecipitation without time-consuming subcloning into different vectors and without specific antibodies.

Both contain strong yeast promoters which causes a high sensitivity in detecting protein-protein interactions. On the other hand, these vectors might have the disadvantage of a higher rate of false positive interactions.

5.1.4   Features and disadvantages of the Y2H system

During the past few years, the Y2H system has become an important technique for detecting protein-protein interactions in large-scale projects.

The Y2H system produces a significant number of false positive and false negative results.

The largest group of false positives is caused by so-called self-activating baits. These proteins encode polypeptides that, when fused to a binding domain, can activate transcription in the absence of any interacting partner protein. They can easily be identified by including a negative control into the screen, e.g. the empty vector pGADT7.

False positives can be caused by mutations in the reporter gene or in the vector. They can be identified by repeating the screen at least once (here quadruplicates were made of each pairwise combination). In previous studies, the authors tried to reduce false positive interactions by statistical means or estimated true-positive interactions by extrapolating the results of a biochemical analysis of a small subset of interactions. Here, we tested all positive Y2H interactions in parallel by CoIPs.

False negatives can be caused by different characteristics of the Y2H system. First, one or both proteins may fail to enter into the yeast nucleus (e.g. transmembrane proteins). Second, a protein may be unable to function as a fusion protein due to steric hindrance. Third, the interaction between the two proteins may depend on post-transcriptional modifications that are absent in the yeast cell.

A comparison of the two independent large-scale screens in *Sacharomyces cerevisiae* may provide some insight into how much false data is produced by this approach (Ito et al., 2000; Uetz et al., 2000). Ito and colleagues constructed a DNA-binding domain hybrid and an activation domain hybrid for each of the ≈ 6000 predicted yeast proteins. This approach resulted in 4,549 two-hybrid positives. Uetz and colleagues used another strategy: individual DNA-binding domain fusion proteins were tested against an array of ≈ 6000 separate activation domain transformants, and individual DNA-binding domain transformants tested against a library of all activation domain hybrids. This study resulted in the identification of 957 putative interactions. There is only a small overlap in the results among all three approaches, and neither the first nor the second study recapitulate more than $\approx 13\%$ of the published interactions detected up to now by using conventional single protein analysis (Hazbun and Fields, 2001). Not only does this rather small fraction of overlapping interactions hint at a high number of false negatives, it also suggests that genome 'interactomes' are larger than estimated by earlier studies.

5.1.5   Validation of Y2H interactions by co-immunoprecipitation

Most studies that have attempted to validate large-scale two-hybrid data have postulated that these data sets contain up to 50% false positives (Deane et al., 2002; Mrowka et al., 2001). When we verified our two-hybrid data by co-immunoprecipitation, we found a similar percentage. To circumvent the need for producing specific antibodies for co-immunoprecipitation, bait and prey proteins were fused to an epitope-tag. An antibody directed against the tag – instead of the protein itself – was used for complex retrieval. But even for co-immunoprecipitation, there are some limitations: First, antibodies may exhibit cross-reactivity with proteins other than the immunogen. In this case several proteins not related to the interacting protein might be precipitated, which essentially leads to the generation of false positives. In overexpression systems, the CoIP might be false positive due to unspecific binding. The artificially introduced tag may interfere with protein folding, protein function, or the ability to interact with other proteins.

5.2 Local analysis of the KSHV interaction map

Recently, the interactome of vaccinia virus, which is a member of the other family of large DNA viruses, poxviruses, was reported (McCraith et al., 2000). In this study, only 37 viral protein interactions were detected among 266 ORFs tested (~0,14 interactions / ORF). In this study, we identified 125 viral protein interactions among the 88 ORFs in KSHV (~1.4 interactions / ORF), i.e. an approximately 10-fold higher frequency (Uetz et al., 2004). Several of these protein interactions have been shown before for KSHV or homologous proteins of other herpesviruses, thus confirming the effectiveness of our approach. The majority, however, has not been reported before. We identified 15 viral hubs with >5 protein interactions, including ORF29b (16 protein interactions), K10 (16), ORF60 (14), ORF67.5 (12), ORF28 (10), ORF23 (9), K11 (8), K5 (7), ORF31 (7), ORF57 (7), ORF9 (6), ORF41 (6) and ORF61 (6) (Figure 23a-c). The 15 viral hubs represent all functional classes and include three proteins ORF23, ORF28 and ORF31 with unknown function. Since viral hubs tend to be conserved between herpesviral subfamilies, they are potential targets for drug design.
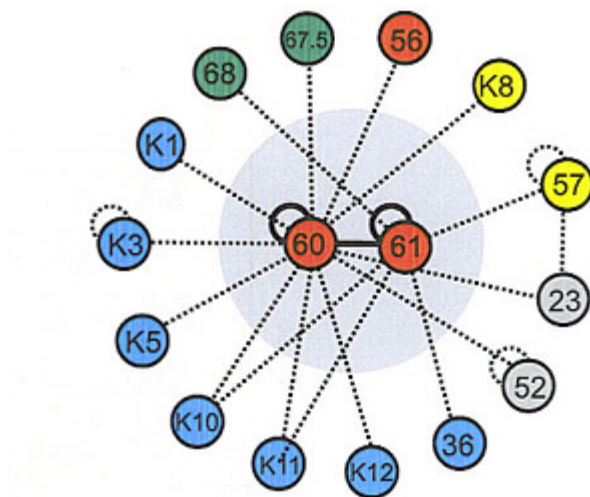
Figure 23a: Local viral subnet involving the ribonucleotide reductase subunits ORF60 and ORF61.
The ORF60 and ORF61 ribonucleotide reductase subunit proteins were found to homodimerize. They also interact with numerous other proteins, especially with proteins involved in *host interaction*. Interactions between proteins of the same functional group were indicated by solid, between proteins of different functional groups by hatched bars.
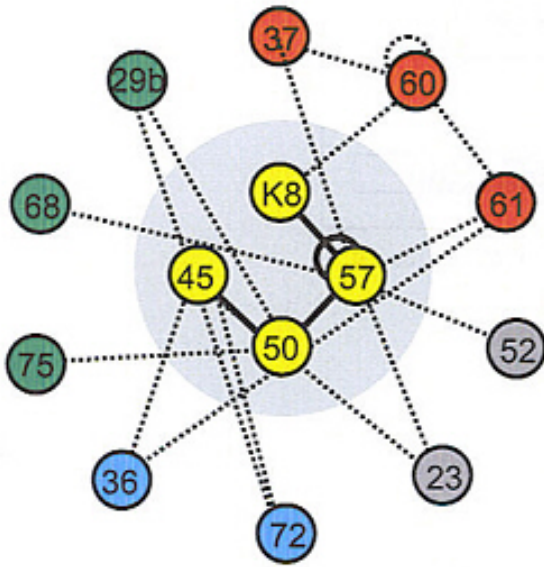
Figure 23b: Local viral subnet involving the immediate early proteins ORF45, ORF50, ORF57 and K8.1.
These four proteins belong to the class of *gene regulation and signalling* and they are immediate early proteins. In addition ORF57 was found to homodimerize.
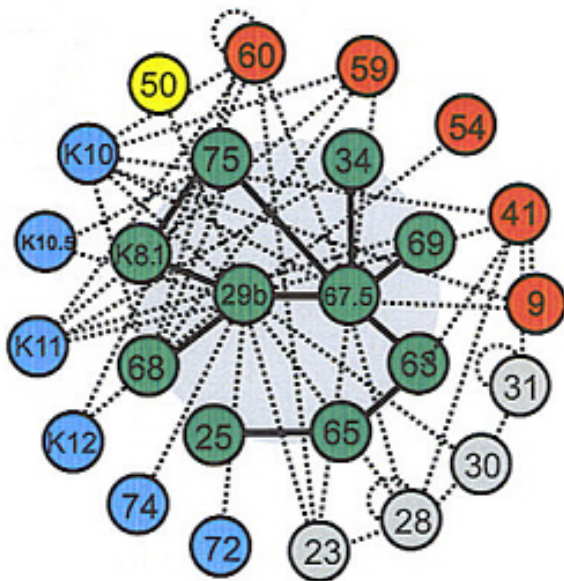
Figure 23c: Local viral subnet involving the packaging proteins ORF29b and ORF67.5.
ORF29b and ORF67.5 are DNA packaging proteins. ORF29b and ORF67.5 act as major hubs with 15 and 12 viral interaction partners, respectively.

5.3 Biological implications of particular protein-protein interactions

The interacting proteins were grouped into five functional categories: DNA-replication, nucleotide metabolism, gene regulation, virion structure / morphogenesis, virus-host interactions, and unknown function. Out of the 125 KSHV Y2H interactions, a small subset of interactions shall be described in more detail. This subset was chosen on the basis of the following criteria: 1) the viral interaction has formerly been described in small-scale experiments, and 2) both interaction partners are known and the interaction appears to be both plausible and interesting.

Table 4: Previously reported protein interactions in KSHV (including KSHV orthologs in other herpesviruses).

Interaction	Virus	Protein	Reference
Orf9 – Orf41	HSV-1	polymerase and helicase subunit	H. S. Marsden et al., *J.Virol.* 71, 6390-6397 (1997).
Orf25 – Orf65	KSHV	major and small capsid proteins	P. Lo, X. Yu, I. Atanasov, B. Chandran, Z. H. Zhou, *J.Virol.* 77, 4291-4297 (2003)
Orf29b – Orf67.5	HSV-1	Packaging proteins (HSV-1 UL15 homolog) and Orf67.5 (HSV-1 UL33 homolog)	P. M. Beard, N. S. Taus, J. D. Baines, *J.Virol.* 76, 4785-4791 (2002).
Orf36 – Orf45	KSHV	Kinase	A. von Geelen et al. *personal communication*
Orf45 - K8	*KSHV*	*immediate early proteins*	*K. Ueda et al. personal communication*
Orf57 – Orf57	KSHV HSV-1	Immediate early protein HSV-1: ICP27	P. Malik and J.B. Clements, *Nucleic Acids Research* 32, 5553–5569 (2004) Y. Zhi et al. *Virology.* 257341-51(1999):.
Orf50 (RTA) – Orf57	KSHV	The immediate early transcriptional activators	P. Malik et al. J.Gen.Virol. 85:2155-2166 (2004)
Orf50 (RTA) – K8	*KSHV*	*The immediate early transcriptional activators*	*Y. Izumiya et al., J.Virol. 77, 1441-1451 (2003).*
Orf60 – Orf61	KSHV	Ribonucleotide reductase subunits	Y. Sun and J. Conner, *Biochem.J.* 347 Pt 1, 97-104 (2000).

Orf60 – Orf60	HSV-1	homodimerization of ribonucleotide reductase subunit (HSV-1 UL40)	J. Conner et al., *Biochemistry* 32, 13673-13680 (1993).
Orf61 - Orf61	HSV-1	homodimerization of ribonucleotide reductase subunit (HSV-1 UL39)	J. Conner et al., *Biochemistry* 32, 13673-13680 (1993).
K12 – K12	KSHV	homodimerization of kaposin	S. Kliche et al., *Mol.Cell* 7, 833-843 (2001).

5.3.1   Structural viral proteins and proteins involved in morphogenesis

KSHV particles comprise an icosaedric capsid surrounded by a protein matrix termed tegument and a plasma membrane containing a variety of glycoproteins termed envelope. The capsid consists of the mayor (ORF25) and minor (ORF26) capsid proteins constituting hexon and penton structures. The small basic capsid protein (ORF65) is located at the tip of the hexon structures and was suggested to connect capsid with tegument. In this study, we detected that ORF65 interacts with ORF25 as shown before, but also with the tegument protein ORF63. On the other hand, ORF63 interacts with the protein ORF67.5, which is involved in packaging viral DNA into capsids. The two packaging and terminase proteins ORF29b and ORF67.5 act as major hubs with 15 and 12 viral interaction partners, respectively (Figure 23c). They constitute the most complex interaction subnet in this study and are connected to DNA packaging (ORF68), capsid (ORF25, ORF65), tegument (ORF34, ORF75) and even envelope proteins (K8.1), as well as to proteins involved in capsid egress (ORF69). Their homologs in HSV-1, UL15 and UL33, form a heteromultimeric complex with UL28. However, they also interact with proteins involved in viral replication, including the ORF9 polymerase, ORF41 helicase and ORF59 processivity factor. Moreover, ORF9 and ORF59 interact with the third packaging protein, ORF68, suggesting that the three ORF29b-ORF67.5-ORF68 packaging proteins link viral replication to virion assembly. Another interesting outcome within this functional class is the high connectivity of several proteins with unknown function including ORF23, ORF28 and ORF30 with the packaging proteins ORF29b and ORF67.5 suggesting a similar or related role for these proteins (Figure 23c).

5.3.2 Ribonucleotide reductase subunits ORF60 and ORF61

ORF60, which interacts with 13 other viral proteins, is one of the major hubs of this analysis. The small and large subunits of the viral ribonucleotide reductase, ORF60 and ORF61, interact with each other, similar to their cellular and vaccinia virus homologs (Kashlan et al., 2002, McCraith et al., 2000). The ribonucleotide reductase catalyses the conversion of all four ribonucleoside diphosphates to the corresponding desoxyribonucleoside diphosphates and thus plays an essential role in the *de novo* synthesis of DNA in all living organisms. Both ORF60 and ORF61 also self-interact. Such homodimerization was also reported for the HSV-1 homologues UL39 and UL40 (Conner et al., 1993). These characteristics suggest a heterotetrameric structure similar to eukaryotic class Ia ribonucleotide reductases and the ribonucleotide reductases of HSV-1 and EHV-4 (Kashlan et al., 2002; Sun and Conner, 2000). Not all herpesviral ribonucleotide reductases possess enzymatic reductase activity, and thus probably have adapted distinct biological functions during the evolution (Sun and Conner., 1999). HSV-1 UL40 (R1) for example has kinase activity in the C-terminal domain (missing in KSHV) and was suggested to act as a chaperone (Aurelian, 1998; Chabaud et al., 2003; Chung et al., 1989). A chaperone function might explain the multiplicity of interactions found for KSHV ORF60.

HSV-2 R1 was reported to have anti-apoptotic properties able to protect cells against death triggered by TNF-receptor family (Langelier et al., 2002).

In CMV, the ribonucleotide reductase homolog UL45 is an anti-apoptotic protein and mandatory for viral growth in endothelial cells (Brune et al., 2001).

HSV-1 ribonucleotide reductase is a target for antiviral chemotherapy. Synthetic peptides inhibit the viral protein by preventing subunit association at the critical carboxy terminus of the small subunit (R2) (Liuzzi et al., 1994).
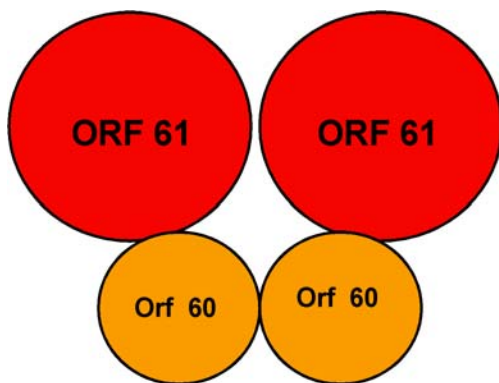
Figure 24: Putative heterotetrameric structure of RR-complex.

5.3.3 The dUTPase ORF54

The dUTPAse ORF54 is conserved in all three herpesvirus subfamilies and is also encoded by poxviruses and certain retroviruses. (Elder et al., 1992; McGeoch, 1990; Preston and Fisher, 1984). dUTPase is an enzyme involved in maintaining a low dUTP / dTTP ratio to minimize the lethal misincorporation of uracil into DNA by hydrolysing dUTP to dUMP and pyrophosphate (Shlomai and Kornberg, 1978). dUMP is a substrate for thymidylate synthase for the *de novo* dTTP synthesis. Herpesviral dUTPase-knock-out mutants have been reported to have an attenuated neurovirulence, a lacking ability to reactivate virus replication from latency (Pyles et al., 1992) and to possess an increased frequency of mutant formation (Pyles and Thompson, 1994). Most dUTPase active enzymes are homo-trimeric complexes (e.g. the human or the *E. coli* enzyme), The monomeric dUTPases are exclusively found in herpesviruses (McGeoch et al., 1995). There are several reports, suggesting that herpesviral dUTPase could be a target for specific chemotherapeutic agents, since there are additionally differences in the substrate specifity and the kinetics of dUTPase of viruses and their host cells (Kremmer et al., 1997; Williams, 1988, Studebaker et al., 2001; Studebaker et al., 2004). In this study, a bidirectional interaction between ORF54 and the kinase ORF36 was detected. A phosphorylation of the dUTPase was reported for the cellular dUTPase, vaccinia virus dUTPase and the dUTPase of EBV (Lirette et al., 1990; Sommer et al., 1996; Strahler et al., 1993). Since both proteins, ORF54 and ORF36 are conserved in all three herpesvirus subfamilies and the CMV ORF36 homolog UL97 is known to be responsible for ganciclovir resistance, this interaction might be a possible target for the development of inhibitors (Mendez et al., 1999).

5.3.4. Cluster of four immediate early proteins ORF45, ORF50, ORF 57 and K8.

We detected an interaction between the four immediate early proteins ORF50, ORF57, K8 and ORF45, as well as a dimerization of ORF57 (Figure 23b).

Immediate early (IE) genes are the first class of the viral genes expressed after primary infection or reactivation. This class of genes is defined by their transcription following primary infection or reactivation. IE genes encode regulatory

proteins that modulate the expression of viral and cellular genes early after infection. They also play a crucial role in the switch from latency to the lytic life cycle. ORF 50 is known to be the most important protein during reactivation and functions as a strong transcriptional activator of the early and late genes of KSHV (Lukac et al., 1999). ORF 50 was shown to act as a transcriptional activator of the ORF 57 and K8 promotors and is mandatory for lytic replication of KSHV, similar to its EBV homolog RTA (AuCoin et al., 2004). It binds to the transcription factor RBP-Jκ and contains a transcriptional activation sequence at the C-terminus (Liang et al., 2002).

ORF 57 is a spliced gene that is conserved throughout the herpesvirus family. It has a Herpes Simplex Virus type 1 homologue termed ICP27, which is an essential regulatory protein and acts at both transcriptional and post-transcriptional levels.

Similar to ICP27, ORF 57 was shown to be a strong effector that can act on several levels to augment viral gene expression (Kirshner et al., 2000). Both, ICP27 and ORF 57 protein were reported to shuttle between nucleus and cytoplasm (Bello et al., 1999; Mears et al., 1998).

The results of this screen report a homodimerization of ORF 57, which was also shown for the HSV-1 protein ICP27 (Zhi, et al., 1999). The self-interaction of the KSHV ORF 57 was later on also shown by Malik and Clements (2004), who succeeded to report the interaction by GST-pull-down assay.

The two ORF 50 and ORF 57 proteins are connected in several ways to each other. Both act post-transcriptionally and transcriptionally to regulate viral lytic gene expression and synergistically activate certain early and late KSHV promoters. ORF 50 was reported to transactivate its own promotor and those of K8 and ORF 57 (Byun et al., 2002).

Here we detected the direct interaction between the two proteins ORF 50 and ORF 57. This interaction was recently reported by Malik and colleagues (Malik et al., 2004). A physical association between ORF50 and ORF57 was shown by pull-down assays, leading to the upregulation of the ORF50 promotor with augmentation of ORF50 activity by ORF57 protein, and vice versa.

The immediate-early gene ORF45 is known as a phoshorylated tegument protein which can be found in virus particles, localizes in the cytoplasm and inhibits IRF-7, a cellular transcription factor inducing type I interferons (Zhu et al., 2002; Zhu and Yuan, 2003; Zhu et al., 2005).

ORF50, ORF57, K8 and ORF45 could either form a static heteromultimeric complex, or sequentially interact with each other. Their different localization supports the latter. Since the expression of ORF57 and K8 is transcriptionally regulated by ORF50, the ORF50-ORF57-K8 complex might be involved in a feedback loop.

In our screen, ORF45 also interacts with ORF36, an autophosphorylated serine protein kinase located in the nucleus. This is remarkable, since ORF 45 is known to be a tegument protein, located in the cytoplasm. ORF 45 was reported to be phosphorylated by Park et al (Park et al., 2000). Our data suggest that ORF36 regulates ORF45 by phosphorylation. On the basis of our results this interaction was confirmed by von Geelen and colleagues from the University of California, Davis, who found that ORF 36 binds ORF 45 and phoshorylated ORF 45 on a threonine residue (von Geelen, personal communication).

The viral protein kinase, encoded by ORF 36 in KSHV, is conserved among all herpesviruses. Because of its low homology to cellular kinases and the fact, that the homologues of ORF36 in α-, β- and γ-herpesviruses have been reported to be essential for optimal virus growth (Besser et al., 2003; Gershburg and Pagano, 2002; Prichard et al., 1999), this viral protein kinase represents an excellent target for novel antiviral drugs.

KSHV ORF36 was reported to activate JNK via MKK4 and MKK7 by phosphorylation. Activated JNK in turn regulates transcription by phosphorylating c-Jun, ATF-2, and other transcription factors (Hamza et al., 2004).

5.3.5 Ubiquitin ligases K5 and K3

The antigen presentation pathway of major histocompatibility (MHC) class I plays an important role in alerting the immune system to virally infected cells. MHC class I molecules are expressed on the cell surface of all nucleated cells and present peptide fragments derived from intracellular proteins. These peptides are normally derived from original cell proteins but in a virally infected cell, peptides derived from viral proteins may also be presented. Virus-specific cytotoxic T lymphocytes (CTL) monitor cell surface MHC class I molecules for peptides derived from viral proteins and eliminate infected cells.

Gammaherpesviruses and poxviruses share a family of immune evasion proteins. This family has been termed in several ways: modulators of immune recognition (MIR), Scrapins, or the K3 family (Coscoy et al., 2001b; Fruh et al., 2002; Guerin et

al., 2002). The hallmarks of the viral MIR-family are an amino-terminal RING-CH domain followed by two transmembrane domains. Since poxviruses and herpesviruses are unrelated viral families, it seems plausible that the viral RING-CH proteins originated from eukaryotic hosts (McFadden and Murphy, 2000). The existence of mammalian genes homologous to the MIR-family was confirmed by the reports of several investigators and is termed MARCH family (membrane-associated RING-CH family) (Bartee et al., 2004; Holzerlandt et al., 2002; Jenner and Boshoff, 2002). The Kaposi's Sarcoma associated Herpesvirus encodes two proteins belonging to the MIR-family that share 40% sequence identity: K3 and K5. Expression of one of these proteins causes the rapid internalisation of MHC class I molecules from the plasma membrane by clathrin-dependent endocytosis (Ishido et al., 2000b). The MHC class I molecules are sorted into an acidic endocytic compartment where they are degraded by acidic proteases (Coscoy and Ganem, 2000; Lorenzo et al., 2002). Furthermore, K5 can down-regulate the costimulatory molecules intracellular adhesion molecule-1 (ICAM-1) and B7.2 (Coscoy and Ganem, 2001a; Ishido et al., 2000a). Indeed, a cellular homolog (cMIR) of K3 and K5 has been discovered, which appears to regulate the cell surface expression of B7.2 (Goto et al., 2003). This implies that K3 and K5 have evolved from a gene 'hijacked' by KSHV from the host genome.

Both, K3 and K5 contain two transmembrane domains with cytosolically orientated N- and C-termini (Sanchez et al., 2002). In this study, both cytoplasmatic domains as well as full-length K3 and K5 genes were screened.

A RING finger domain can also be found in some E3 ubiquitin ligases (Capili et al., 2001; Joazeiro et al., 2000). Indeed, K3 and K5 function as E3 ubiquitin ligases. The expression of either protein results in ubiquitinylation of MHC class I molecules (Coscoy et al., 2001b; Hewitt et al., 2002). The addition of ubiquitin to specific lysines in the cytosolic domains of membrane proteins causes their internalization from the plasma membrane and functions as a signal to sort proteins for degradation (Hicke, 1999; Pickart, 2001).

In our screen we found several interactions involving K3 and K5. For example, we observed an interaction between the N- and C-terminal domain of K3, indicating either an intramolecular interaction or a multimerization of several K3 molecules.
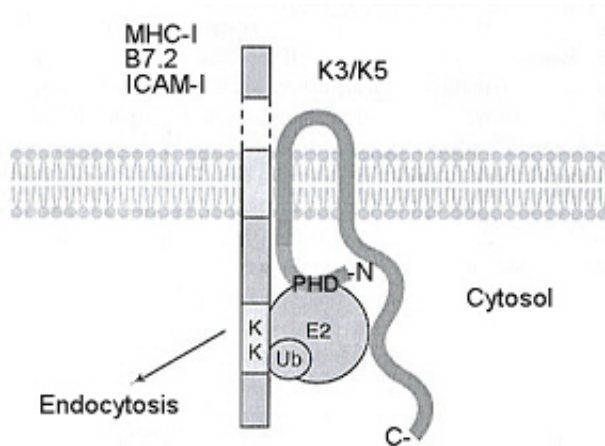
Figure 25:   K3 and K5 are E3 ubiquitin ligases.
The N-terminal PHD domain of K3/K5 (with its associated E2 activity) is directed to the cytosolic tail of the target (MHC-I, B7.2, ICAM-I), where ubiquitinylation (Ub) takes place. The ubiquitinated cytoplasmatic region of the targets are recognized by the endocytic machinery, which promotes their removal from the cell surface and their subsequent degradation by the lysosome. In our yeast two-hybrid screen we observed the interaction of the two cytoplasmatic domains of K3(according to Sanchez et al., 2002).

Interestingly, K3 and K5 both interact with K7, a mitochondrial regulator of apoptosis. K7 connects active caspase-3 to Bcl-2 and thereby inhibits its apototic activity (Wang et al., 2002). Moreover, K7 targets a regulator of the ubiquitin- and proteasome-mediated degradation machinery, PLIC1, to IκB and p53 (Feng et al., 2004). Since K3 and K5 bind to a variety of different viral proteins, our data suggest that K3 or K5 form a complex with K7 which targets and possibly degrades other viral proteins.

5.4   Further investigations concerning the topology of KSHV protein interaction network

While cellular protein interaction networks exist for several model organisms, there had been no viral counterpart to date. In many complex networks (including protein interaction networks), most nodes have few, while some have many interaction partners (so-called hubs). It has been found that their degree distributions follow a power-law decay, and such networks are termed scale-free (Barabasi and Albert, 1999).

KSHV, like its cellular counterparts has relatively many hubs, a key characteristic of scale-free networks. However, in contrast to known cellular protein interaction networks, in which nodes with a single interaction partner are most abundant, the KSHV network has relatively few such "peripheral" nodes lying on the "edge" of the

network. Similar studies in VZV, mCMV and EBV indicated that the same characteristics hold true for other viruses as well (Baiker, Fossum, Kraus et al., personal communication).

In KSHV, the degree distribution peaks at nodes with three neighbours. This unusual characteristic at low node degrees is one of the reasons that the viral networks appear as a single, highly coupled modules and presumably reflects their incompleteness as stand-alone networks. Further bioinformatical analyses revealed that the degree distribution of viral protein networks can be approximated by a power law. In contrast to previously identified cellular networks which possess bigger power coefficients, the power coefficient of the KSHV network was rather low (r=0.95).

The Figures 26-32 were generated by Yu-An Dong, using the results of this study.
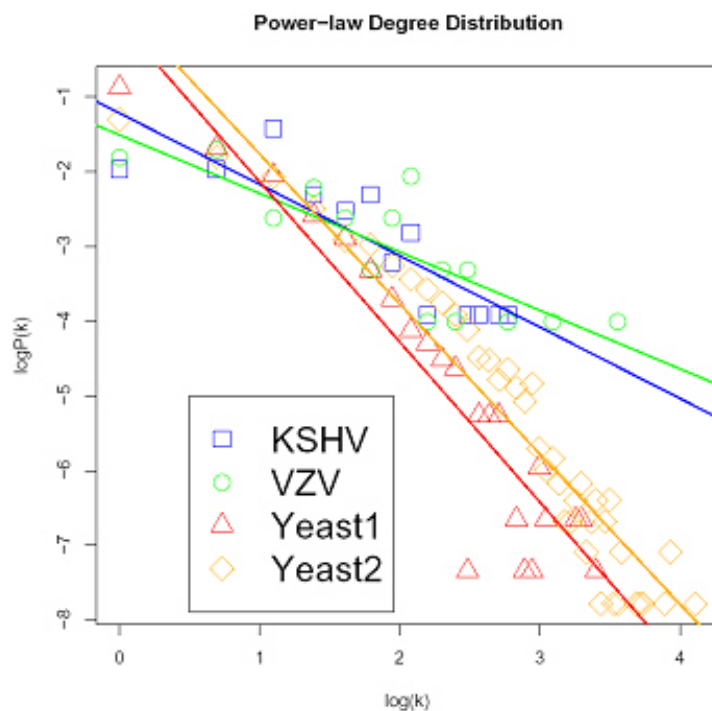
Figure 26: **Power-law degree distribution of two herpesviral (KSHV and VZV) networks in comparison to two high-confidence yeast networks.**
The dataset *Yeast1* is derived from Schwikowski et al., *Yeast2* from the DIP database (October 2004 release). For the analysis of KSHV and VZV, the complete set of interactions detected by Y2H was used. For each network, node degrees k and their relative frequency (i.e. probability) are plotted on a bilogarithmic scale and fitted by linear regression.

Another important characteristic of complex networks is the so-called small-world property (Watts and Strongatz, 1998). In a small-world network the average distance between any two nodes is short (short characteristic path length or the *six degrees of separation* phenomenon) and local neighborhoods are more densely connected (high

clustering coefficient). Both viruses exhibit a short characteristic path length and a short network diameter (the maximum distance between any two nodes), which suggests their coupling as single modules. To assess the viral levels of local clustering, we generated random networks of the same size and degree distribution. Our results show that the level of local clustering is low in KSHV, in fact comparable to equivalent random networks, and thus the KSHV network cannot be classified as small-world. In contrast, all known cellular protein interaction networks are unambiguously small-world, even after the effect on local clustering due to degree distribution and network size, is filtered out.

In *S.cerevisiae*, Maslov and Sneppen demonstrated the existence of a degree correlation by showing that hubs tend to avoid each other while preferring low-connectivity nodes (Maslov and Sneppen, 2002). As a result, the yeast network has well-separated modules, and errors in one module do not easily propagate to other modules. In the viral networks, there is no such declining degree correlation and hubs do not tend to avoid each other, which offers additional evidence that these viral networks could be viewed as single, highly coupled modules. As a consequence of these unusual topological features, viral networks are more resistant to deliberate attacks than other networks, as both network size and characteristic path length remain more stable after the most highly connected nodes are removed.
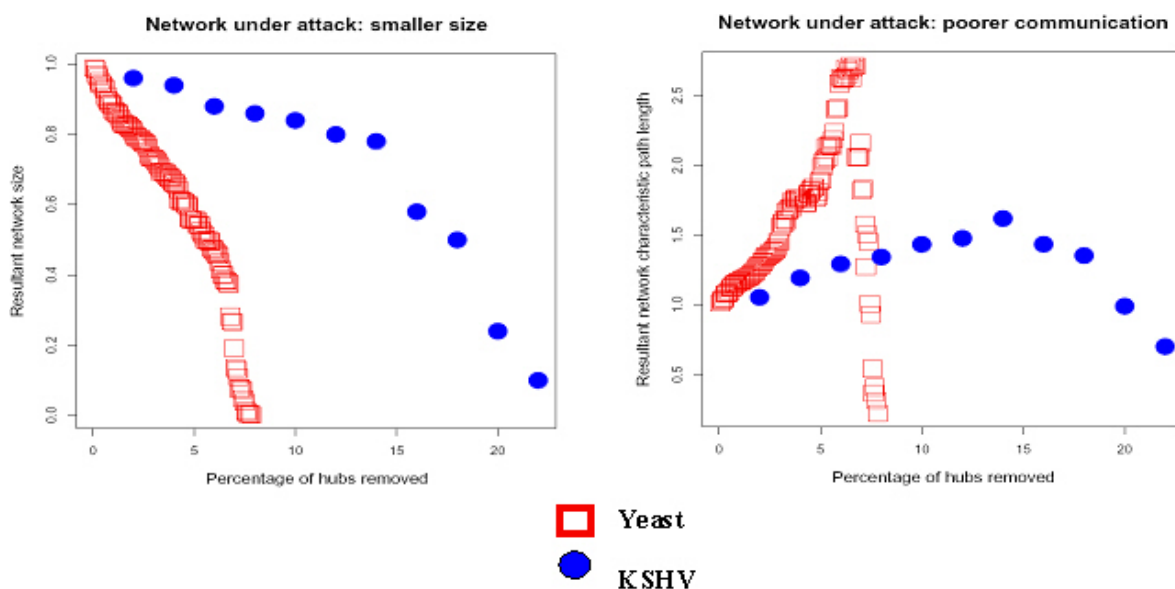
Figure 27:   Simulations of deliberate attack on KSHV and yeast networks by removing their most highly connected nodes.
After each node is removed, the new network characteristic path length (average distance between any two nodes) and size (number of nodes) of the remaining single largest connected component

(SLCC) are computed and plotted as a multiple or fraction of the original parameters. KSHV exhibits much higher attack tolerance, as the increase in path length and the decrease in network size are considerably smaller.

5.5 Relationship between protein interaction and expression profile.

Since the KSHV interactome constitutes the first substantial viral protein interaction dataset on which statistical analysis is possible and in order to get hints on the extent to which global network properties and "super-global" host effect manifest themselves on the local level, we examined the relationship between protein interaction, sequence conservation, expression profile and function in detail. As protein interactions have been shown to be powerful predictors of protein function, we assigned all KSHV proteins into 5 functional classes and analysed which classes preferentially interact with each other (Samanta and Liang, 2003). Only proteins belonging to the "gene regulation" class interacted with proteins of the same class in a statistically significant way, whereas most proteins interacted with proteins of other functional classes, suggesting that many proteins have additional, yet still unknown functions. Interactions between proteins in the "host interaction" class are highly suppressed, probably reflecting missing virus-host interactions.

The 15 viral hubs with >5 interaction partners represent all functional classes and include three proteins Orf23, Orf28 and Orf31 with unknown function. Since viral hubs tend to be conserved across herpesviral subfamilies, they are potential targets for drug design. The combined analysis of expression profile and local network topology gives hints which viral hubs are involved rather in static or dynamic complexes.

Expression Correlation of KSHV

circles represent interactions
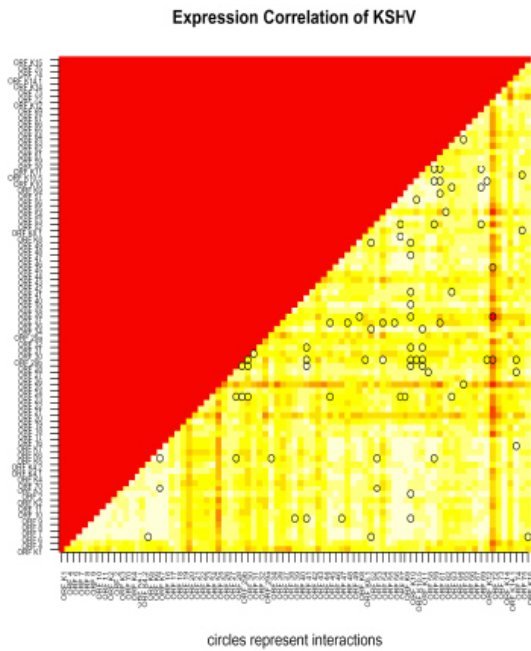
Figure 28:   Correlation between viral protein interactions and expression profile.
Interacting proteins share more similar expression profiles. All pairwise expression profile correlations determined based on results by Jenner et al. were plotted in a matrix for 81 KSHV ORFs (Jenner et al., 2001). Interacting protein pairs are indicated as circles. Standard Pearson correlation of two vectors was used to compute the expression profile correlation of any two KSHV ORFs. The average expression correlation [AEC] for random pairs of ORFs was determined to be 0.804 for random pairs and 0.839 for interacting pairs [p=0.0004].
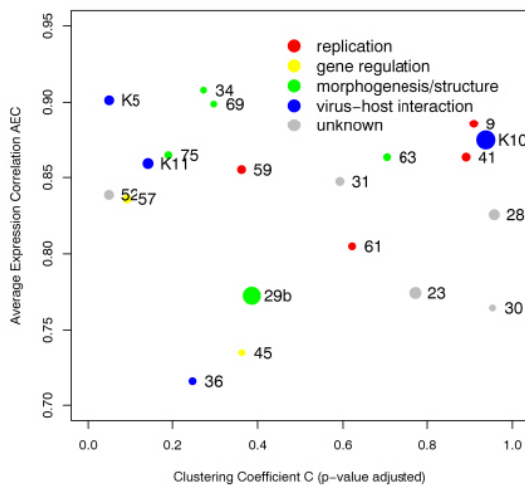
Figure 29:   Dynamic vs. static interactions of viral hubs.
The correlation between AEC and the clustering coefficient C proposes either static or dynamic interactions for viral hubs. The size of the circles indicates the number of interaction partners, the colours refer to the functional class. If interactions are static as in a large complex, proteins are more likely to interact with each other (hence high C) and to be expressed at the same time as their interaction partners (hence high AEC). On the other hand, if interactions take place at different time or place, both C and AEC should be lower. In contrast to previous studies on *party* versus *date* hubs which used raw c values, we evaluated clustering based on its significance (p-value adjusted), which enabled us to use the smaller virus datasets, and filtered out the effect on clustering due to the underlying degree distribution, which was shown to be considerable. For example, the Orf9 polymerase and the Orf41 helicase, which are both involved in replication and most likely form a stable complex, are both high in C and AEC values, whereas the ORF 36 kinase possesses low C and AEC values as anticipated for an enzyme. This analysis implies that K10, one of the major KSHV hubs, probably participates in a stable complex.

90

5.6 Creating an interplay between viral and human protein networks

The network analyses of the KSHV and VZV interactomes revealed unique features of viral systems which also manifested themselves on the local level. Since we hypothesized that many of them could be attributed to missing virus-host interactions, we modeled the interplay between viral and human protein networks. As there is not sufficient experimental interaction data for the human proteome available, we used a prototypical human protein interaction network derived from high-confidence interactions in *S. cerevisiae*, *C. elegans* and *D. melanogaster* (Lehner and Fraser, 2004) Since hardly any published human proteins targeted by KSHV lie within this host network, we connected the viral and host networks by predicting interactions between KSHV and human proteins if both proteins have orthologs in a third organism which are known to interact.

Table 5   Previously published KSHV-human interactions

PubMed ID	KSHV protein	Human protein (Ensembl Gene ID)
12584338*	gB(ORF8)	alpha3integrin(ENSG00000005884)
12584338*	gB(ORF8)	beta1integrin(ENSG00000150093)
11752170*	K15(ORFK15)	HAX-1(ENSG00000143575)
12388711*	K7(ORFK7)	CAML(ENSG00000164615)
11336706*	kaposinA(ORFK12)	cytohesin-1(ENSG00000108669)
11038375*	LANA-1 (ORF73)	ATF4/CREB2(ENSG00000128272)
11425857*	LANA-1 (ORF73)	CBP(ENSG00000005339)
11000236*	LANA-1 (ORF73)	CIR(***)
12829841*	LANA-1 (ORF73)	Gsk-3A(ENSG00000105723)
12829841*	LANA-1 (ORF73)	Gsk-3B(ENSG00000082701)
10562490*	LANA-1 (ORF73)	HistoneH1(ENSG00000189060)
12486118*	LANA-1 (ORF73)	HP1-alpha(ENSG00000094916)
12941895*	LANA-1 (ORF73)	KLIP1(***)
11000236*	LANA-1 (ORF73)	mSin3A(ENSG00000169375)
12768028*	LANA-1 (ORF73)	p53(ENSG00000141510)
10559289*	LANA-1 (ORF73)	RING3(ENSG00000112526)
11000236*	LANA-1 (ORF73)	SAP30(ENSG00000164105)
12477864*	Rap (ORFK8)	C/EBPalpha(***)
12885907*	Rap (ORFK8)	C/EBPalpha(***)
11533213*	Rap (ORFK8)	CBP(ENSG00000005339)
12915577*	Rap (ORFK8)	Cdk2(ENSG00000123374)
12604819*	Rap (ORFK8)	hSNF5(ENSG00000099956)
12885907*	Rap (ORFK8)	p21(ENSG00000124762)
11090200*	Rap (ORFK8)	p53(ENSG00000141510)
12612078*	RTA (ORF50)	Brg1(ENSG00000127616)
12477864*	RTA (ORF50)	C/EBPalpha(***)
11160690*	RTA (ORF50)	CBP(ENSG00000005339)
11390631*	RTA (ORF50)	CBP(ENSG00000005339)

12612078*	RTA (ORF50)	CBP(ENSG00000005339)
11160690*	RTA (ORF50)	c-Jun(ENSG00000177606)
11160690*	RTA (ORF50)	HDAC-1(ENSG00000116478)
11711586*	RTA (ORF50)	MGC2663(ENSG00000130818)
12832621*	RTA (ORF50)	RBP-Jkappa(ENSG00000168214)
11741976*	RTA (ORF50)	STAT3(ENSG00000168610)
12612078*	RTA (ORF50)	TRAP230(ENSG00000184634)
9829980*	vBcl-2(ORF16)	DIVA(ENSG00000137875)
12890756*	vFLIP(ORFK13)	IKK-gamma(ENSG00000073009)
11027294*	vIRF-1 (ORFK9)	p300(ENSG00000100393)
11390621*	vIRF-1 (ORFK9)	p53(ENSG00000141510)
10438822*	vIRF-1 (ORFK9)	ICSBP(ENSG00000140968)
10438822*	vIRF-1 (ORFK9)	IRF1(ENSG00000125347)
10438822*	vIRF-1 (ORFK9)	p300(ENSG00000100393)
10200596*	VIRF-2(ORFK11)	ICSBP(ENSG00000140968)
10200596*	VIRF-2(ORFK11)	IRF-1(ENSG00000125347)
10200596*	VIRF-2(ORFK11)	IRF-1(ENSG00000125347)
10200596*	VIRF-2(ORFK11)	IRF-2(ENSG00000168310)
10200596*	VIRF-2(ORFK11)	p300(ENSG00000100393)
10200596*	VIRF-2(ORFK11)	RelA/p65(ENSG00000173039)
10200596*	VIRF-2(ORFK11)	RelA/p65(ENSG00000173039)
10666184*	vMIP-3(ORFK4.1)	CCR4(ENSG00000183813)
10377196*	vMIP-I(ORFK6)	CCR8(ENSG00000179934)
10736178*	vMIP-II(ORFK4)	CCR5(ENSG00000188239)
11700073*	vMIP-II(ORFK4)	CCR5(ENSG00000188239)
10736178*	vMIP-II(ORFK4)	CXCR4(ENSG00000121966)
10200596*	VIRF-2(ORFK11)	ICSBP(ENSG00000140968)
10200596*	VIRF-2(ORFK11)	IRF-1(ENSG00000125347)
10200596*	VIRF-2(ORFK11)	ICSBP(ENSG00000140968)

* PubMed ID of reference article
*** Unable to be mapped to a unique ENSEMBL gene ID

By this approach, we received 20 high-confidence interactions between 8 KSHV and 20 human proteins which are interconnected within the human network. Nineteen of these 20 virus-host interactions were tested by CoIP and a surprisingly large percentage (13/19 or 68.4%) could be confirmed (Table 6).

While published viral-host interactions tend to involve genes or interactions specific to human or higher eukaryotes (since most human targets have no orthologs or orthologous interactions in the three lower-eukaryotic model organisms), the predicted viral-host interactions involve genes and interactions common from lower eukaryotes to human and hence might reflect more general host-interacting mechanisms.

Table 6   Predicted and verified virus-host interactions.

	viral protein	cellular protein	Y2H	CoIP
1.	ORF2	SDF2	+	+
2.	ORF9	DPD2	+	+
3.	ORF18	121022	-	+
4.	ORF18	ST5A	-	+
5.	ORF18	ST5B	n.d.	n.d.
6.	ORF18	RL4	-	-
7.	ORF36	SERA	-	-
8.	ORF36	XPD	-	+
9.	ORF36	GFA2	+	+
10.	ORF36	CHK1	-	+
11.	ORF36	LSM1	-	-
12.	ORF46	PCNA	-	+
13.	ORF60	U84B	-	+
14.	ORF60	105011	+	+
15.	ORF60	149100	-	+
16.	ORF60	RIR2	-	-
17.	ORF61	RIR1	-	+
18.	ORF72	CDK6	-	+
19.	ORF72	CDK3	+	-
20.	ORF72	CKS2	-	-
	confirmed interactions (percentage)		**5/19 (26.3%)**	**13/19 (68.4%)**

Using the predicted KSHV-human interactions, we were able to dock the two interactomes at each other (Figure 30). Strikingly, the topology of the KSHV network changes completely from a highly coupled module to a more typical scale-free network once it is connected to its host. To rigorously assess the impact of the two systems upon each other, we carried out a combined viral-host network analysis, one level at a time (Figure 31). Starting with the KSHV network (level 0), we first added in their direct human targets together with the interactions they carry (level 1), subsequently we added in those human targets' own interactions partners and their interactions (level 2), and so on, until the viral network is completely assimilated into the host network.
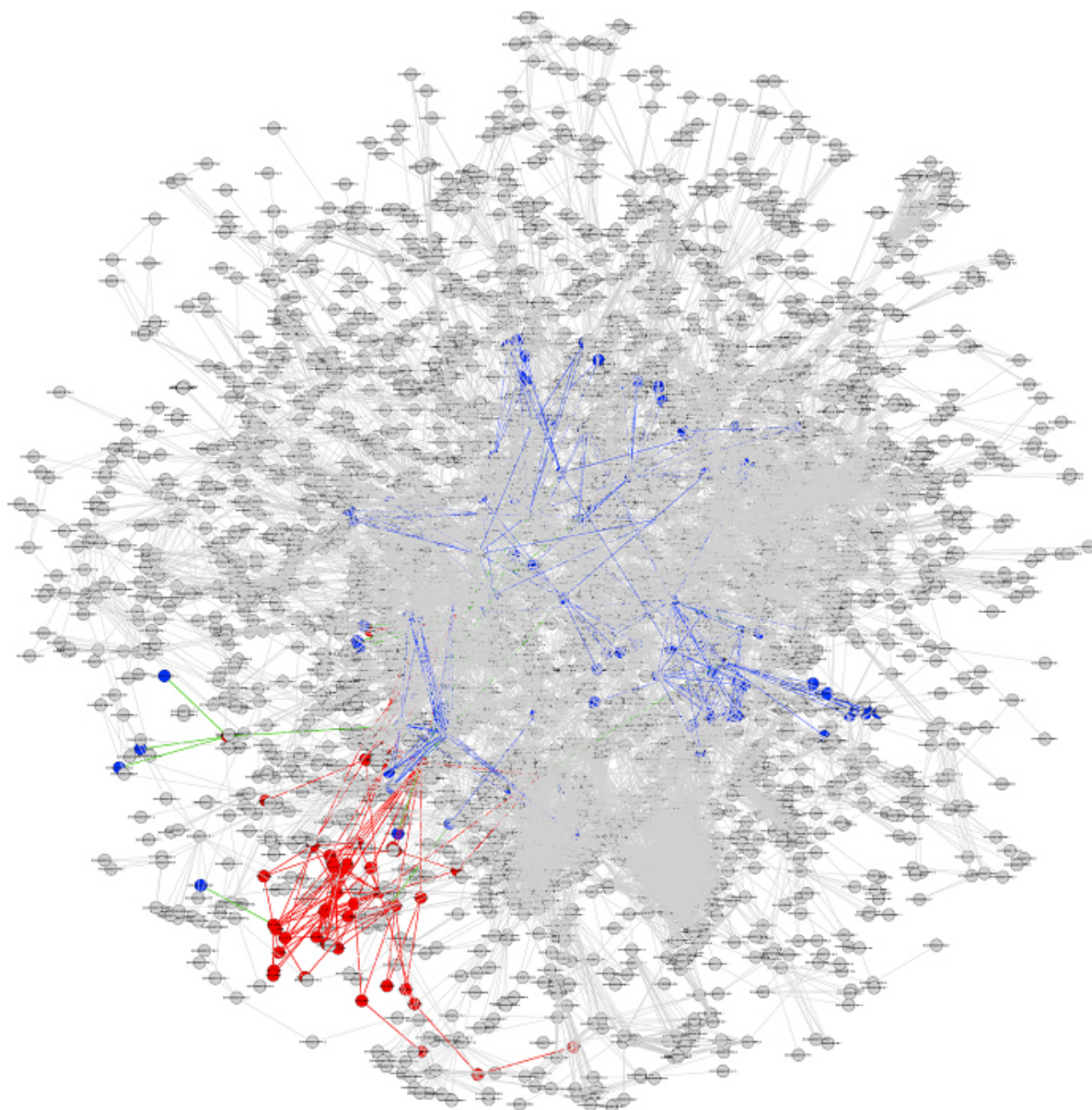
Figure 30:   Global view of the interplay between the KSHV and a predicted high-confidence human interaction network.
The network consists of 10,636 edges among 3,169 nodes. Viral proteins are depicted as red nodes, cellular interacting proteins (level 1 and 2) as blue nodes and cellular proteins (level >2) as grey nodes. Interactions between viral proteins are depicted as red edges, between viral and cellular proteins as green edges and between cellular level 1 and 2 proteins as blue edges.
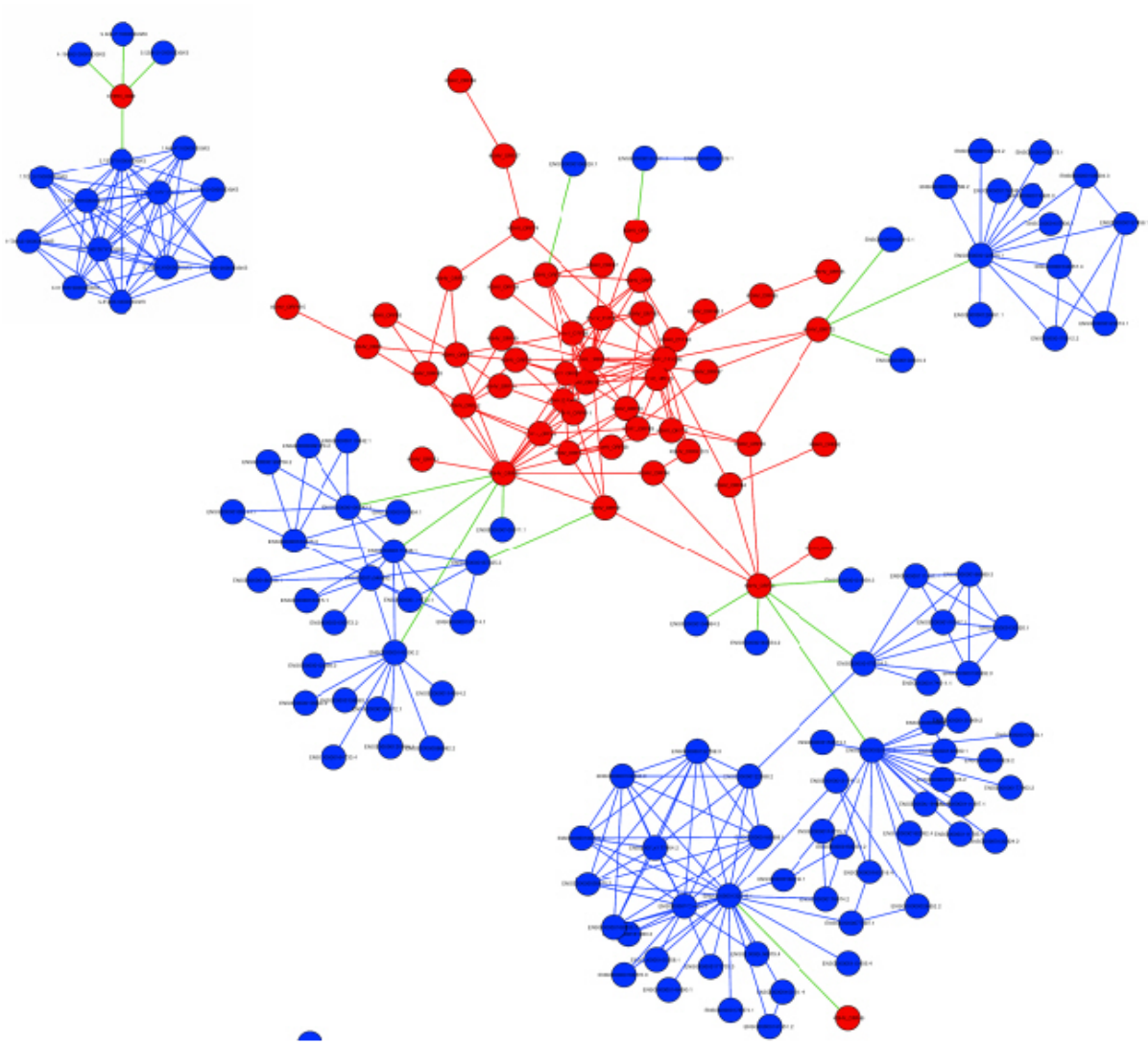
Figure 31: **Local view of the combined viral and host interaction networks (level ≤ 2).**

To evaluate the topology of the combined virus-host network, we reasoned that a correctly combined system should be able to distinguish itself from randomly combined networks. To generate an ensemble of equivalent random viral-host networks, we adopted and compared two separate simulation strategies. Whereas in the first approach human targets were assigned randomly, in the second, even more stringent approach, orthology relationships between KSHV and third organism proteins were randomly shuffled and the whole procedure used to predict KSHV-human interactions was repeated to produce simulated "predictions" (Figure 32).
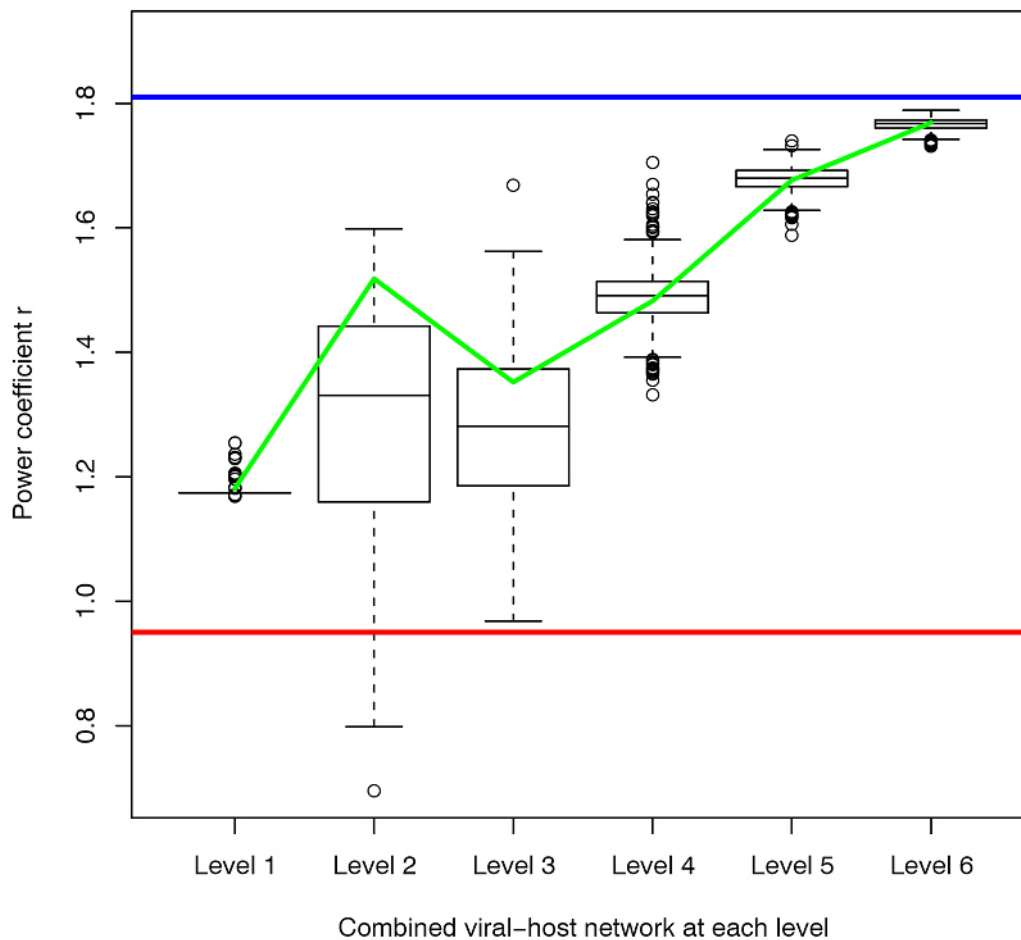
Figure 32: **Power coefficient γ of the combined viral-host interaction network at each level.**
Power coefficient γ of the combined viral-host interaction network at each level. KSHV together with their direct human targets constitute the viral-host network at level 1, the level 1 network together with their own interaction partners constitute the viral-host network at level 2, and so on. The red and the blue lines indicate the power coefficient of the isolated KSHV and human network, respectively. The green line connects the power coefficient γ at each level of the true viral-host network, while the boxplots show the distribution of γ at each level of 100 simulated viral-host networks.

As the level elevates, the viral-host system exhibits an increasing power coefficient indicating that the KSHV network more and more assimilates to the human network. At each level, simulated viral-host systems tend to have smaller power coefficients than the correctly assembled networks, with the most significant distinction at level 2 (empirical p-value < 0.01). Thus, at the level carrying most biological relevance (KSHV's human targets and their own interaction partners in turn) and suffering from minimal noise (level 3 already includes a sizable fraction of the human network and many of the interactions are conceivably no longer relevant to the viral-host context), the combined virus-host network significantly assimilates human network properties.

While we have shown that virus and host interactomes possess a distinct network topology, their interplay may lead to emergent new system properties representing specific features of the viral pathogenesis. Obviously, numerous biological hypotheses resulting from our study remain to be investigated in detail. The availability of protein interaction networks in other herpesviruses and large-scale virus-host interaction data in the near future will boost our knowledge on the function of many still poorly characterised viral proteins and the phylogeny of herpesviruses. It will eventually lead to a considerably improved understanding of viral pathogenesis and evoke novel therapeutic strategies.

6 REFERENCES

(1) Ablashi, D.V.; Chatlynne, L.G.; Whitman, J.E., Jr.; Cesarman, E. "Spectrum of Kaposi's sarcoma-associated herpesvirus, or human herpesvirus 8, diseases." Clin.Microbiol.Rev. 15.3 (2002): 439-64.

(2) Ahmed, A.; Isa, M.S.; Garba, H.A.; Kalayi, G.D.; Muhammad, I.; Egler, L.J. "Influence of HIV infection on presentation of Kaposi's sarcoma." Trop.Doct. 31.1 (2001): 42-45.

(3) Antman, K. and Chang, Y. "Kaposi's sarcoma." N.Engl.J.Med. 342.14 (2000): 1027-38.

(4) Arvanitakis, L.; Mesri, E.A.; Nador, R.G.; Said, J.W.; Asch, A.S.; Knowles, D.M.; Cesarman, E. "Establishment and characterization of a primary effusion (body cavity-based) lymphoma cell line (BC-3) harboring kaposi's sarcoma-associated herpesvirus (KSHV/HHV-8) in the absence of Epstein-Barr virus." Blood 88.7 (1996): 2648-54.

(5) AuCoin, D.P.; Colletti, K.S.; Cei, S.A.; Papouskova, I.; Tarrant, M.; Pari, G.S. "Amplification of the Kaposi's sarcoma-associated herpesvirus/human herpesvirus 8 lytic origin of DNA replication is dependent upon a cis-acting AT-rich region and an ORF50 response element and the trans-acting factors ORF50 (K-Rta) and K8 (K-bZIP)." Virology. 318.2 (2004): 542-55.

(6) Aurelian, L."Herpes simplex virus type 2: Unique biological properies include neoplastic potential mediated by the PK domain of the large subunit of ribonuleotide reductase." Frontiers in Bioscience 3 (1998): 237-49.

(7) Barabasi, A.L. and Albert, R. "Emergence of scaling in random networks" Science 286 (1999): 509-512

(8) Bartee, E.; Mansouri, M.; Hovey Nerenberg, B.T.; Gouveia, K.; Fruh, K. „Downregulation of major histocompatibility complex class I by human ubiquitin ligases related to viral immune evasion proteins." J Virol. 78.3 (2004): 1109-20.

(9) Bartel, P.L.; Roecklein, J.A.; SenGupta, D.; Fields, S. "A protein linkage map of Escherichia coli bacteriophage T7." Nat.Genet. 12.1 (1996): 72-77.

(10) Beard, J.M.; Taus, N.S. and J. D. Baines "DNA Cleavage and Packaging Proteins Encoded by Genes U_L28, U_L15, and U_L33 of Herpes Simplex Virus Type 1 Form a Complex in Infected Cells" J Virol. 76.10(2002): 4785–4791.

(11) Bello, L.J.; Davison, A.J.; Glenn, M.A.; Whitehouse, A.; Rethmeier, N.; Schulz, T.F.; Barklie, Clements J. "The human herpesvirus-8 ORF 57 gene and its properties." J.Gen.Virol. 80 (Pt 12) (1999): 3207-15.

(12)   Besser, J.; Sommer, M.H.; Zerboni, L.; Bagowski, C.P.; Ito, H.; Moffat, J.; Ku, C.C.; Arvin, A.M. "Differentiation of varicella-zoster virus ORF47 protein kinase and IE62 protein binding domains and their contributions to replication in human skin xenografts in the SCID-hu mouse." J Virol. 77.10 (2003): 5964-74.

(13)   Boshoff, C.; Endo, Y.; Collins, P.D.; Takeuchi, Y.; Reeves, J.D.; Schweickart, V.L.; Siani, M.A.; Sasaki, T.; Williams, T.J.; Gray, P.W.; Moore, P.S.; Chang, Y.; Weiss, R.A. "Angiogenic and HIV-inhibitory functions of KSHV-encoded chemokines." Science 278.5336 (1997): 290-94.

(14)   Boshoff, C.; Schulz, T.F.; Kennedy, M.M.; Graham, A.K.; Fisher, C.; Thomas, A.; McGee, J.O.; Weiss, R.A.; O'Leary, J.J. "Kaposi's sarcoma-associated herpesvirus infects endothelial and spindle cells." Nat.Med. 1.12 (1995): 1274-78.

(15)   Boulton, S.J.; Gartner, A.; Reboul, J.; Vaglio, P.; Dyson, N.; Hill, D.E.; Vidal, M. "Combined functional genomic maps of the C. elegans DNA damage response." Science 295.5552 (2002): 127-31.

(16)   Brune, W.; Menard, C.; Heesemann, J.; Koszinowski, U.H. "A ribonucleotide reductase homolog of cytomegalovirus and endothelial cell tropism" Science.;291.5502 (2001): 303-5.

(17)   Byun, H.; Gwack, Y.; Hwang, S.; and Choe, J. "Kaposi' s Sarcoma-associated Herpesvirus Open Reading Frame (ORF) 50 Transactivates K8 and ORF57 Promoters via Heterogeneous Response Elements" Mol Cells.14.2 (2002): 185-191

(18)   Cagney, G., P. Uetz, and S. Fields. "High-throughput screening for protein-protein interactions using two-hybrid assay." Methods Enzymol. 328 (2000): 3-14.

(19)   Capili, A.D.; Schultz, D.C.; RauscherIII, F.J.; Borden, K.L. "Solution structure of the PHD domain from the KAP-1 corepressor: structural determinants for PHD, RING and LIM zinc-binding domains." EMBO J. 20.1-2 (2001): 165-77.

(20)   Castleman, B., L. Inverson, and V.P. Menendez "Localized mediastinal lymphnode hyperplasia resembling thymoma." Cancer 9.4 (1956): 822-30.

(21)   Cesarman, E.; Chang, Y.; Moore, P.S.; Said, J.W.; Knowles, D.M. "Kaposi's sarcoma-associated herpesvirus-like DNA sequences in AIDS-related body-cavity-based lymphomas." N.Engl.J.Med. 332.18 (1995): 1186-91.

(22)   Cesarman, E.; Moore, P.S.; Rao, P.H.; Inghirami, G.; Knowles, D.M.; Chang, Y. "In vitro establishment and characterization of two acquired immunodeficiency syndrome-related lymphoma cell lines (BC-1 and BC-2)

containing Kaposi's sarcoma-associated herpesvirus-like (KSHV) DNA sequences." Blood. 86.7 (1995): 2708-14.

(23)   Chabaud, S.; Lambert, H.; Sasseville, A.M.; Lavoie, H.; Guilbault, C.; Massie, B.; Landry, J.; Langelier, Y. "The R1 subunit of herpes simplex virus ribonucleotide reductase has chaperone-like activity similar to Hsp27." FEBS Lett. 545.2-3 (2003):213-8.

(24)   Chandran, B.; Bloomer, C.; Chan, S.R.; Zhu, L.; Goldstein, E.; Horvat, R. "Human herpesvirus-8 ORF K8.1 gene encodes immunogenic glycoproteins generated by spliced transcripts." Virology 249.1 (1998): 140-49.

(25)   Chang, Y.; Cesarman, E.; Pessin, M.S.; Lee, F.; Culpepper, J.; Knowles, D.M.; Moore, P.S. "Identification of herpesvirus-like DNA sequences in AIDS-associated Kaposi's sarcoma." Science 266.5192 (1994): 1865-69.

(26)   Chee, M.S.; Bankier, A.T.; Beck, S.; Bohni, R.; Brown, C.M.; Cerny, R.; Horsnell, T.; Hutchison, C.A., III; Kouzarides, T.; Martignetti,J.A. "Analysis of the protein-coding content of the sequence of human cytomegalovirus strain AD169." Curr.Top.Microbiol.Immunol. 154 (1990): 125-69.

(27)   Choi, I.R.; Stenger, D.C.; French, R. "Multiple interactions among proteins encoded by the mite-transmitted wheat streak mosaic tritimovirus" Virology 267.2 (2000a): 185-98.

(28)   Choi, J.K.; Lee, B.S.; Shim, S.N.; Li, M.; Jung, J.U. "Identification of the novel K15 gene at the rightmost end of the Kaposi's sarcoma-associated herpesvirus genome." J.Virol. 74.1 (2000b): 436-46.

(29)   Chung, T.D.; Wymer, J.P.; Smith, C.C.; Kulka, M.; Aurelian, L. "Protein kinase activity associated with the large subunit of herpes simplex virus type 2 ribonucleotide reductase (ICP10)" J Virol. 63.8 (1989): 3389-98.

(30)   Conner, J.; Furlong, J.; Murray, J.; Meighan, M.; Cross, A.; Marsden, H.; Clements, J.B. "Herpes simplex virus type 1 ribonucleotide reductase large subunit: regions of the protein essential for subunit interaction and dimerization." Biochemistry. 32.49 (1993): 13673-80.

(31)   Coscoy, L. and D. Ganem. "Kaposi's sarcoma-associated herpesvirus encodes two proteins that block cell surface display of MHC class I chains by enhancing their endocytosis." Proc.Natl.Acad.Sci.U.S.A 97.14 (2000): 8051-56.

(32)   Coscoy, L. and D. Ganem. "A viral protein that selectively downregulates ICAM-1 and B7-2 and modulates T cell costimulation." J.Clin.Invest 107.12 (2001a): 1599-606.

(33)   Coscoy, L., D. J. Sanchez, and D. Ganem. "A novel class of herpesvirus-encoded membrane-bound E3 ubiquitin ligases regulates endocytosis of proteins involved in immune recognition." J.Cell Biol. 155.7 (2001b): 1265-73.

(34)   Cuconati, A.; Wenkai, X.; Lahser, F.; Pfister, T.; Wimmer, E. "A protein linkage map of the P2 nonstructural proteins of Poliovirus." <u>Journal of Virology</u> 72.2 (1998): 1297-1307.

(35)   Davy, A.; Bello, P.; Thierry-Mieg, N.; Vaglio, P.; Hitti, J.; Doucette-Stamm, L.; Thierry-Mieg, D.; Reboul, J.; Boulton, S.; Walhout, A.J.; Coux, O.; Vidal, M. "A protein-protein interaction map of the Caenorhabditis elegans 26S proteasome." <u>EMBO Rep.</u> 2.9 (2001): 821-28.

(36)   Deane, C.M.; Salwinski, L.; Xenarios, I.; Eisenberg, D. "Protein interactions: two methods for assessment of the reliability of high throughput observations." <u>Mol.Cell Proteomics.</u> 1.5 (2002): 349-56.

(37)   Dittmer, D.P. "Transcription profile of Kaposi's sarcoma-associated herpesvirus in primary Kaposi's sarcoma lesions as determined by real-time PCR arrays." <u>Cancer Res.</u> 63.9 (2003): 2010-15.

(38)   Dupin, N.; Diss, T.L.; Kellam, P.; Tulliez, M.; Du, M.Q.; Sicard, D.; Weiss, R.A.; Isaacson, P.G.; Boshoff, C. "HHV-8 is associated with a plasmablastic variant of Castleman disease that is linked to HHV-8-positive plasmablastic lymphoma." <u>Blood</u> 95.4 (2000): 1406-12.

(39)   Elder, J.H.; Lerner, D.L.; Hasselkus-Light, C.S.; Fontenot, D.J.; Hunter, E.; Luciw, P.A.;Montelaro, R.C. & Phillips, T.R. "Distinct subsets of retroviruses encode dUTPase" <u>J Virol.</u> 66 (1992): 1791–94.

(40)   Ensoli, B., S.Z. Salahuddin, and R.C. Gallo. "AIDS-associated Kaposi's sarcoma: a molecular model for its pathogenesis." <u>Cancer Cells</u> 1.3 (1989): 93-96.

(41)   Feng, P.; Scott, C.W.; Cho, N.H.; Nakamura, H.; Chung, Y.H.; Monteiro, M.J.; Jung, J.U. "Kaposi's sarcoma-associated herpesvirus K7 protein targets a ubiquitin-like/ubiquitin-associated domain-containing protein to promote protein degradation." <u>Mol.Cell Biol.</u> 24.9 (2004): 3938-48.

(42)   Fields, S. and O. Song. "A novel genetic system to detect protein-protein interactions." <u>Nature</u> 340.6230 (1989): 245-46.

(43)   Flajolet, M.; Rotondo, G.; Daviet, L.; Bergametti, F.; Inchauspe, G.; Tiollais, P.; Transy, C.; Legrain, P. "A genomic approach of the hepatitis C virus generates a protein interaction map." <u>Gene</u> 242.1-2 (2000): 369-79.

(44)   Flexner, C. "HIV-protease inhibitors." <u>N.Engl.J.Med.</u> 338.18 (1998): 1281-92.

(45)   Fruh, K.; Bartee, E., Gouveia, K.; Mansouri, M. "Immune evasion by a novel family of viral PHD/LAP-finger proteins of gamma-2 herpesviruses and poxviruses." <u>Virus Res.</u> 88.1-2 (2002): 55-69.

(46)   Fuerst,T.R.; Niles, E.G.; Studier, F.W.; and Moss, B. "Eukaryotic transient-expression system based on recombinant vaccinia virus that synthesizes bacteriophage T7 RNA polymerase." <u>Proc. Natl. Acad. Sci. U. S. A</u>, 83 (1986): 8122-8126.

(47)   Ganem, D. "KSHV and Kaposi's sarcoma: the end of the beginning?" Cell 91.2 (1997): 157-60.

(48)   Gershburg, E.; Pagano, J.S. "Phosphorylation of the Epstein-Barr virus (EBV) DNA polymerase processivity factor EA-D by the EBV-encoded protein kinase and effects of the L-riboside benzimidazole 1263W94." J Virol. 76.3 (2002): 998-1003.

(49)   Giot, L.; Bader, J.S.; Brouwer, C.; Chaudhuri, A.; Kuang, B.; Li, Y.; Hao, Y.L.; Ooi, C.E.; Godwin, B.; Vitols, E.; Vijayadamodar, G.; Pochart, P.; Machineni, H.; Welsh, M.; Kong, Y.; Zerhusen, B.; Malcolm, R.; Varrone, Z.; Collis, A.; Minto, M.; Burgess, S.; McDaniel L.; Stimpson E.; Spriggs F.; Williams J.; Neurath K.; Ioime N.; Agee, M.; Voss, E.; Furtak, K.; Renzulli, R.; Aanensen, N.; Carrolla, S.; Bickelhaupt, E.; Lazovatsky, Y.; DaSilva, A.; Zhong, J.; Stanyon, C.A.; Finley, R.L. Jr.; White, K.P.; Braverman, M.; Jarvie, T.; Gold, S.; Leach, M.; Knight, J.; Shimkets, R.A.; McKenna, M.P.; Chant, J.; Rothberg, J.M. A protein interaction map of Drosophila melanogaster. Science. 302 (2003):1727-36.

(50)   Glenn, M.; Rainbow, L.; Aurade, F.; Davison, A.; Schulz, T.F. "Identification of a spliced gene from Kaposi's sarcoma-associated herpesvirus encoding a protein with similarities to latent membrane proteins 1 and 2A of Epstein-Barr virus." J.Virol. 73.8 (1999): 6953-63.

(51)   Goto, E.; Ishido, S.; Sato, Y.; Ohgimoto, S.; Ohgimoto, K.; Nagano-Fujii, M.; Hotta, H. "c-MIR, a human E3 ubiquitin ligase, is a functional homolog of herpesvirus proteins MIR1 and MIR2 and has similar activity." J.Biol.Chem. 278.17 (2003): 14657-68.

(52)   Gradoville, L.; Gerlach, J.; Grogan, E.; Shedd, D.; Nikiforow, S.; Metroka, C.; Miller, G. "Kaposi's sarcoma-associated herpesvirus open reading frame 50/Rta protein activates the entire viral lytic cycle in the HH-B2 primary effusion lymphoma cell line." J.Virol. 74.13 (2000): 6207-12.

(53)   Gruffat, H.; Portes-Sentis, S.; Sergeant, A.; Manet, E. "Kaposi's sarcoma-associated herpesvirus (human herpesvirus-8) encodes a homologue of the Epstein-Barr virus bZip protein EB1." J.Gen.Virol. 80 (Pt 3) (1999): 557-61.

(54)   Guerin, J.L.; Gelfi, J.; Boullier, S.; Delverdier, M.; Bellanger, F.A.; Bertagnoli, S.; Drexler, I.; Sutter, G.; Messud-Petit, F. "Myxoma virus leukemia-associated protein is responsible for major histocompatibility complex class I and Fas-CD95 down-regulation and defines scrapins, a new group of surface cellular receptor abductor proteins." J Virol. 76.6 (2002): 2912-23.

(55)   Guo, D.; Rajamäki, M.L.; Saarma, M.; Valkonen, J.P. "Towards a protein Interaction map of potyviruses: protein interaction matrixes of two potyviruses based on the yeasttwo-hybrid system." J.Gen.Virol. 82 (2001): 935-39.

(56)   Hamza, M.S.; Reyes, R.A.; Izumiya, Y.; Wisdom, R.; Kung, H.J.; Luziw, P.A. "ORF36 Protein Kinase of Kaposi's Sarcoma Herpesvirus Activates the c-Jun N-terminal Kinase Signaling Pathway" <u>J.Biol.Chem.</u> 279.37 (2004): 38325-30.

(57)   Hazbun, T.R. and S. Fields. "Networking proteins in yeast." <u>Proc.Natl.Acad.Sci.U.S.A</u> 98.8 (2001): 4277-78.

(58)   Harper, J.W.; Adami, G.R.; Wei, N.; Keyomarsi, K.; Elledge, S.J. "The p21 Cdk-interacting protein Cip1 is a potent inhibitor of G1 cyclin-dependent kinases" <u>Cell</u> 75.4 (1993): 805-16.

(59)   Hewitt, E.W.; Duncan, L.; Mufti, D.; Baker, J.; Stevenson, P.G.; Lehner, P.J. "Ubiquitylation of MHC class I by the K3 viral protein signals internalization and TSG101-dependent degradation." <u>EMBO J.</u> 21.10 (2002): 2418-29.

(60)   Hicke, L. "Gettin' down with ubiquitin: turning off cell-surface receptors, transporters and channels." <u>Trends Cell Biol.</u> 9.3 (1999): 107-12.

(61)   Hofmann, K. and W. Stoffel. "TMBASE—a database of membrane spanning protein segments." <u>*Biol. Chem. Hoppe-Seyler.*</u> 374 (1993):166.

(62)   Holzerlandt, R.; Orengo, C.; Kellam, P.; Alba, M.M. "Identification of new herpesvirus gene homologs in the human genome." <u>Genome Res.</u> 12.11 (2002): 1739-48.

(63)   Honess, R.W. and B. Roizman. "Regulation of herpesvirus macromolecular synthesis. I. Cascade regulation of the synthesis of three groups of viral proteins." <u>J.Virol.</u> 14.1 (1974): 8-19.

(64)   Ishido, S.; Choi, J.K.; Lee, B.S.; Wang, C.; DeMaria, M.; Johnson, R.P.; Cohen, G.B.; Jung, J.U. "Inhibition of natural killer cell-mediated cytotoxicity by Kaposi's sarcoma-associated herpesvirus K5 protein." <u>Immunity.</u> 13.3 (2000a): 365-74.

(65)   Ishido, S.; Wang, C.; Lee, B.S.; Cohen, G.B.; Jung, J.U. "Downregulation of major histocompatibility complex class I molecules by Kaposi's sarcoma-associated herpesvirus K3 and K5 proteins." <u>J.Virol.</u> 74.11 (2000b): 5300-09.

(66)   Ito, T.; Tashiro, K.; Muta, S.; Ozawa, R.; Chiba, T.; Nishizawa, M.; Yamamoto, K.; Kuhara, S.; Sakaki, Y. "Toward a protein-protein interaction map of the budding yeast: A comprehensive system to examine two-hybrid interactions in all possible combinations between the yeast proteins." <u>Proc.Natl.Acad.Sci.U.S.A</u> 97.3 (2000): 1143-47.

(67)   Jenner, R.G.; Alba, M.M.; Boshoff, C.; Kellam, P. "Kaposi's sarcoma-associated herpesvirus latent and lytic gene expression as revealed by DNA arrays." <u>J.Virol.</u> 75.2 (2001): 891-902.

(68)   Jenner, R.G.; Boshoff, C. „The molecular pathology of Kaposi's sarcoma-associated herpesvirus." <u>Biochim Biophys Acta.</u> 1602.1 (2002): 1-22.

(69)   Joazeiro, C.A. and A.M. Weissman. "RING finger proteins: mediators of ubiquitin ligase activity." <u>Cell</u> 102.5 (2000): 549-52.

(70)   Kashlan, O.B.; Scott, C.P., Lear, J.D. Cooperman, B.S. "A comprehensive model for the allosteric regulation of mammalian ribonucleotide reductase. Functional consequences of ATP- and dATP-induced oligomerization of the large subunit." <u>Biochemistry</u>.;41.2 (2002): 462-74.

(71)   Kirshner, J.R.; Lukac, D.M.; Chang, J.; Ganem, D. "Kaposi's sarcoma-associated herpesvirus open reading frame 57 encodes a posttranscriptional regulator with multiple distinct activities." <u>J.Virol.</u> 74.8 (2000): 3586-97.

(72)   Kremmer, E. ; Sommer, P., Grasser, F.A. "Epstein-Barr virus-encoded deoxyuridine triphosphate nucleotidohydrolase (dUTPase): a potential target for drug therapy." <u>Transplant Proc</u>. 29.1-2 (1997): 812-4.

(73)   Lagunoff, M. and D. Ganem. "The structure and coding organization of the genomic termini of Kaposi's sarcoma-associated herpesvirus." <u>Virology</u> 236.1 (1997): 147-54.

(74)   Langelier, Y.; Bergeron, S.; Chabaud, S.; Lippens, J.; Guilbault C.; Sasseville, A.M.; Denis, S.; Mosser, D.D.; Massie, B. „The R1 subunit of herpes simplex virus ribonucleotide reductase protects cells against apoptosis at, or upstream of,caspase-8 activation" <u>J.Gen.Virol.</u> 83 (2002): 2779-89.

(75)   Lee, H.; Veazey, R.; Williams, K.; Li, M.; Guo, J.; Neipel, F.; Fleckenstein, B.; Lackner, A.; Desrosiers, R.C.; Jung, J.U. "Deregulation of cell growth by the K1 gene of Kaposi's sarcoma-associated herpesvirus." <u>Nat.Med.</u> 4.4 (1998): 435-40.

(76)   Lehner, B and A.G. Fraser " A first-draft human protein-interaction map." Genome Biol. 5.9 (2004):R63

(77)   Liang, Y.; Chang, J.; Lynch, S.J.; Lukac, D.M.; Ganem, D. "The lytic switch protein of KSHV activates gene expression via functional interaction with RBP-Jkappa (CSL), the target of the Notch signaling pathway." <u>Genes Dev</u>. 16.15 (2002): 1977-89.

(78)   Lin, S.F.; Robinson, D.R.; Miller, G.; Kung, H.J. "Kaposi's sarcoma-associated herpesvirus encodes a bZIP protein with homology to BZLF1 of Epstein-Barr virus." <u>J.Virol.</u> 73.3 (1999): 1909-17.

(79)   Lirette, R.; Caradonna, S. "Inhibition of phosphorylation of cellular dUTP nucleotidohydrolase as a consequence of herpes simplex virus infection." <u>J Cell</u> <u>Biochem.</u> 43.4 (1990): 339-53.

(80)   Liuzzi, M.; Deziel, R.; Moss, N.; Beaulieu, P.; Bonneau, A.M.; Bousquet, C.; Chafouleas, J.G.; Garneau, M.; Jaramillo, J.; Krogsrud, R.L.; Lagracé, L.; McCollum, R.S.; Nawoot, S.; Guindon,Y. "A potent peptidomimetic inhibitor of HSV ribonucleotide reductase with antiviral activity in vivo." <u>Nature.</u> 372.6507 (1994): 695-8.

(81)   Lo, P.; Yu, X.; Atanasov, I.; Chandran, B.; Zhou, Z.H. "Three-dimensional localization of pORF65 in Kaposi's sarcoma-associated herpesvirus capsid." <u>J.Virol.</u> 77.7 (2003): 4291-97.

(82)   Lorenzo, M.E., J.U. Jung, and H.L. Ploegh. "Kaposi's sarcoma-associated herpesvirus K3 utilizes the ubiquitin-proteasome system in routing class major histocompatibility complexes to late endocytic compartments." <u>J.Virol.</u> 76.11 (2002): 5522-31.

(83)   Lubyova, B. and P.M. Pitha. "Characterization of a novel human herpesvirus 8-encoded protein, vIRF-3, that shows homology to viral and cellular interferon regulatory factors." <u>J.Virol.</u> 74.17 (2000): 8194-201.

(84)   Lukac, D.M., J.R. Kirshner, and D. Ganem. "Transcriptional activation by the product of open reading frame 50 of Kaposi's sarcoma-associated herpesvirus is required for lytic viral reactivation in B cells." <u>J.Virol.</u> 73.11 (1999): 9348-61.

(85)   Lukac, D.M.; Renne, R.; Kirshner, J.R.; Ganem, D. "Reactivation of Kaposi's sarcoma-associated herpesvirus infection from latency by expression of the ORF 50 transactivator, a homolog of the EBV R protein." <u>Virology</u> 252.2 (1998): 304-12.

(86)   Malik, P.; Blackbourn, D.J.; Cheng, M.F.; Hayward, G.S.; Clements, J.B. "Functional co-operation between the Kaposi's sarcoma-associated herpesvirus ORF57 and ORF50 regulatory proteins." <u>J Gen Virol.</u> 85.8 (2004): 2155-66.

(87)   Malik, P. and Clements, J.B. "Protein kinase CK2 phosphorylation regulates theinteraction of Kaposi's sarcoma-associated herpesvirus regulatory protein ORF57 with its multifunctional partner hnRNP K" <u>Nucleic Acids Research</u>, 32.18 (2004): 5553–5569

(88)   Marsden, H.S.; McLean, G.W.; Barnard, E.C.; Francis, G.J.; MacEachran, K.; Murphy, M., McVey, G.; Cross, A.; Abbotts, A.P.; Stow, N.D. „The catalytic subunit of the DNA polymerase of herpes simplex virus type 1 interacts specifically with the C terminus of the UL8 component of the viral helicase-primase complex."<u>J Virol.</u> 71.9 (1997):6390-7.

(89)   Maslov, S. and K. Sneppen "Specificity and Stability in Topology of Protein Networks" _Science_ 296 (2002): 910-913

(90)   McCraith, S.; Holtzman, T.; Moss, B.; Fields, S."Genome-wide analysis of vaccinia virus protein-protein interactions." Proc.Natl.Acad.Sci.U.S.A 97.9 (2000): 4879-84.

(91)   McFadden, G.; Murphy, P.M. "Host-related immunomodulators encoded by poxviruses and herpesviruses." Curr Opin Microbiol. 3.4 (2000): 371-8.

(92)   McGeoch, D.J. "Protein sequence comparisons show that the 'pseudoproteases' encoded by poxviruses and certain retroviruses belong to the deoxyuridine triphosphate family." Nucleic Acids Research 18 (1990): 4105–10.

(93)   McGeoch, D.J.; Cook, S.; Dolan, A.; Jamieson, F.E.; Telford, E.A. "Molecular phylogeny and evolutionary timescale for the family of mammalian herpesviruses." J Mol Biol. 247.3 (1995):443-58.

(94)   McGeoch, D.J. and A.J. Davison. "The descent of human herpesvirus 8." Semin.Cancer Biol. 9.3 (1999): 201-09.

(95)   Mears, W. E. and Rice, S. A. "The herpes simplex virus immediate-early protein ICP27 shuttles between nucleus and cytoplasm. " Virology 242 (1998):128–137.

(96)   Mendez, J.C.; Sia, I.G.; Tau, K.R.; Espy, M.J.; Smith, T.F.; Chou, S.; Paya, C,V. "Novel mutation in the CMV UL97 gene associated with resistance to ganciclovir therapy." Transplantation. 67.5 (1999): 755-7.

(97)   Milgram, S."The Small World Problem" Psychology Today (1967): 60-67

(98)   Miller, G.; Heston, L.; Grogan, E.; Gradoville, L.; Rigsby, M.; Sun, R.; Shedd, D.; Kushnaryov, V.M.; Grossberg, S.; Chang, Y. "Selective switch between latency and lytic replication of Kaposi's sarcoma herpesvirus and Epstein-Barr virus in dually infected body cavity lymphoma cells." J.Virol. 71.1 (1997): 314-24.

(99)   Miller, G.; Rigsby, M.O.; Heston, L.; Grogan, E.; Sun,R.; Metroka, C.; Levy, J.A.; Gao, S.J.; Chang, Y.; Moore, P. "Antibodies to butyrate-inducible antigens of Kaposi's sarcoma-associated herpesvirus in patients with HIV-1 infection." N.Engl.J.Med. 334.20 (1996): 1292-97.

(100) Monini, P.; Carlini, F.; Sturzl, M.; Rimessi, P.; Superti, F.; Franco, M.; Melucci-Vigo, G.; Cafaro, A.; Goletti, D.; Sgadari, C.; Butto', S.; Leone, P.; Chiozzini, C.; Barresi, C.; Tinari, A.; Bonaccorsi, A.; Capobianchi, M.R.; Giuliani, M.; di Carlo, A.; Andreoni, M.; Rezza, G.; Ensoli, B. "Alpha interferon inhibits human herpesvirus 8 (HHV-8) reactivation in primary effusion lymphoma cells and reduces HHV-8 load in cultured peripheral blood mononuclear cells." J.Virol. 73.5 (1999): 4029-41.

(101) Moore, P.S.; Gao, S.J.; Dominguez, G.; Cesarman, E.; Lungu, O.; Knowles, D.M.; Garber, R.; Pellett, P.E.; McGeoch, D.J.; Chang, Y. "Primary characterization of a herpesvirus agent associated with Kaposi's sarcomae." <u>J.Virol.</u> 70.1 (1996): 549-58.

(102) Mrowka, R., A. Patzak, and H. Herzel. "Is there a bias in proteome research?" <u>Genome Res.</u> 11.12 (2001): 1971-73.

(103) Nealon, K.; Newcomb, W.W.; Pray, T.R.; Craik, C.S.; Brown, J.C.; Kedes, D.H. "Lytic replication of Kaposi's sarcoma-associated herpesvirus results in the formation of multiple capsid species: isolation and molecular characterization of A, B, and C capsids from a gammaherpesvirus." <u>J.Virol.</u> 75.6 (2001): 2866-78.

(104) Neipel, F.; Albrecht, J.C.; Ensser, A.; Huang, Y.Q.; Li, J.J.; Friedman-Kien, A.E.; Fleckenstein, B. "Human herpesvirus 8 encodes a homolog of interleukin-6." <u>J.Virol.</u> 71.1 (1997): 839-42.

(105) Neipel, F., J. C. Albrecht, and B. Fleckenstein. "Cell-homologous genes in the Kaposi's sarcoma-associated rhadinovirus human herpesvirus 8: determinants of its pathogenicity?" <u>J.Virol.</u> 71.6 (1997): 4187-92.

(106) Nicholas, J.; Zong, J.C.; Alcendor, D.J.; Ciufo, D.M.; Poole, L.J.; Sarisky, R.T.; Chiou, C.J.; Zhang, X.; Wan, X.; Guo, H.G.; Reitz, M.S.; Hayward, G.S. "Novel organizational features, captured cellular genes, and strain variability within the genome of KSHV/HHV8." <u>J.Natl.Cancer Inst.Monogr.</u>23 (1998): 79-88.

(107) Oksenhendler, E.; Carcelain, G.; Aoki, Y.; Boulanger, E.; Maillard, A.; Clauvel, J.P.; Agbalika, F. "High levels of human herpesvirus 8 viral load, human interleukin-6, interleukin-10, and C reactive protein correlate with exacerbation of multicentric castleman disease in HIV-infected patients." <u>Blood</u> 96.6 (2000): 2069-73.

(108) Oksenhendler, E.; Duarte, M.; Soulier, J.; Cacoub, P.; Welker, Y.; Cadranel, J.; Cazals-Hatem, D.; Autran, B.; Clauvel, J.P.; Raphael, M. "Multicentric Castleman's disease in HIV infection: a clinical and pathological study of 20 patients." <u>AIDS</u> 10.1 (1996): 61-67.

(109) Palella, F.J.,Jr.; Delaney, K.M.; Moorman, A.C.; Loveless, M.O.; Fuhrer, J.; Satten, G.A.; Aschman, D.J.; Holmberg, S.D. "Declining morbidity and mortality among patients with advanced human immunodeficiency virus infection. HIV Outpatient Study Investigators." <u>N.Engl.J.Med.</u> 338.13 (1998): 853-60.

(110) Park, J.; Lee, D.; Seo, T.; Chung, J.; Choe, J. "Kaposi's sarcoma-associated herpesvirus(human herpesvirus-8) open reading frame 36 protein is a serine protein kinase" <u>J Gen Virol.</u> 81 (2000): 1067-71.

(111) Paulose-Murphy, M.; Ha, N.K.; Xiang, C.; Chen, Y.; Gillim, L.; Yarchoan, R.; Meltzer, P.; Bittner, M.; Trent, J.; Zeichner, S. "Transcription

program of human herpesvirus 8 (kaposi's sarcoma-associated herpesvirus)." J.Virol. 75.10 (2001): 4843-53.

(112) Penn, I. "Development of cancer in transplantation patients." Adv.Surg. 12 (1978): 155-91.

(113) Pickart, C.M., "Ubiquitin enters the new millennium." Mol.Cell 8.3 (2001): 499-504.

(114) Poole, L.J.; Zong, J.C.; Ciufo, D.M.; Alcendor, D.J.; Cannon, J.S.; Ambinder, R.; Orenstein, J.M.; Reitz, M.S.; Hayward, G.S. "Comparison of genetic variability at multiple loci across the genomes of the major subtypes of Kaposi's sarcoma-associated herpesvirus reveals evidence for recombination and for two distinct types of open reading frame K15 alleles at the right-hand end." J.Virol. 73.8 (1999): 6646-60.

(115) Preston, V.G. and Fisher, F.B. "Identification of the herpes simplex virus type 1 gene encoding the dUTPase. " Virology 138 (1984): 58–68.

(116) Prichard, M.N.; Gao, N.; Jairath, S.; Mulamba, G.; Krosky, P.; Coen, D.M.; Parker, B.O.; Pari, G.S. "A recombinant human cytomegalovirus with a large deletion in UL97 has a severe replication deficiency." J Virol. 73.7 (1999): 5663-70.

(117) Pyles, R.B.; Sawtell, N.M. and Thompson, R.L. "Herpes simplex virus type 1 dUTPase mutants are attenuated for neurovirulence, neuroinvasiveness, and reactivation from latency." J Virol. 66.11 (1992): 6706–13.

(118) Pyles, R.B. and Thompson, R.L." Mutations in accessory DNA replicating functions alter the relative mutation frequency of herpes simplex virus type 1 strains in cultured murine cells." J Virol 68.7 (1994): 4514-24.

(119) Rain, J.C.; Selig, L.; De Reuse, H.; Battaglia, V.; Reverdy, C.; Simon, S.; Lenzen, G.; Petel, F.; Wojcik, J.; Schachter, V.; Chemama, Y.; Labigne, A.; Legrain, P. "The protein-protein interaction map of Helicobacter pylori." Nature 409.6817 (2001): 211-15.

(120) Rawlinson, W.D., H.E. Farrell, and B.G. Barrell. "Analysis of the complete DNA sequence of murine cytomegalovirus." J.Virol. 70.12 (1996): 8833-49.

(121) Reboul, J.; Vaglio, P.; Rual, J.F.; Lamesch, P.; Martinez, M.; Armstrong, C.M.; Li, S.; Jacotot, L.; Bertin, N.; Janky, R.; Moore, T.; Hudson, J.R., Jr.; Hartley, J.L.; Brasch, M.A.; Vandenhaute, J.; Boulton, S.; Endress, G.A.; Jenna, S.; Chevet, E.; Papasotiropoulos, V.; Tolias, P.P.; Ptacek, J.; Snyder, M.; Huang, R.; Chance, M.R.; Lee, H.; Doucette-Stamm, L.; Hill, D.E.; Vidal, M. "C. elegans ORFeome version 1.1: experimental verification of the genome annotation and resource for proteome-scale protein expression." Nat.Genet. 34.1 (2003): 35-41.

(122) Renne, R.; Lagunoff, M.; Zhong, W.; Ganem, D. "The size and conformation of Kaposi's sarcoma-associated herpesvirus (human

herpesvirus 8) DNA in infected cells and virions." J.Virol. 70.11 (1996a): 8151-54.

(123) Renne, R.; Zhong, W.; Herndier, B.; McGrath, M.; Abbey, N.; Kedes, D.; Ganem, D. "Lytic growth of Kaposi's sarcoma-associated herpesvirus (human herpesvirus 8) in culture." Nat.Med. 2.3 (1996b): 342-46.

(124) Reynolds, W.A., R.K. Winkelmann, and E.H. Soule. "Kaposi's sarcoma: a clinicopathologic study with particular reference to its relationship to the reticuloendothelial system." Medicine (Baltimore) 44.5 (1965): 419-43.

(125) Rivas, C.; Thlick, A.E.; Parravicini, C.; Moore, P.S.; Chang, Y. "Kaposi's sarcoma-associated herpesvirus LANA2 is a B-cell-specific latent viral protein that inhibits p53." J.Virol. 75.1 (2001): 429-38.

(126) Roizman, B. and Pellett, P. E. "The family *Herpesviridae*: a brief introduction" *In* D. M. Knipe and P. M. Howley (ed.), Fields virology. Lippincott-Raven Publishers, Philadelphia, Pa. . (2001): 2381-2397

(127) Russo, J.J.; Bohenzky, R.A.; Chien, M.C.; Chen, J.; Yan, M.; Maddalena, D.; Parry, J.P.; Peruzzi, D.; Edelman, I.S.; Chang, Y.; Moore, P.S. "Nucleotide sequence of the Kaposi sarcoma-associated herpesvirus (HHV8)." Proc.Natl.Acad.Sci.U.S.A 93.25 (1996): 14862-67.

(128) Safai, B. and R.A. Good."Kaposi's sarcoma: a review and recent developments." Clin.Bull. 10.2 (1980a): 62-69.

(129) Safai, B.; Mike, V.; Giraldo, G.; Beth, E.; Good, R.A. "Association of Kaposi's sarcoma with second primary malignancies: possible etiopathogenic implications." Cancer 45.6 (1980b): 1472-79.

(130) Samanta, M.P. and S. Liang "Predicting protein functions from redundancies in large-scale protein interaction networks" PNAS 100 (2003): 12579-83

(131) Sanchez, D.J., L. Coscoy, and D. Ganem. "Functional organization of MIR2, a novel viral regulator of selective endocytosis." J.Biol.Chem. 277.8 (2002): 6124-30.

(132) Sarid, R.; Flore, O.; Bohenzky, R.A.; Chang, Y.; Moore, P.S. "Transcription mapping of the Kaposi's sarcoma-associated herpesvirus (human herpesvirus 8) genome in a body cavity-based lymphoma cell line (BC-1)." J.Virol. 72.2 (1998): 1005-12.

(133) Schulz, T.F. "Kaposi's sarcoma-associated herpesvirus (human herpesvirus 8): epidemiology and pathogenesis." J.Antimicrob.Chemother. 45 Suppl T3 (2000): 15-27.

(134) Schwikowski, B.; Uetz, P. and S. Fields „A network of protein−protein interactions in yeast" Nat. Biotechnol. 18 (2000): 1257-61

(135) Seaman, W.T.; Ye, D.; Wang, R.X.; Hale, E.E.; Weisse, M.; Quinlivan, E.B. "Gene expression from the ORF50/K8 region of Kaposi's sarcoma-associated herpesvirus." Virology 263.2 (1999): 436-49.

(136) Selik, R.M., E.T. Starcher, and J.W. Curran. "Opportunistic diseases reported in AIDS patients: frequencies, associations, and trends." AIDS 1.3 (1987): 175-82.

(137) Shlomai, J. & Kornberg, A. "Deoxyuridine triphosphatase of Escherichia coli. Purification, properties, and use as a reagent to reduce uracil incorporation into DNA." Journal of Biological Chemistry 253 (1978): 3305-12.

(138) Simas, J.P. and S. Efstathiou. "Murine gammaherpesvirus 68: a model for the study of gammaherpesvirus pathogenesis." Trends Microbiol. 6.7 (1998): 276-82.

(139) Sommer, P.; Kremmer, E.; Bier, S.; Konig, S.; Zalud, P.; Zeppezauer, M.; Jones, J.F.; Mueller-Lantzsch, N.; Grasser, F.A. " Cloning and expression of the Epstein-Barr virus-encoded dUTPase: patients with acute, reactivated or chronic virus infection develop antibodies against the enzyme. " J Gen Virol. 77.11 (1997): 2795-805.

(140) Soulier, J.; Grollet, L.; Oksenhendler, E.; Cacoub, P.; Cazals-Hatem, D.; Babinet, P.; d'Agay, M.F.; Clauvel, J.P.; Raphael, M.; Degos, L. "Kaposi's sarcoma-associated herpesvirus-like DNA sequences in multicentric Castleman's disease." Blood 86.4 (1995): 1276-80.

(141) Staskus, K.A.; Zhong, W.; Gebhard, K.; Herndier, B.; Wang, H.; Renne, R.; Beneke, J.; Pudney, J.; Anderson, D.J.; Ganem, D.; Haase, A.T. "Kaposi's sarcoma-associated herpesvirus gene expression in endothelial (spindle) tumor cells." J.Virol. 71.1 (1997): 715-19.

(142) Strahler, J.R.; Zhu, X.X.; Hora, N.; Wang, Y.K.; Andrews, P.C.; Roseman, N.A.; Neel, J.V.; Turka, L.; Hanash, S.M."Maturation stage and proliferation-dependent expression of dUTPase in human T cells." Proc Natl Acad Sci U S A. 90.11 (1993): 4991-5.

(143) Studebaker, A.W.; Balendiran, G.K.; Williams, M.V." The Herpesvirus Encoded dUTPase as a Potential Chemotherapeutic Target "Current Protein and Peptide Science, 2 (2001): 371-79.

(144) Studebaker, A.W.; Ariza, M.E.; Balendiran, G.K.; Williams, M.V."Novel Approaches for Modulating dUTPase and Uracil-DNA Glycosylase: Potential Uses for Cancer and Viral Chemotherapy" Drug Design Reviews - Online, 1 (2004): 1-13.

(145) Sun, R.; Lin, S.F.; Gradoville, L.; Yuan, Y.; Zhu, F.; Miller, G. "A viral gene that activates lytic cycle expression of Kaposi's sarcoma-associated herpesvirus." Proc.Natl.Acad.Sci.U.S.A 95.18 (1998): 10866-71.

(146) Sun, R.; Lin, S.F.; Staskus, K.; Gradoville, L.; Grogan, E.; Haase, A.; Miller, G. "Kinetics of Kaposi's sarcoma-associated herpesvirus gene expression." J.Virol. 73.3 (1999): 2232-42.

(147) Sun, Y. and Conner, J. "The U28 ORF of human herpesvirus-7 does not encode a functional ribonucleotide reductase R1 subunit." Journal of General Virology 80 (1999): 2713–2718.

(148) Sun, Y. and Conner, J. "Characterization of heterosubunit complexes formed by the R1 and R2 subunits of herpes simplex virus1 and equine herpes virus 4 ribonucleotide reductase" Biochem. J. 347 (2000): 97-104

(149) Taylor, J.F.; Templeton, A.C.; Vogel, C.L.; Ziegler, J.L.; Kyalwazi, S.K. "Kaposi's sarcoma in Uganda: a clinico-pathological study." Int.J.Cancer 8.1 (1971): 122-35.

(150) Templeton, A.C. and D. Bhana. "Prognosis in Kaposi's sarcoma." J.Natl.Cancer Inst. 55.6 (1975): 1301-04.

(151) Trus, B.L.; Heymann, J.B.; Nealon, K.; Cheng, N.; Newcomb, W.W.; Brown, J.C.; Kedes, D.H.; Steven, A.C. "Capsid structure of Kaposi's sarcoma-associated herpesvirus, a gammaherpesvirus, compared to those of an alphaherpesvirus, herpes simplex virus type 1, and a betaherpesvirus, cytomegalovirus." J.Virol. 75.6 (2001): 2879-90.

(152) Tusnàdy G.E. and I.Simon "The HMMTOP transmembrane topology prediction server" Bioinformatics 17.9 (2001): 849-50.

(153) Uetz, P.; Giot, L.; Cagney, G.; Mansfield, T.A.; Judson, R.S.; Knight, J.R.; Lockshon, D.; Narayan, V.; Srinivasan, M.; Pochart, P.; Qureshi-Emili, A.; Li,Y.; Godwin, B.; Conover, D.; Kalbfleisch, T.; Vijayadamodar, G.; Yang, M.; Johnston, M.; Fields, S.; Rothberg, J.M. "A comprehensive analysis of protein-protein interactions in Saccharomyces cerevisiae." Nature 403.6770 (2000): 623-27.

(154) Uetz, P.; Rajagopala, S.V.; Dong Y.A.; Haas, J. "From ORFeomes to Protein Interaction Maps in Viruses" Genome Research 10B (2004): 2029-33.

(155) Walhout, A.J.; Sordella, R.; Lu, X.; Hartley, J.L.; Temple, G.F.; Brasch, M.A.; Thierry-Mieg, N.; Vidal, M. "Protein interaction mapping in C. elegans using proteins involved in vulval development." Science 287.5450 (2000): 116-22.

(156) Wang, H.W.; Sharp, T.V.; Koumi, A.; Koentges, G.; Boshoff, C. "Characterization of an anti-apoptotic glycoprotein encoded by Kaposi's sarcoma-associated herpesvirus which resembles a spliced variant of human survivin." EMBO J. 21.11 (2002): 2602-15.

(157) Watts, D.J. and Strongatz, S.H. "Collective dynamics of 'small world' networks" Nature 393 (1998): 440-442

(158) Williams, M.V. "Herpes simplex virus-induced dUTPase: target site for antiviral chemotherapy." <u>Virology</u>.166.1 (1988):262-4.

(159) Wu, L.; Lo, P.; Yu, X.; Stoops, J.K.; Forghani, B.; Zhou, Z.H. "Three-dimensional structure of the human herpesvirus 8 capsid." <u>J.Virol.</u> 74.20 (2000): 9646-54.

(160) Zhi, Y.; Sciabica, K.S.; Sandri-Goldin, R.M. "Self-interaction of the herpes simplex virus type 1 regulatory protein ICP27." <u>Virology</u>. 257.2 (1999):341-51.

(161) Zhong, W.; Wang, H.; Herndier, B.; Ganem, D. "Restricted expression of Kaposi sarcoma-associated herpesvirus (human herpesvirus 8) genes in Kaposi sarcoma." <u>Proc.Natl.Acad.Sci.U.S.A</u> 93.13 (1996): 6641-46.

(162) Zhu, F.X., T. Cusano, and Y. Yuan. "Identification of the immediate-early transcripts of Kaposi's sarcoma-associated herpesvirus." <u>J.Virol.</u> 73.7 (1999): 5556-67.

(163) Zhu, F.X.; King, S.M.; Smith, E.J.; Levy; D.E.; Yuan, Y. "Kaposi's sarcoma-associated herpesviral protein inhibits virus-mediated induction of type I interferon by blocking IRF-7 phosphorylation and nuclear accumulation." <u>Proc Natl Acad Sci</u> <u>U S A.</u> 99.8 (2002): 5573-8.

(164) Zhu, F.X.; Yuan, Y. "The ORF45 protein of Kaposi's sarcoma-associated herpesvirus is associated with purified virions." <u>J Virol.</u> 77.7 (2003): 4221-30.

(165) Zhu, F.X.; Chong, J.M. ; Wu, L.; Yuan, Y. "Virion Proteins of Kaposi's Sarcoma-Associated Herpesvirus" <u>Virol.</u> 79.2 (2005): 800–811.

7 FIGURES AND TABLES

Figures:

Tables

8   ABBREVIATIONS

μ	micro (10^{-6})
°C	degrees Celsius
AD	activation domain
AIDS	acquired immun deficiency syndrome
Ap^r	ampicillin resistence
ATP	adenosine triphoshate
BCBL	body cavity-based lymphomas
BD	binding domain
bp	base pair
BSA	bovine serum albumin
bZIP	basic region - leucine zipper
C.elegans	Caenorhabditis elegans
cDNA	complementary DNA
CIP	calf intestinal alkaline phosphatase
Cm^r	chloramphenicol resistence
CMIR	cellular modulator of immune recognition
CMV	Cytomegalovirus
CoIP	coimmunoprecipitation
cyt	cytoplasmatic
DBD	DNA-binding domain
DDR	DNA damage response
DHFR	dihydrofolate reductase
DMEM	Dulbecco's modified Eagle's medium
DMSO	dimethylsulfoxid
DNA	deoxyribonucleic acid
dNTP	deoxyribonucleoside triphosphate
DTT	dithiothreitol
E	early
E. coli	Escherichia coli
e.g.	exempli gratia (Lat. = for instance)
EBV	Epstein-Barr-Virus
EDTA	ethylene-diamine-tetraacidic acid
EHV	equine herpesvirus type
ER	endoplasmatic reticulum
et al.	et alii (Lat. = and others)
EtOH	ethanol
ext	external
FCS	fetal calf serum
fig.	figure
FL	full length
FLIP	FLICE-inhibitory protein
g	gram
gDNA	genomic DNA
Gm^r	gentamycin resistence
h	hour(s)
H. pylori	Heliobacter pylori
HA	hemagglutinin
HAART	highly active antiretroviral threapy
HCl	hydrochloric acid
HCMV	human cytomegalovirus
HCV	hepatitis C virus
HHV	human herpesvirus
HIS	histidine
HIV	human immundeficiency Virus
HSV	Herpes simplex virus
HVS	herpesvirus saimiri
ICAM-1	intracellular adhesion molecule-1

115

IE	immediate-early
JNK	c-Jun N-terminal kinase;
kb	kilobases
kDa	kilo Dalton
Km^r	kanamycin resistence
KS	Kaposi's sarcoma
KSHV	Kaposi's sarcoma-associated herpesvirus
L	late
l	litre
LAMP	latency-associated membrane protein
LANA	latency-associated nuclear antigen
LB	Luria Bertani medium
LEU	leucin
m	milli (10^{-3})
Mab	monoclonal antibody
MARCH	membrane-associated RING-CH
Mat	mating type
MCD	multicentric Castleman's diseases
MCP	major capsid protein
MHC	major histocompatibility
min	minute(s)
MIR	modulator of immune recognition
MKK	mitogen-activated protein kinase kinase;
MOI	multiplicity of infection
mRNA	messenger RNA
n	nano (10^{-9})
NLS	nuclear localization signal
ORF	open reading frame
PBS	phosphate buffered saline
PCR	polymerase chain reaction
PEL	primary effusion lymphoma
PLIC1	protein-linking integrin-associated protein and cytoskeleton 1
PMA	phorbol myristate acetate
PMSF	phenylmethylsulfonfluoride
PRV	pseudorabies virus
PsbMV	pea seed-borne mosaic virus
PVA	potato virus A
RC	recombinatorial cloning
RNA	ribonucleic acid
RNAi	RNA-mediated interference
rpm	revolutions per minute
RR	ribonucleotide reductase
RT	room temperature
Rta	replication and transcriptional activator
s	second(s)
S. cerevisiae	Saccharomyces cerevisiae
SDS	sodium dodecylsulfat
SsDNA	single-stranded DNA
TA	transcription activator
tab.	table
TEMED	tetramethylethylendiamin
TK	thymidine kinase
TPA	tissue plasminogen activator
TRI	triplex
TRP	tryptophan
TS	thymidylate synthase
UBA	ubiquitin-associated
UBL	ubiquitin-like
UV	ultraviolett
vADH	viral adhesin

vCBP	viral complement-binding protein
vCYC	viral cyclin
vGCR	viral G-protein-coupled receptor
vIL	viral interleukin
vIRF	viral interferon regulatory factor
vMIP	viral macrophage inflammatory protein
VZV	varizella zoster virus
WSMV	wheat streak mosaic virus
Y2H	yeast two-hybrid
YPD	yeast peptone dextrose medium

9 ACKNOWLEDGEMENT

We thank Yuan Ghang, Don Ganem, Shou-Yiang Gao, Wolfgang Hammerschmidt, Patrick Moore, Frank Neipel, Paula Pitha-Rowe, Thomas Schulz, Charles Wood and Yan Yuan for plasmids containing KSHV genes or genomes. Recombinant T7 vaccinia virus was received through courtesy of Bernhard moss by NIH AIDS repository.

DANKSAGUNG

An dieser Stelle möchte ich mich sehr herzlich bei all jenen bedanken, ohne deren Hilfe und Unterstützung diese Arbeit nicht zustande gekommen wäre.

Besonders bedanken möchte ich mich bei PD Dr.med. Dr.rer.nat. Jürgen Haas für die hervorragende Unterstützung und Betreuung meiner Doktorarbeit am Max-von-Pettenkofer Institut für Virologie am Genzentrum.

Herrn Prof. Ulrich Koszinowski danke ich für die Bereitstellung des Labors und die exzellente Unterstützung

Dem FöFoLe Promotionsstudiengang „Molekulare Medizin" unter Herrn Prof. Heesemann danke ich für die Begleitung, die finanzielle Unterstützung, sowie der Organisation der Methodenkolloquien, der Ringvorlesungen und des Wochenendseminares. Meinen Kollegen aus dem Promotionsstudiengang und ihren Betreuern danke ich für Gestaltung der obengenannten Veranstaltungen, sowie für den regen geistigen Austausch.

Peter Uetz danke ich für die Bereitstellung seines Labors zur Durchführung des Y2H-Screens und für die fachlichen Unterstützung, ihm und Yu-An Dong danke ich für die mathematische Bearbeitung des Projektes und die zahlreichen eingebrachten Ideen.

Der Arbeitsgruppe Haas danke ich für die Mitarbeit und die zahllosen Hilfestellungen, insbesondere Christine Atzler, Dietlind Rose und Maria Roupelieva für die

10 PUBLICATIONS

Herpesviral Protein Networks and their Interaction with the Human Proteome
Peter Uetz, Yu-An Dong, Christine Zeretzke, Christine Atzler, Armin Baiker, Bonnie Berger, Seesandra V. Rajagopala, Maria Roupelieva, Dietlind Rose, Even Fossum, Jürgen Haas
Submitted on 30 June 2005; accepted 21 November 2005, published online 8 December 2005; Science DOI: 10.1126/science.1116804 (Science Express Reports)

Abstracts:
1. Systematic analysis of protein-protein interactions in the human gamma herpesvirus KSHV
Christine Zeretzke, Yu-An Dong, Maria Roupelieva, Ulrich Hentschel, Dietlind Rose, Christine Atzler, Peter Uetz and Juergen Haas
Jahrestagung der Deutschen Gesellschaft fuer Virologie
17.-20.3.04 Tuebingen, Germany

2. Systematic analysis of protein-protein interactions in KSHV
Peter Uetz, Christine Zeretzke, Yu-An Dong, Maria Roupelieva, Ulrich Hentschel, Dietlind Rose, Christine Atzler, and Juergen Haas
7th International Workshop on KSHV and Related Agents,
22.-25.8.2004 Santa Cruz, U.S.A.

3. Systematic analysis of protein-protein interactions in KSHV
Peter Uetz, Christine Zeretzke, Yu-An Dong, Maria Roupelieva, Ulrich Hentschel, Dietlind Rose, Christine Atzler and Juergen Haas
30th International Herpesvirus Workshop
30.7.05-4.8.05 Turku, Finland

4. Distinct topology of cellular and herpesvirus protein interaction networks
Peter Uetz, Yu-An Dong, Christine Zeretzke, Armin Baiker, Even Fossum, Maria Roupelieva, Bonnie Berger, Seesandra Rajagopala, Christine Atzler, Dietlind Rose and Juergen Haas
8th International Workshop on KSHV and Related Agents,
221.-25.8.2004 Wildbad Kreuth, Germany

11 CURRICULUM VITAE

Persönliche Daten:

Name:	Christine Zeretzke
Anschrift:	Bozener Str. 8, 81547 München
Geburtsdatum:	03. September 1978
Geburtsort:	Münster
Eltern:	Werner und Hannelore Zeretzke, geb. Altfeld
Staatsangehörigkeit:	deutsch
Familienstand:	ledig

Ausbildung:

1988 – 1997	Kopernikus-Gymnasium, Rheine Abschluß: Abitur
1998 – 2005	Studium der Humanmedizin an der Ludwig-Maximilians Universität in München.
2001 – 2003	Dissertation am Max-von-Pettenkofer-Institut, Genzentrum der Ludwig-Maximilians-Universität München unter der Betreuung von PD Dr. Dr. Jürgen Haas. Thema: „A *genome-wide analysis of protein-protein interactions in Kaposi's sarcoma-associated herpesvirus (KSHV)"* Die Dissertation wurde gefördert durch den FöFoLe Promotionsstudiengang „Molekulare Medizin".
Seit Juni 2005	Assistenzärztin an der Medizinischen Poliklinik der Universität München